

https://dspace.org/

GIS-Based dynamic flood modelling along Jukskei River, Johannesburg, South Africa

Asante-Manteaw, Theophilus

2024-03

University of the Witwatersrand, Johannesburg

https://hdl.handle.net/10539/46683

Asante-Manteaw, Theophilus. (2024). GIS-Based dynamic flood modelling along Jukskei River, Johannesburg, South Africa. [Master's dissertation, University of the Witwatersrand, Johannesburg]. WIReDSpace. https://hdl.handle.net/10539/46683

Downloaded from a DSpace repository. https://dspace.org/

GIS-BASED DYNAMIC FLOOD MODELLING ALONG JUKSKEI RIVER, JOHANNESBURG, SOUTH AFRICA

By

Theophilus Asante-Manteaw (2635242)

Supervisor: Dr Iqra Atif

Submitted in partial fulfilment of the requirements for the degree of **Master of Science in Geographic Information Systems and Remote Sensing** in the School of Geography, Archaeology and Environmental Studies, Faculty of Science, University of the Witwatersrand, Johannesburg, South Africa.

March 2024

DECLARATION

I, Theophilus Asante-Manteaw, affirm that the research titled "GIS-BASED DYNAMIC FLOOD MODELLING ALONG JUKSKEI RIVER, JOHANNESBURG, SOUTH AFRICA" conducted during my Master of Science program in Geographical Information Systems and Remote Sensing at the University of the Witwatersrand, Johannesburg, is entirely my own original work. I have adhered to ethical standards and properly acknowledged all sources used. This research has not been submitted elsewhere for any academic qualification. I take full responsibility for the integrity and authenticity of the research findings.



…….

Signature of candidate

…..23rd…… day of ……March……20…24……in …Johannesburg….

ABSTRACT

This research focuses on utilizing Geographic Information Systems (GIS) for dynamic flood modelling along the Jukskei River in Johannesburg, South Africa. The study aims to enhance flood risk assessment by integrating GIS technology with hydraulic model. Through spatial data analysis and flood scenario simulations, the research seeks to provide insights into water surface elevation (WSE), vulnerability, and flood impact in the catchment area. The model utilized several parameters: the DEM was STRM data obtained from USGS, precipitation data was acquired from CHIRPS, LULC data was obtained from South Africa's Department of Forestry, Fisheries, and the Environment (DFFE), and soil types were acquired from the international soil reference and information centre. The spatial data analysis included examining trends in precipitation spanning a period of 20 years (2000 - 2020), reclassifying land use land cover (LULC), and outlining river channels using digital elevation models (DEM) and reprojection to common coordinate reference system (CRS). Furthermore, the flood scenario simulations were conducted by combining different factors (DEM, LULC, soil types, and precipitation) and assigning and adjusting Manning's n values for different LULC classes to calibrate the model. From the analysis of the precipitation data spanning two decades (2000 - 2020) with the aid of RStudio, it was noted that certain months exhibited sporadic instances of elevated precipitation throughout the study period, showing a rising trend. The examination indicated that spring, summer, and autumn experienced the highest levels, with the peak observed in autumn at 142.03mm, while the lowest maximum average was 35.23mm. This notable precipitation contributed significantly to flooding within the catchment area, with an R-squared value of 0.0638. The flood depth map, WSE maps, and flood inundation maps indicated that with 28mm of precipitation, 1473 buildings were affected within an area of 324,268 square meters, with a flood depth of 2.64 meters. Similarly, with a precipitation level of 49.43mm, 2803 buildings faced vulnerability within an area of 526,217 square meters, with a flood depth of 5.76 meters. Furthermore, at the highest observed precipitation of 142.03mm, 7242 buildings were at risk within an area of 1,137,908 square meters, with a flood depth measuring 8.41 meters.

ACKNOWLEDGEMENTS

I wish to show my greatest appreciation to Dr Iqra Atif, a professor at the School of Geography, Archaeology, and Environmental Studies (GAES) at the University of Witwatersrand, Johannesburg, South Africa. Dr Atif provided vital support and essential resources. This helped me finish this research successfully. Her guidance, knowledge, and encouragement improved the quality of this research greatly.

Additionally, I want to express my gratitude to Samuel Yaw Asante for his huge support throughout this research journey. His help and constant encouragement were key to overcoming difficulties and reaching milestones.

I must express my sincerest gratitude to the lecturers who taught me. Their knowledge and skills in Geographical Information Systems (GIS) and Remote Sensing were invaluable. I appreciate their dedication to teaching. They willingly shared their expertise, shaping my understanding in this specialized field.

The staff within the program and School of Geography, Archaeology, and Environmental Studies deserve my deepest thanks. Their administrative guidance was helpful. The technical assistance they provided was crucial. Their collaborative efforts greatly facilitated this research work's progress.

TABLE OF CONTENTS

DECLARATION i

ABSTRACT ii

ACKNOWLEDGEMENTS iii

LIST OF TABLES vi

LIST OF FIGURES viii

LIST OF EQUATIONS ix

LIST OF ACRONYMS x

CHAPTER 1: INTRODUCTION AND BACKGROUND 1

1.1 Introduction 1

1.2 Background 2

1.3 Research Motivation 3

1.4 Aim and Objectives 5

1.4.1 Aim 5

1.4.2 Objectives 5

1.5 Layout Of Thesis 5

CHAPTER 2: LITERATURE REVIEW 7

2.1 Natural Disasters 7

2.2 Influence of Climate Change on Floods 8

2.3 Floods 8

2.4 Causes And Factors Influencing Floods 9

2.5 Impacts Of Flooding 10

2.6 Flood Management Approaches 11

2.7 Geospatial Technologies in Flood Management 12

2.8 RStudio for Geospatial Analysis 14

2.8.1 Understanding R-Value in Spatial and Temporal Analysis 15

2.8.2 The Role of P-Value in Spatial and Temporal Data Analysis 15

2.9 Flood Modelling Techniques 15

2.10 Hydrological And Hydraulic Modelling 16

2.11 Static And Dynamic Flood Models 17

2.12 GIS In Dynamic Flood Modelling 19

2.13 Watershed Modelling System (WMS) 20

2.14 Hec-Ras for Dynamic Flood Modelling 21

2.14.1 Applications of Saint Venant Equation in Flood Modelling 22

2.14.2 Applications of Diffusion Wave Equation in Flood Modelling 23

CHAPTER 3: MATERIALS AND METHODOLOGY 24

3.1 Study Area 24
3.2 Methodological Approach 25
3.3 Research Design 26
3.4 Research Parameters 27
3.5 Pre-Processing 27
3.5.1 DEM 28
3.5.2 Soil types 28
3.5.3 Precipitation 28
3.5.4 LULC 29
3.5.5 Ras Mapper and Ras Geometry 29
3.6 Post-Processing 30
3.6.1 1D Steady Flow 30
3.6.2 2D Unsteady Flow 30
3.6.3 Calibration And Validation 32
3.6.4 Flood Mapping 32
CHAPTER 4: RESULTS AND DISCUSSION 33
4.1 Rainfall Data Analysis 33
4.2 Flood Area Mapping 47
4.3 Flood Hazard Maps 51
4.4 Flood Risk Map 54
4.5 Water Surface Elevational (WSE) Maps 57
4.6 Flood Velocity Map 60
4.7 Model Calibration and Validation 61
4.8 Discussion 62
4.8.1 Effect of precipitation 63
4.8.2 Effect of LULC 63
4.8.3 Effect of DEM (Topography) 64
4.8.4 Effect of Manning's roughness 64
4.8.5 Model Calibration and Validation 64
4.8.6 Hydraulic Model 65
CHAPTER 5: CONCLUSION AND RECOMMENDATIONS 67
5.1 Conclusion 67
5.2 Recommendations 69
REFERENCES 71

LIST OF TABLES

Table 1 Shows parameter requirements. 27
Table 2 Precipitations against WSE, depth and water volume. 48
Table 3 Flood inundation and affected buildings. 48
Table 4 Distance travelled by flood from the reach along cross sections. 48
Table 5 Reference table for Manning roughness based on Chow-1959 (Soliman *et al*., 2022b). 61

LIST OF FIGURES

Figure 1. The study area map of Jukskei River, Johannesburg. 25
Figure 2. Detailed methodological flow chart. 26
Figure 3. Spatial variation of precipitation (mm) over 10 years interval for **A** (2000-2010) and **B** (2011-2020). 36
Figure 4. Maximum monthly precipitation from CHIRPS for a period of 20 years (2000-2020). 37
Figure 5. The three seasons (spring, summer, and winter) pattern with high rainfall in South Africa in A, B, C, and D. 41
Figure 6. Yearly precipitation for (A) maximum, (B) average and (C) minimum period of 20 years (2000 to 2020). 43
Figure 7. Map of DEM (SRTM) covering Alexandra. 44
Figure 8. Map of LULC covering Alexandra. 45
Figure 9. Map of soil types covering Alexandra. 46
Figure 10. Maximum flood depth map of Alexandra. 50
Figure 11. flood hazard map at 28mm of precipitation. 51
Figure 12. flood hazard map at 49.43mm of precipitation. 52
Figure 13. flood hazard map at 142.03mm of precipitation. 53
Figure 14. flood risk map at 28mm of precipitation. 54
Figure 15. flood risk map at 49.43mm of precipitation. 55
Figure 16. flood risk map at 142.03mm of precipitation. 56
Figure 17. Cross-section showing depth at different amounts of precipitation at **A** (28mm), **B** (49.43mm) and **C** (142.03mm) at Alexandra. 59
Figure 18. Flood hazard map of Alexandra, Johannesburg. 60
Figure 19. Validation imagery for the calibrated model. Source (Mawasha & Britz, 2022) 62

LIST OF EQUATIONS

Equation 1 Conservation of mass (continuity):..... 22
Equation 2 Conservation of momentum: 23
Equation 3 Manning's N value 29
Equation 4 Energy equation 30
Equation 5 Continuity Equation:..... 31
Equation 6 Momentum Equation: 31

LIST OF ACRONYMS

WMS	Watershed Modelling System
HEC	Hydrologic Engineering Centre
HEC-RAS	HEC river analysis system
HEC-HMS	HEC hydrologic modelling system
TIN	Triangular Irregular Network
DEM	Digital Elevation Model
SRTM	Shuttle Radar Topographic Mission
SPPs	Satellite Precipitation Products
FHI	Flood Hazard Index
MCDA	Multi-criteria Decision Analysis
SCS	Soil Conservation Service
WSE	Water Surface Elevation
NRCS	Natural Resources Conservation Service
GIS	Geographic Information Systems
LULC	Land Use Land Cover
OECD	Organisation for Economic Co-operation and Development
DFFE	Department of Forestry, Fisheries, and the Environment

CHAPTER 1: INTRODUCTION AND BACKGROUND

1.1 Introduction

A natural hazard involves the exposure of infrastructure and human population to catastrophic events of natural origin, that require management, mitigation, and impact reduction through prediction and control measures (Echogdali *et al*., 2018; Priya *et al*., 2020; Stoleriu *et al*., 2020). Of these, floods are one of the frequent disasters that affect South Africa almost every year. According to the World Bank Group, the increase in rainfall in South Africa and other various regions of the world by 2021 is due to erratic climate change, leading to a higher risk of damaging floods. Similarly, from the year 2000, about 73% of all floods have been categorized as riverine floods, 16% as flash floods, and just under 2% as coastal floods (with the remaining 9% not classified) as reported by OECD, 2016. This growing trend has been attributed to the development of flood zones, which has been identified as a key driver for the rising incidence and losses due to floods and is projected that exposures will increase significantly as a result. As a result, this situation poses an increased risk for developing and underdeveloped nations which underscores the significance of the interaction between runoff from rooftops to river channels in basin flooding. Understanding the physics involved in forecasting and partial control of flood impact through management, mitigation, and reduction measures can be modelled using suitable methods, including static and dynamic flood models (Yariyan *et al*., 2020). In addition, the integration of GIS technology into flood modelling has enhanced the ability to incorporate vast amounts of spatial and temporal data such as buildings, roads, and bridges, among others. These integrated models serve various purposes, such as precise flood prediction, the design of water structures, and the formulation of policies to prevent extreme value hydrological events (Hoseini, 2022). For instance, a study on the El Maleh River showed that using available hydrological data, models can forecast the likelihood of flooding at different frequencies and assess flood magnitude, including factors such as flood depth and velocity (Echogdali *et al*., 2018). In addition, the impact of the HEC-RAS flood prediction model for the Dikrong River also established the anticipated velocity and Water Surface Elevation (WSE) (Goswami *et al*., 2023).

1.2 Background

Flood is defined as the submersion of an area, typically low-lying, underwater. As estimated across Africa and the world, riverine floods are the most prevalent among pluvial (surface) floods and coastal (surge) floods. Research by Prastica *et al*., (2018) on Bengawan Solo River in Indonesia revealed that the floodwater loading exceeded the full bank capacity elevation of the river which could be attributed to increased riverbed height caused by changes in deposited materials and Land Use and Land Cover (LULC) in the river's vicinity. Moreover, according to (CIWEM, 2020), cities and urban areas in Africa are currently identified as high-risk zones for flood disasters. This is partly due to the rise of unplanned urbanization. Owing to this, in 2022, South Africa encountered one of the worst floods in its history, leading to over 400 fatalities during a single event resulting in the declaration of a state of emergency (IFRC, 2022). According to the (South African Weather Service, 2023), indications of increased aridity have been observed in the western regions of the Western Cape and Northern Cape Provinces in South Africa. However, drought conditions persisted in certain areas of the Eastern Cape Province especially Gauteng Province, which is densely populated and has been frequently experiencing flash-flood events during summer. One such event was the heavy rainfall on November 10, 2016, in Alexandra, where multiple media outlets reported the incident which led to the displacement of communities, six (6) casualties, and substantial damage to infrastructure (Floodlist, 2016).

Within the health sector, Theron *et al*., 2022 emphasized that severe weather events, including droughts, floods, wildfires, cyclones, and heatwaves, played a significant part in the emergence of life-threatening health conditions. These conditions encompass heat-related illnesses, traumatic injuries, exacerbations of asthma, behavioural health disorders, cardiovascular disease, and the escalation of vector-borne diseases such as malaria.

Despite the inability to eradicate flooding, incorporating adequate and efficient adaptive measures, including those focused on management plans, strategies, and disaster risk reduction is expected to enable developing countries to mitigate natural hazards and risks linked to severe climate patterns (Khan *et al*., 2021). The diverse social and economic impact, understanding dynamic floods is becoming

significantly important to developing countries due to the disaster afterwards. This means studying the complex and difficult mechanisms underlying dynamic flood events enough to predict them (Kim *et al*., 2020).

In most cases, prediction and vulnerability assessment aims to support hydrological and hydraulic characteristics for modelling flood risk. Although floods in headwater streams are primarily caused by high rainfall. In flood modelling, the magnitude and extent of floods may be affected by various factors such as evapotranspiration, temperature, landscape gradient, topography, soil infiltration rate, type of soil, land drainage, land use land cover, river channel alterations and soil saturation level including structures for water retention and flood control (Marr & Swemmer, 2023). However, the physics of flood modelling is categorized into two, namely static and dynamic for which various research with statistical and numerical methodologies have been developed over time. These include but are not limited to the analytic hierarchy process (AHP), frequency ratio (FR) model, analytic network process (ANP), hydrologic models, and hydraulic models by (Khadraoui *et al*., 2023; Singh *et al*., 2021; Yariyan *et al*., 2020). Regardless of technological advancement, the computer modelling tools, specifically the Hydrologic Engineering Centre - River Analysis System (HEC-RAS) in WMS, have proven to be reliable software for analysing channel flow and delineating floodplains in the field of river hydraulics (Razi *et al*., 2022).

1.3 Research Motivation

Dynamic flooding, among other natural disasters, involves the erosion and transport of soil material and debris within a watershed at varying velocities through river channels. This process generates forces, which interacts with man-made structures and river bends, affecting the flow dynamics and potential flood impacts. Although extensive research has been conducted on flood modelling globally. However, in the South African context, there is a lack of focus on studying flood risk and its quantitative consequences on informal settlements.

In South Africa, the emergence of informal settlements can be traced back to South Africa's industrialization in the early 1913s, coinciding with the surge in natural resource mining activities, which has since generated a myriad of interconnected

effects on both the environment and society. These effects persist today, manifesting in the proliferation of informal communities. As documented in the 2016 census conducted by Statistics South Africa, Johannesburg city hosts 333,570 informal settlements (shacks), accounting for 18% of the total population of Gauteng Province. Qumba and colleagues (2022) found through their research that following development in Johannesburg, approximately 35% of LULC was designated for settlements, demonstrating a substantial impact of urbanization and the presence of informal settlements on the city's landscape (Qumba *et al*., 2022) including Alexandra (commonly known as Alex), situated near the upper-class suburb of Sandton and adjacent to the Jukskei River watershed. The environmental and societal repercussions of urbanization are significant and include alterations in LULC, rising rainfall and temperatures (creating heat islands), changes in soil properties, shifts in the landscape, insufficient sanitation infrastructure, and associated health risks. Additionally, the modification of the terrain resulting from earth material displacement for industrial purposes and infrastructure development leads to shifts in soil characteristics and changes in precipitation patterns due to heat islands, potentially influencing both soil moisture levels and composition (Gurung *et al*., 2021).

In recent years, Alexandra, a town in South Africa's Gauteng province, has experienced a significant surge in flooding due to a rise in rainfall and the implications of climate change. As stated by the Greenbook report of South Africa CISR, Gauteng province experienced four severe floods between 2015 and 2018. The floods were responsible for the loss of 12 lives, the displacement of 165 people and extensive damage to infrastructure, homes and vehicles. Numerous efforts have been made to assess the flood impacts in Gauteng Province, particularly in areas like Alexandra within Johannesburg city. Mawasha & Britz, (2022) carried out a study in Alexandra to evaluate the effects of urban flood hazards resulting from LULC changes over a 28-year period within the catchment. The study also considered flood velocity and depth associated with river discharge. Their findings indicated a rapid expansion of the community, accompanied by a doubling in depth-velocity over the specified period. This issue has raised concerns among governing bodies and the community. Observations from local authorities indicate that

littering and illegal dumping of waste into the Jukskei River contribute to the flooding. However, the extent and severity of flooding in Alexandra township remain uncertain, as no attempt has been made to measure the impact caused by precipitation such as affected settlements, water depth, velocities, and inundations, along with other relevant parameters. Thus, the objective of this research is to quantify the impact of dynamic flooding using the HEC-RAS model over a 20-year period (2000-2020) along the Jukskei River in Alexandra, Johannesburg City.

1.4 Aim and Objectives

1.4.1 Aim

This study aims to develop a GIS-based dynamic flood modelling system to map flood-inundated areas along Jukskei River from Bertrams to Waterfall City, Midrand, Johannesburg, South Africa.

1.4.2 Objectives

The objectives of this research are:

1. To investigate the spatial and temporal precipitation of satellite datasets for the period between 2000 to 2020.
2. To simulate flood hazards using a calibrated and validated HEC-RAS model.
3. To develop a flood risk map.

1.5 Layout Of Thesis

The thesis comprises five key chapters. The first chapter provides a comprehensive overview of flood hazards, exploring their global, African, and South African implications. It includes a synthesis of existing literature and outlines the research background, problem statement, objectives, significance, and scope. The second chapter offers a concise overview of published literature on natural hazards, with a focus on floods and their management, as well as showcasing statistical and technological approaches for flood modelling and prediction. The third chapter details the adopted study procedure, materials, and methods applied in the studies. The fourth chapter is dedicated to presenting research findings and facilitating

discussions, while the fifth chapter delves into the practical implications of the research, addressing its environmental, economic, and societal impacts.

CHAPTER 2: LITERATURE REVIEW

2.1 Natural Disasters

Natural disasters have been a significant concern for scholars and practitioners across various disciplines for many years (Saleh & Bba, n.d.). The increase in the intensity and occurrence of natural calamities such as droughts, floods, and environmental crises has been attributed to the effects of climate change and extreme weather phenomena (W. Chen *et al*., 2020; Kao *et al*., 2017). These disasters have had profound impacts on both human and natural environments, leading to substantial economic damages and loss of property and life (Bhardwaj *et al*., 2021; Schardong *et al*., 2019; B. Zhang *et al*., 2021). The occurrence of natural disasters beyond the levels of socio-economic planning has been linked to the unpredictable nature of climate, including more frequent and intense extremes (Nastos & Dalezios, 2016). The impacts of natural disasters extend beyond immediate damages, affecting ecosystem services, urban infrastructure, and the health of communities (Irwin *et al*., 2016; Sandifer *et al*., 2017). Furthermore, vulnerability of specific groups, such as women, to the economic impacts of natural disasters has been highlighted as an area requiring further study (Khaskhelly *et al*., 2021). As a response to these challenges, disaster risk reduction strategies have been explored, including the implementation of ecosystem-based approaches to safeguard societies from the negative impacts of disasters and climate change (Monty *et al*., n.d.). Additionally, community-centric methods for disaster risk reduction and early warning systems have been proposed to improve societal resilience (Baudoin *et al*., 2016). Efforts to minimise the effects of natural disasters have also involved the socialization of disaster mitigation and the development of adaptive management mechanisms to address the risks posed by climate change (Kirana & Sufyan Bature, 2022; Nikitin *et al*., 2022). Historical disaster research has been identified as a valuable tool for contributing to reconstruction efforts, management, and mitigation, as well as avoiding disasters among at-risk populations (Ahmad *et al*., 2021).

2.2 Influence of Climate Change on Floods

Climate change has contributed to a rise in the severity and frequency of natural hazard-related disasters, resulting in significant impacts on cities and historic areas (Lindner *et al*., 2021; Yigitcanlar *et al*., 2022). The negative impacts of natural disasters and climate change on the economy have been widely acknowledged (J. Fang *et al*., 2019). However, it is crucial to highlight that vulnerability is a primary driver of disasters, and while climate change impacts hazards, it is not the sole or most fundamental contributor to disaster risk (Kelman, 2017; Kelman *et al*., 2015). Climate change, particularly through extreme weather events, has been identified as a factor increasing the impacts and risk of disasters (Nemakonde & Van Niekerk, 2023). Disparities exist in understanding the interaction involving climate change and non-atmospheric natural disasters, highlighting the need for further research and knowledge dissemination (Phillips *et al*., 2015). The implications of climate change are becoming progressively visible through more severe wildfires, hurricanes, and flooding (Hai & Perlman, 2022). In relation to industrial supply chains, climate change adaptation and disaster reduction risk present significant challenges, necessitating the development of integrated frameworks (L.-L. Chen & Tseng, 2019). Agriculture and fishery enterprises are experiencing fluctuating impacts because of variations in precipitation, temperature, and the development of new types of natural hazards (Do *et al*., 2021). Small islands are facing the increasing impact and frequency of climate change and natural disasters, prompting the need for practical fiscal policy frameworks (Nakatani, 2019). The influence of climate change on extreme weather events has led to rising frequency and intensity, impacting the stock market and contributing to increased volatility (U-Din *et al*., 2022).

2.3 Floods

Floods are a significant concern in relation to climate change, with studies indicating both increases and decreases in river floods as climate patterns change Blöschl *et al*. (2019). The severity and frequency of floods have been observed to be on the rise, attributed to climate change and increasing exposure (Bruijn *et al*., 2022; Alifu *et al*., 2022). Extreme flood disasters have been found to have serious impacts on the environment and local ecology, emphasizing the comprehensive

impact and assessment of such events (Qian *et al*., 2022). The nexus between flood disaster risk, climate change, and food security has been studied, highlighting the interconnectedness of these factors in regions such as Northern Ghana (Atanga & Tankpa, 2021). Additionally, the social acceptance of flood control methods under climate change has been explored, emphasizing the need for contingent valuation methods to assess the effectiveness of such strategies (Maghsood *et al*., 2019). Furthermore, the seasonality nature of climatic factors of flood variations in the United States has been investigated, shedding light on the complex interplay between climate patterns and flood occurrences (Dickinson *et al*., 2019). Collectively, they underline the diversity of impacts from floods about to climate change, encompassing environmental, social, and economic dimensions. The recommendations emphasise the need to undertake a comprehensive assessment, resilient management, and integration of flood protection strategies in efforts to adapt to climate change.

2.4 Causes And Factors Influencing Floods

The causes and factors influencing floods are multifaceted and encompass a wide range of natural and human-induced elements. Natural factors contributing to floods include high tides, high flood intensity, and heavy rainfall (HIRCA & SÖNMEZ, 2019). Additionally, heavy and sudden rainfalls, snowmelt, and meteorological factors have been identified as key natural contributors to flooding (Hannum *et al*., 2022; Toonen, 2019). Changes in watershed characteristics, such as rainfall intensity, land use, and slope, have also been found to influence flood characteristics (H. Wang *et al*., 2022). Moreover, shifts in flood generation processes have been observed to exacerbate regional flood anomalies, leading to biases in flood risk estimates (Supriatna *et al*., 2022).

Human-induced factors, such as blocked or damaged drainage channels, improper land use, and heavy deforestation, have been recognized as significant contributors to flood occurrences (Odm *et al*., 2022). Deforestation has caused increased the risk of flooding and soil erosion (X. Yang *et al*., 2016). Land use/cover change has been highlighted as a crucial factor influencing flood characteristics and the hydrological process (Q. Yang *et al*., 2020a). Furthermore, urbanization and limitations of

municipal drainage systems have been identified as factors contributing to urban flooding (Alhassan, 2020). The socio-economic characteristics of farmers, institutional factors, and farm-level factors have been found to influence their response to flood events, with variations based on specific regions or countries (Santosa, 2023). Additionally, economic factors have been shown to significantly influence the formation of flood resilience in urban communities (Morote & Hernández, 2020). Climate change has been recognized as a significant variable influencing flood risks and flood potential (S. Huang *et al*., 2021; Supriatna *et al*., 2022). The interdependence of influencing factors and their indirect effects on flood inundation have been highlighted, emphasizing the complexity of flood disaster-causing factor chains (X. D. Huang *et al*., 2018). Moreover, the temporal and spatial patterns in nonstationary flood frequency have been linked to the forest landscape and rainfall, indicating the pivotal role of these factors in triggering flood event alterations.

2.5 Impacts Of Flooding

The effects of flooding are diverse and encompass various aspects of human life, the environment, and infrastructure. Coastal flooding, intensified by climate change, is predicted to disproportionately impact people living in river deltas, leading to significant social and economic consequences (Edmonds *et al*., 2020). Floods can have ambiguous impacts, as they are natural phenomena, and ecosystems in floodplains are adapted to flooding, although adverse effects can still occur (Thieken *et al*., 2016). Flash flood events, caused by intense precipitation, disrupt road transportation and are expected to continue, affecting mobility and economic activities (Ntakiyimana *et al*., 2022). Flood risk continues to rise, and infrastructure and communities are being challenged by the negative impact of climate change (W. Wang *et al*., 2020). Floods affect natural habitats and ecosystems in particular, which has a major impact on the environment and ecology of regions (Yu *et al*., 2022). Additionally, floods can affect critical infrastructure, disrupt transportation networks, and lead to economic and societal damage, including loss of lives (Quintero *et al*., 2018). The agricultural sector is also significantly impacted by floods, causing over-saturation, infertility, and soil

erosion, leading to damage to crop fields and affecting food security (Aldardasawi & Eren, 2021). Furthermore, floods can have immediate effects on transportation systems by means of physical destruction of infrastructure and indirect effects due to a cascade of adverse impacts, severely impacting critical infrastructure (Rebally *et al*., 2021). Flooding can also affect city infrastructure, interrupting services and impacting the economy for prolonged periods (Echendu, 2020). The influence of flooding on the developed environment includes damage to human shelters, roads, bridges, and dams, affecting the structural integrity of communities (Dube *et al*., 2018). The environmental impact of flooding includes damage to natural habitats, public health risks, and the need for flood protection measures to mitigate adverse effects on the environment and public health (Šoltész *et al*., 2021). Moreover, flooding can increase flood depths in urban areas, leading to property damage and affecting the resilience of urban communities (Muthusamy *et al*., 2019). The tangible and intangible flood damage evaluation includes assessing changes in road networks, safe havens, and flood warnings to mitigate potential loss of property and life (Frongia *et al*., 2016).

2.6 Flood Management Approaches

Flood management approaches have indeed evolved to encompass a broad range of techniques aimed at enhancing resilience and minimising the impacts of flooding (Hegger *et al*., 2016). The coordination, alignment, and diversification of flood risk management techniques have been proposed to enhance urban agglomerations' resilience to flood risks, modifying strategies to the intensity and various forms of flooding, such as coastal, fluvial, flash floods, and pluvial, and focusing on both probability and consequence-reducing approaches. A paradigm shifts from flood defence to increasingly dynamic approaches, embedding resilience into the management of flood risk has been observed, stressing the necessity for an extensive understanding of flooding and its impacts (Mehring *et al*., 2022). This shift involves a move towards managing flooding in a more adaptive manner, considering in-the-moment impacts and integrating resilience into flood risk management. A critical study of flood risk control and selecting appropriate strategies highlighted the distinction between indirect and direct implications of

floods, emphasizing the need to address both types of impacts in flood risk management planning (Tariq *et al*., 2020). This method recognizes the importance of mitigating the consequences of flooding and acknowledges that entirely preventing floods is not always feasible. Integrated flood management approaches, flood resilience systems, managing green open spaces, and sustainable drainage systems have been proposed as part of efforts to minimize flood risk and improve welfare in highly demographic flood-prone areas (Hegger *et al*., 2016). These approaches aim to integrate various measures to enhance flood endurance and reduce the impacts of flooding on communities. Dynamic flood risk mitigation planning utilizing a complete flood risk framework has been proposed to bridge the gap between flood defence management procedures and spatial preparation practice, aiming to reconcile different approaches and enhance flood risk management effectiveness (Klijn *et al*., 2015). The Japanese government adopted a basin-wide and trans-sectoral strategy as part of its comprehensive management of floods to accelerate planning for increasingly severe floods caused by climate change (Yamamoto *et al*., 2021). Their approach emphasizes the importance of an integrated and comprehensive flood management approach, taking into consideration the likely influence of climate change on flood risk.

2.7 Geospatial Technologies in Flood Management

Geospatial technologies have significantly advanced flood management strategies, offering valuable tools for flood risk assessment, mapping, and mitigation. The incorporation of remote sensing, geospatial analysis, and GIS has revolutionized flood management by providing innovative solutions for flood vulnerability assessment, flood mapping, and disaster risk reduction. For instance, studies such as "Artificial Intelligence in Geospatial Analysis for Flood Vulnerability Assessment" (Tamiru & Dinka, 2021) and "Development of Digital Elevation Model (DEM) for the assessment of flood vulnerable areas" (Sudalaimuthu *et al*., 2022) have proved the application of geospatial approaches, including remote sensing and GIS, for flood vulnerability assessment and the development of digital elevation models to identify flood-prone areas. These approaches integrate multi-criteria decision analysis tools and hydrological factors to analyse parameters

influencing urban floods. Furthermore, research such as "Assessment of runoff potential for disaster risk reduction using geospatial technology" (Oladotun, 2022) and "A WEB-GIS PLATFORM FOR FLOODS RISK MAPPING" (A Web-GIS Platform for Floods Risk Mapping Case Study: The Floodplain of Khartoum State, 2022) has emphasized the effectiveness of geospatial technology for flood prediction, disaster risk reduction, and flood risk mapping. These studies highlight the importance of hydrologic assessment techniques and geospatial technology for effective flood forecasting and management. Moreover, the application of free geospatial technologies for coastal mapping asset and management (Paul *et al*., 2022), 3D city models for evaluating flash flood risks (Kalbani & Rahman, 2022), and the application of geospatial big data (Li *et al*., 2021) have demonstrated the versatility and the relevance of geospatial technologies in diverse flood management contexts. Additionally, the integration of optical earth observation and SAR with hydraulic modelling for mapping floods and their impact assessment (Psomiadis *et al*., 2020a) and the development of a combined GIS multi-criteria decision-making approach for dynamic flood mapping (Y. Wang *et al*., 2019) have showcased the integrated use of remote sensing products and hydraulic simulation for flood impact estimation and flood dynamic mapping. In terms of emerging technologies, the evaluation of hydrological models such as WATFLOOD, HBV-EC, HSPF, and HEC-HMS for functional flood prediction in a Canadian Prairie catchment demonstrates the use of hydrological models as operational flood forecasting tools (Unduche *et al*., 2018). Additionally, the integration of hydrological modelling and LULC change forecasting for determining the impact of LULC modification on flow rate in Sari Watershed, Sumbawa Island, Indonesia showcases the power of CA-Markov and GIS/ remote sensing technology for evaluating LULC dynamics (Setiawan & Nandini, 2022). Furthermore, the use of HEC-RAS and HEC-HMS models in forecasting flood extent areas of Attanagalu Oya highlights the efficiency of these models for flood analysis (Anuruddhika *et al*., 2022). Additionally, the combination of Monte Carlo simulation, flood inundation modelling, fuzzy vertex analysis, and depth damage function derivation for quantitative microbial risk assessment and urban sewer flooding demonstrates the integration of multiple methods for comprehensive flood analysis (Addison-

Atkinson *et al*., 2022). Moreover, the relevance of socio-hydrological modelling for understanding flood-risk trends is demonstrated by the comparison of the technological systems and resilience of green (Ciullo *et al*., 2017). The research emphasizes that flood risks are dynamically evolving with changing determinants, such as climate and environmental changes, highlighting the unsteady characteristics of flood risks (Zischg, 2022). The assessment of flood hazards in the Yasooj region, Iran, applying multi-criteria decision assessment and GIS demonstrates the application of AHP and GIS approaches for flood hazard potential assessment (Rahmati *et al*., 2016). Most importantly, the study and use of important technologies for the unsteady management of basin water levels in flood season outlines major real-time operating technologies for the unsteady management of basin water levels (J. Zhang *et al*., 2021). Moreover, the assessment of flood coverage using integrated 1D/2D hydraulic modelling in hilly watersheds bordering the coastline of Southeast China demonstrates the effectiveness of the coupled 1D/2D model in studying flood propagation attributes (W. Zhang *et al*., 2020). The Aqueduct Global Flood Analyzer for flood risk assessment in Zimbabwe demonstrates the use of advanced tools for flood risk analysis (Samu & Akıntuğ, 2020).

2.8 RStudio for Geospatial Analysis

RStudio is a development environment that is integrated (IDE) for the R statistical language, playing a crucial role in geospatial and statistical techniques. has been instrumental in enabling researchers to access and analyse geospatial data. It has been used in conjunction with statistical software packages such as INLA for spatiotemporal mapping of major trauma, demonstrating its role in facilitating complex statistical modelling and analysis in geospatial research (Beck *et al*., 2021). Additionally, RStudio has been employed in the teaching of introductory statistical classes, indicating its significance in statistical education and its positive association with students' attitudes toward statistics (Silva & Moura, 2020).

2.8.1 Understanding R-Value in Spatial and Temporal Analysis

The Pearson correlation coefficient (r) is a measure in statistics applied to evaluate the direction and strength of a linear correlation involving two independent parameters. The r value varies between -1 and 1, with 1 indicating an ideal positive linear connection, -1 suggesting a complete negative linear relationship, and 0 representing no linear association between the parameters (Schober & Schwarte, 2018). The impact of the r value reflects the strength of the correlation, with values closer to 1 or -1 suggesting a more robust correlation (Kiss *et al*., 2018). For example, $0 \leq r \leq 0.69$ indicates a little correlation, $0.70 \leq r \leq 0.89$ indicates a medium correlation, and $r > 0.90$ indicates a strong connection (Kiss *et al*., 2018). Whenever the r value is 0, it suggests no linear relationship between the variables (Schober & Schwarte, 2018).

2.8.2 The Role of P-Value in Spatial and Temporal Data Analysis

The p-value in statistics is a metric that indicates how strong the evidence is as opposed to the null assumption. It represents the likelihood of detecting an effect at least as strong as the one noted, provided the null assumption is accurate, and a low p-value indicates that the noted data is not probable under the null assumption, resulting in the dismissal of the null assumption in support of the alternative assumption (Greenland *et al*., 2016). For instance, given that the p-value falls beneath a preset significance level (e.g., 0.05), it is considered statistically significant, suggesting that the outcomes are unlikely to have happened by chance (Cordell *et al*., 2020).

2.9 Flood Modelling Techniques

Modelling is the act of developing a simplified representation or simulation of a system, phenomenon, or process to understand, analyse, predict, or control its behaviour (Everett *et al*., 2017). In the field of remote sensing image classification, modelling encompasses the improvement of algorithms and computational models that will analyse and classify remote sensing imagery based on specific features and patterns. This involves creating models that can effectively interpret and classify remote sensing data, contributing to applications such as environmental monitoring,

natural resource management, and land cover mapping (Ishikawa *et al*., 2023). Flood modelling is the application of mathematical, computational, and statistical tools to simulate and forecast the patterns of floods in various environments. It encompasses a wide range of methodologies and technologies aimed at understanding, predicting, and managing flood events. Flood modelling includes the development of predictive models, the investigation of flood risk, and the evaluation of potential flood impacts. In addition to the application of federated learning for flood forecasting (Farooq *et al*., 2023), studies report the use of stochastic conflict resolution optimization models for flood control (Nematollahi *et al*., 2022), and the assessment of flood hazard mapping methods (Bezak *et al*., 2018). The application of deep learning for flood prediction dependent on weather parameters (Sankaranarayanan *et al*., 2020), the development of spatial flood risk evaluation frameworks (Luu *et al*., 2020), and the combination of optical earth observation and SAR with hydrodynamic simulation for impact assessment and flood mapping (Psomiadis *et al*., 2020b) are noteworthy developments; notwithstanding the challenges in modelling and predicting droughts and floods (Brunner *et al*., 2021), the analysis of flood risk mapping applying analytic hierarchy process and machine learning models (Q. Yang *et al*., 2020b), and the application of flood forecasting and uncertainty assessment using machine learning (Gude *et al*., 2020).

2.10 Hydrological And Hydraulic Modelling

Hydrologic flood modelling and hydraulic flood modelling are two distinct, yet interconnected approaches used in flood analysis and management. Hydrological flood modelling involves the use of computational models to simulate and analyse the processes that lead to flooding, focusing on the behaviour of water within catchments, watersheds, and river basins. It encompasses the study of precipitation, evapotranspiration, infiltration, runoff, and streamflow to understand the dynamics of water movement and the factors contributing to flood events (Dept. of Transport and Main Roads & State of QLD, 2019; Hoseini *et al*., 2017). Hydrological floods are governed by a range of factors, including soil textural properties, rainfall-runoff characteristics, flood peak distributions, flood scaling properties, post-event

analysis, urbanization, groundwater flood hazards, organic carbon concentrations, precipitation inputs, and watershed characteristics. These properties play a critical function in understanding and predicting the behaviour of floods in various hydrological settings (Arafat *et al*., 2020; Garvelmann *et al*., 2015).

Furthermore, hydraulic flood modelling incorporates the application of computational models to simulate the behaviour of floodwaters within river channels, floodplains, and urban areas. It focuses on the hydraulic aspects of floods, such as flow velocities, water depths, and flood extents (Kemter *et al*., 2020). Hydraulic models are used to predict how floodwaters propagate through river systems and urban areas, providing valuable insights for flood risk management and assessment. The properties of hydraulic flooding are caused by different factors, such as the hydraulic characteristics of the water movement, the topography of the affected region, the velocity and depth of the floodwaters, and the duration of the flooding event. Additionally, the hydraulic properties of the floodwaters, such as their flow dynamics, sediment transport, and erosional potential, perform a significant role in analysing the impact and magnitude of hydraulic flooding (Cui *et al*., 2019; Pekárová *et al*., 2016). The reaction of rivers with ecological factors is a critical aspect of hydraulic modelling, especially in balancing frictional losses with gravity-induced flow in the river reach. Manning's equation is frequently employed to achieve equilibrium in river systems, even though it adopts a simplified method for determining parameters like stage constant roughness and velocity-depth exponents. It underscores the significance of establishing ethical values for habitat suitability according to ecosystem biology, particularly in mountainous water bodies characterized by unique ecological factors such as hydrological alterations (Książek *et al*., 2019).

2.11 Static And Dynamic Flood Models

A static flood model is a simplified representation of flood hazard that does not account for dynamic changes in flood conditions over time. It typically assumes a fixed water level or flood extent, often based on a specific extreme event or scenario. Static flood models are restricted in their capability to capture the complicated and evolving nature of flood hazards, as they do not consider spatial

or temporal variations in flood conditions resulting from diverse flooding factors such as riverine discharge and storm tides (Ramirez *et al*., 2016). For instance, (Vousdoukas *et al*., 2016) discuss the limitations of the static approach in coastal flood hazard mapping, highlighting that it can lead to significant exaggeration of flood inundation in comparison with dedicated hydraulic models, particularly in more level terrains. Similarly, (Stephens *et al*., 2021) noted that static models anticipate flood inundation which is only defined by terrain and that the highest storm-tide river heights are preserved for an unlimited time frame, overlooking the dynamic nature of flood procedures. Rucker *et al*., 2021 discussed the reduction of instantaneous coastal flooding forecasting for decision-making support, noting that the static method may be adequate for research of flooding caused by a surge in storm, in relation to the spatial scales of the challenge. (Didier *et al*., 2019) compared bathtub and numerical modelling in an open estuary for coastal flood mapping. The study concluded that the bathtub approach resulted in significant differences in flood extent compared to numerical modelling, highlighting the limitations of static flood modelling in capturing the complexity of flood dynamics. Dynamic flood models are computational models that simulate the evolving behaviour of floods over time, accounting for changes in water levels, flow velocities, and flood extents. These models consider the dynamic nature of flood events, capturing the temporal and spatial variations in flood conditions resulting from diverse flooding factors such as riverine flow rate, storm tides, and other hydrological processes (Zischg, 2022). In particular, (Wu *et al*., 2019) established a dynamic 3D model simulation for flood risk integrating hydrodynamic models and spatio-temporal GIS. This model provides refined, dynamic, real-time, and quantitative information for decisions by simulating flood progression, evaluating hydraulic engineering facilities, and managing disasters. (Van Khanh Triet *et al*., 2017) investigated a dyke construction impact in the Vietnamese Mekong Delta on flood hazard. The research employed an upgraded model to assess how the construction of elevated embankments affects flood characteristics. The updated model was found to be reliable and produced realistic inundation dynamics, providing valuable insights into the shifting flood hazard downstream due to dyke development. Despite technological advancement, various researchers have

conducted studies on hydrologic and hydraulic modelling using different methods. The following are studies by some researchers (Ahmadisharaf & Kalyanapu, 2019) that developed a hydraulic and hydrologic coupled probabilistic model framework to examine the unknowns of flood loss projections. The study utilized a hydraulic model that operates in two dimensions and dynamically simulates the extent of flooding. Mahapatra *et al*., 2022 conducted dynamic flow assessment applying hydrodynamic and hydrological models for instantaneous flood prediction in the Vamsadhara River reservoir. Ahmadisharaf *et al*., 2017 also implemented a long-term viability-based flood hazard mapping framework for the Swannanoa River catchment. The framework utilized a hydraulic model of unsteady two-dimension for flood and simulation. In their research, Sathya and colleagues employed the HEC-RAS one-dimensional unsteady flow model to replicate water depth and flow velocity, specifically for reconstructing flash flood disasters in the Sempor River (Sathya *et al*., 2021). Studies conducted by (Amarnath & Thatikonda, 2020) converted flood discharge data to water level projections by applying an unsteady and steady flow hydrodynamic model, such as HEC-RAS.

2.12 GIS In Dynamic Flood Modelling

GIS plays a critical role in dynamic flood modelling, offering a wide range of advantages in flood susceptibility analysis, flood hazard assessment, and flood risk control (Y. Wang *et al*., 2019). By integrating spatial data, GIS provides a comprehensive platform for understanding and visualizing the flood extent spatially, identifying flood-prone regions, and supporting effective decision-making for flood risk reduction (Y. Wang *et al*., 2019).

One of the key advantages of GIS in dynamic flood modelling is its capability to consider comprehensive spatial data, including topography, land use, soil type, and hydrological features. Swain and colleagues employed Geographic Information Systems (GIS) to perform flood susceptibility mapping using the Analytic Hierarchy Process (AHP) technique. Their study illustrates the significance of each factor in prioritizing flood susceptibility (Swain *et al*., 2020). This approach allowed for the integration of diverse spatial data, providing an extensive knowledge of the drivers leading to flood susceptibility and hazard. GIS also

enables spatial analysis and visualization, allowing for the detection of high-risk flood areas and flood extent visualization. (Sofia *et al*., 2017) conducted a study on flood dynamics in urbanized landscapes, highlighting the statistical contributions of both climate and land use to the improvement in the number of flooded regions. Furthermore, GIS-based spatial multi-index models have been applied to assess flood risk in large river basins, contributing to further scientific study on flood mitigation and prediction (D. Zhang *et al*., 2020). The integration of GIS with hydraulic and hydrological models has enabled the assessment of flood hazards, including flood susceptibility mapping, flood risk analysis, and floodplain delineation, providing valuable insights for flood planning and management. In addition, GIS has been instrumental in improving flood inundation mapping, allowing for the visualization and analysis of the spatial extent of floods. (Dang & Kumar, 2017) applied GIS-based hydrological modelling for analysis of flood risk in Ho Chi Minh City, Vietnam, demonstrating the effectiveness of GIS in mapping and assessing the impacts of flooding. The spatial visualization capabilities of GIS have facilitated the development of flood extent maps, which are essential for understanding flood impacts and planning prevention measures. Moreover, GIS has been used to analyse the interactions between urbanization and flood risk, providing valuable insights for risk assessment and flood vulnerability mapping. (Raufu *et al*., n.d.) applied remote sensing and GIS to assess and present outcomes on flood risk, supporting effective and immediate decision-making on floods. The integration of GIS with remote sensing data has enhanced the accuracy and reliability of flood modelling and mapping, facilitating a more comprehensive understanding of flood dynamics.

2.13 Watershed Modelling System (WMS)

The WMS is a comprehensive application tool used for preparing and running hydrological models such as HSPF and HEC-HMS (Bailey *et al*., 2017). It provides capabilities for automating watershed delineation, parameter calculation, and hydrologic modelling program execution, as well as for viewing the results of these programs. Additionally, the WMS has been utilized for manipulating Digital Elevation Models (DEMs) and generating necessary data for watershed modelling.

Furthermore, the code applies the Engineered Resilient Systems (ERS) XmsMesh meshing applications, developed by Aquaveo, to develop a mesh for watersheds that conforms to the geometry and spacing for each catchment within a watershed shapefile (Mcknight *et al*., 2019). The use of WMS in watershed modelling has been instrumental in simulating flow, understanding rainfall-runoff processes, and assessing the potential for urban flooding and flash floods in watersheds. By incorporating GIS with other software, WMS has been capable of capturing the hydrological processes that develop in a watershed region (Rauf *et al*., 2021). Moreover, the potential of a model to simulate the watershed structure relies on how well-watershed procedures are defined by the model and how the input of the model determines the effectiveness of the watershed mechanism. (Alsilibe & Bene, 2022). Furthermore, WMS inculpates a range of leading river storm and hydraulics drain models, consisting of HSPF, EPA SWMM, CE-QUAL-W2, HEC-RAS, NFF, GSSHA, HEC-HMS, TR-20, Rational MODRAT, HEC-1, TR-55, SMPDBK, and others (Environmental Modeling Research Laboratory of Brigham Young University & Aquaveo LLC, 2016).

2.14 Hec-Ras for Dynamic Flood Modelling

The Hydrologic Engineering Centre-River Analysis System (HEC-RAS) is a widely known and extensively used model for assessing floods in both scientific research and practical applications (Costabile *et al*., 2020). It was invented by the US Army Corps of Engineers and is employed for various flood modelling purposes, including calculating breach hydrographs (Sattar *et al*., 2020). HEC-RAS can simulate super-elevation of flow along reach bends, multidirectional flows, and sediment entrainment in dynamic flow modelling, making it suitable for modelling sudden-onset floods such as glacial lake outburst floods (GLOFs) (Hagg *et al*., 2021; Kougkoulos *et al*., 2018). Additionally, it also indicates that dynamic flow modelling is likely to involve sediment entrainment, which could improve the accuracy of flood models (Kougkoulos *et al*., 2018). The software is extensively accepted for its proficiency in analysing river systems and has currently added features such as 1D-2D river-floodplain coupling, making it a valuable tool for flood modelling and risk assessment (Roy *et al*., 2021). HEC-RAS has been applied

to develop flood extent maps, assess flood-prone areas, and estimate economic losses in affected areas (Marselina *et al*., 2022; Razi *et al*., 2023; Riswanto & Nanda, 2023). Furthermore, it is utilized for flood forecasting when data is limited, or gauging stations are not available in the study area (T. H. Yang & Liu, 2020). The model has also been applied to simulate accurate river flow, particularly for flood incidents, and to analyse hydraulic systems and perform development planning (Armain *et al*., 2021; Deshays *et al*., 2021). In all, HEC-RAS is a versatile and extensively used application for modelling hydraulic floods, offering capabilities for flood mapping, breach hydrograph calculation, sediment entrainment simulation, and flood risk assessment. Its applications range from simulating sudden-onset floods to analysing channel flows and flood inundation, making it an indispensable tool for water resources managers and hydrologists. Additionally, the software enables quasi-unsteady flow modelling, which is a simplified flow modelling in dynamic conditions based on the energy equation (Dysarz, 2018). Users can simulate unsteady flow by applying optionally the Saint Venant computations or diffusion wave formulae using an inherent restricted volume technique (Dhungel *et al*., 2019).

2.14.1 Applications of Saint Venant Equation in Flood Modelling

The Saint Venant equation, additionally known as the shallow water equations (SWEs), is extensively used to model urban floods with complicated velocity trends and river depth variations. It is developed on the principles of protection of momentum and mass and is particularly suitable for modelling unsteady flow in rivers and open channels (Gillies & Smith, 2015). The SWEs are fundamental for simulating the spatially varied dynamic flow in open channels and are mostly used as the governing equations for this purpose (Sh Abed *et al*., 2020). Additionally, the Saint Venant equations are crucial for studying water flow in open channels, simulating flood propagation in rivers, and analysing flood inundation in urban areas (Diogo & do Carmo, 2019).

Equation 1 Conservation of mass (continuity):

$$\frac{\partial Q}{\partial x} + \frac{\partial A}{\partial t} + I = 0 \qquad \text{Equation 1}$$

(Gillies & Smith, 2015)

Equation 2 Conservation of momentum:

$$\frac{1}{Ag}\frac{\partial Q}{\partial t} + \frac{2Q}{A^2 g}\frac{\partial Q}{\partial x} + \left(1 - \frac{Q^2 T}{A^3 g}\right)\frac{\partial y}{\partial x} = S_0 - S_f \qquad \text{Equation 2}$$

(Gillies & Smith, 2015)

where Q is the discharge ($m^3 s^{-1}$), A is the cross-sectional area of flow (m^2), x is the distance (m), t is time (s), I is the soil infiltration rate ($m^3 m^{-2} s^{-1}$), y is the depth of flow (m), g is the acceleration due to gravity ($m s^{-2}$) and S_0 and S_f are the bed slope and friction slope (dimensionless), respectively. (Gillies & Smith, 2015b)

2.14.2 Applications of Diffusion Wave Equation in Flood Modelling

This is another approach used in dynamic flood modelling. It is known for its ability to capture the process of flood propagation in rivers due to changes in discharge or water level (Haba, 2020). The diffusion wave equation is particularly useful for modelling the movement of substances taking into account anisotropic diffusion, making it more suitable for modelling pollutant movement related to floods in urban or farmland environments (S. Fang *et al.*, 2022). Furthermore, the diffusion wave equation is employed to better capture momentum losses along segments of channels, especially in large, gently sloped channels, where the kinematic wave equation may not match flood wave timings effectively (Ghobadian & Khalaj, 2015).

CHAPTER 3: MATERIALS AND METHODOLOGY

3.1 Study Area

Alexandra is a township in the City of Johannesburg located at Lat -26.103705, Lon 28.106941 and is predominantly black African (99%). The township's total population was estimated at 179,524 people, spread over an area of 26,000 km^2, according to the 2011 census. The township, often referred to as Alex, is close to Sandton, one of the more affluent suburbs in the area, as well as Marlboro, Wynberg and Kelvin. Despite its proximity to wealthier neighbourhoods, Alex is known to be one of the most impoverished areas of the city, with many residents living in informal settlements like kiosks popularly called "shacks" (Alexandra, South Africa - Wikipedia, n.d.). The flood-prone town of Alexandra, located approximately 14 km from Johannesburg in the northeast along the Jukskei River, presents a critical area for flood studies. The catchment area of the Jukskei River, one of the largest in the Gauteng province, encompasses densely populated, industrialized, and urbanized regions, with the northern belt featuring urbanized and farming activities. The area experiences a dry and sunny climate, with maximum rainfall occurring in summer and minimum in spring. The study area, stretching from Alexandra to Waterfall City in Midrand, encounters rainfall primarily between September and March, constituting 70% to 90% of the rainy season. The mean temperature ranges from 16°C to 25°C in summer and from 13°C to below freezing in winter. The Jukskei River, approximately 394 km long, originates from Bertram in Johannesburg and flows through Alexandra Township to a point approximately 7 km above Lanseria International Airport, North-East of Johannesburg. The flooding in Alexandra is attributed to factors such as informal settlement encroachment, inflows from the main city, low floodplain, low gradient, and clayey soil (Plinthosols) along the river.

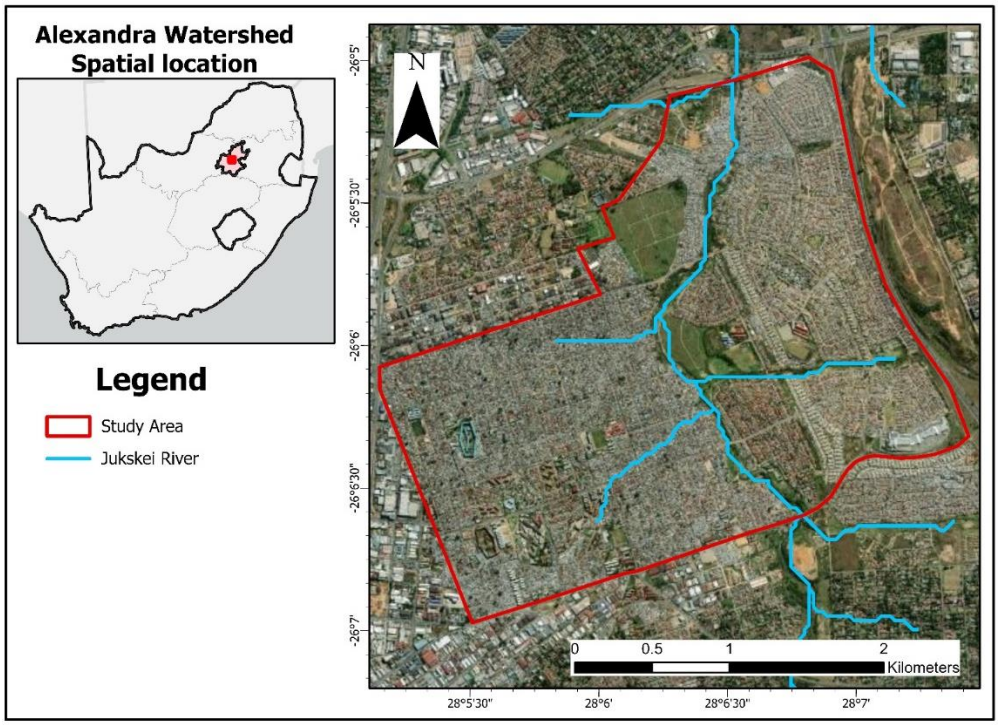

Figure 1. The study area map of Jukskei River, Johannesburg.

3.2 Methodological Approach

The study is structured into three distinct stages: the first stage involves organizing the dataset, converting it into a single coordinate reference system (CRS) and converting necessary raster datasets to vectors for modelling purposes; the second stage focuses on constructing and validating of a dynamic flood model (HEC-RAS) for the hazard risk mapping; and the third stage aims to produce a flood hazard map that delineates the impacted regions at Alexandra, Johannesburg along the Jukskei River. This study follows the dataset and methodology commonly embraced by other researchers. The dataset employed in this research aligns with those frequently utilized in other studies, encompassing soil properties, precipitation, LULC, and digital DEM. Additional sources of secondary data, such as digital satellite imagery and synthetic unit hydrographs were incorporated.

3.3 Research Design

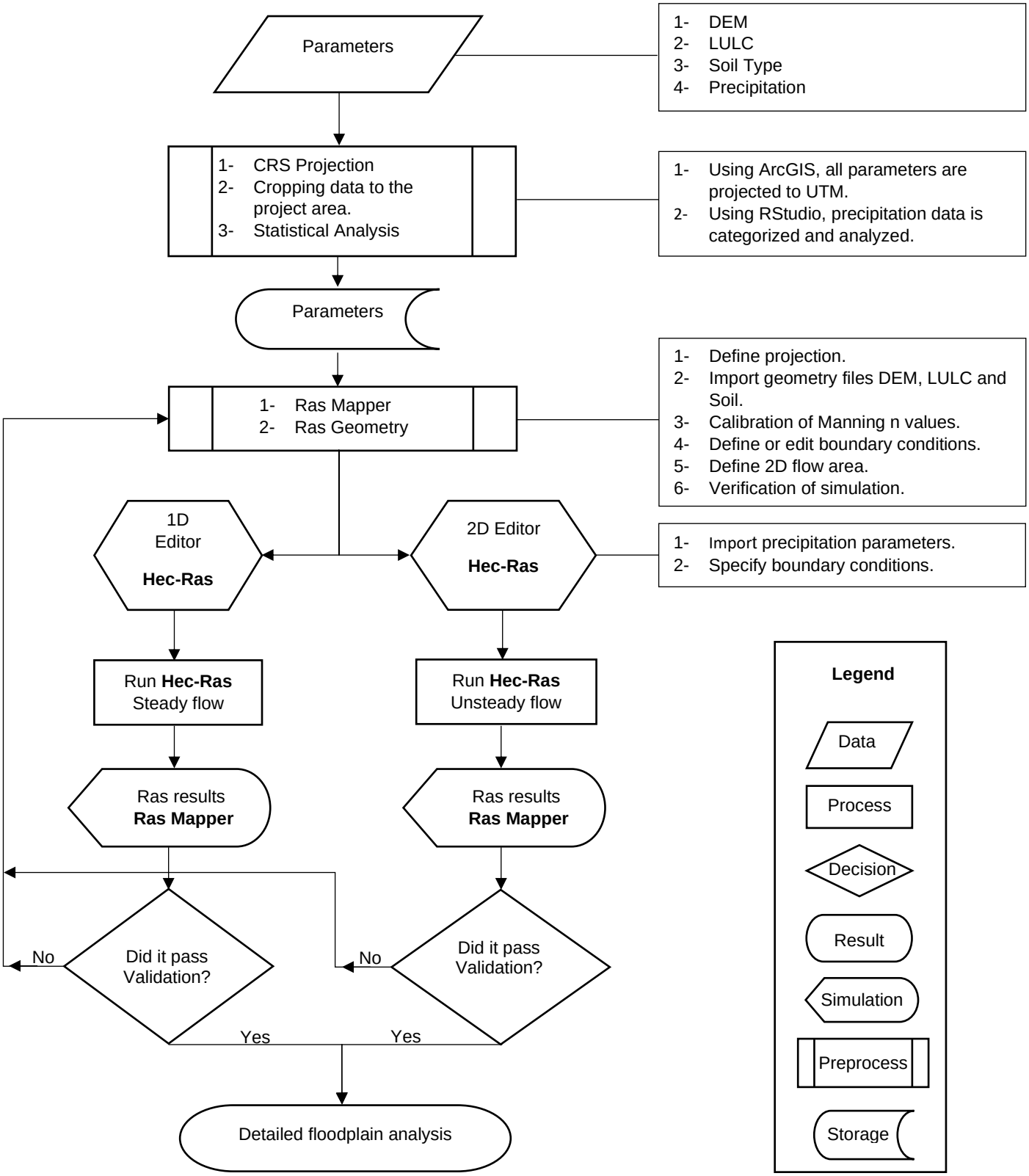

Figure 2. Detailed methodological flow chart.

3.4 Research Parameters

This study utilizes parameters comprising a digital DEM, LULC data, soil information, and precipitation data. Table 1 presents a summary of the parameter sources utilized in this study for dynamic flood modelling and hazard mapping.

Table 1. Shows parameter requirements.

Parameters	Details	Source
Digital Elevation Model (DEM)	Name: **SRTM** Data format: **GeoTiff** Spatial resolution: **30m (1 band)** Spatial coverage: **Gobal**	Managed by: NASA. Website: Earth Data (Open Source) https://search.earthdata.nasa.gov/search
Precipitation	Name: **CHIRPS** Data format: **CSV** Spatial resolution: **0.05 degrees** Spatial coverage: **Global** Temporal Extent**: 2000 – 2020**	Managed by: SERVIR. Website: https://climateserv.servirglobal.net/map
Soil	Data Modelling: **ESRI shapefile format,With soil attributes database.**	International Soil Reference and Information Centre (ISRIC) Website
Land Use and Land Cover	Data format: **GeoTIFF** Spatial resolution: **30 x 30m** Temporal Extent: **2020** Coverage: **South Africa**	Managed by: Department of Forestry, Fisheries, and the Environment (DFFE) Website: https://egis.environment.gov.za/gis_data_downloads

3.5 Pre-Processing

Prior to utilizing the parameters in the analysis, it is pre-processed. This involves various mapping processes, including reprojection, masking, and statistical analysis. These steps are necessary due to factors such as variations in data sources,

types, and formats, which require post-processing to ensure compatibility and consistency.

3.5.1 DEM

According to the version of the SRTM dataset, it can be used for various applications, including landslide susceptibility mapping (Das & Lepcha, 2019), and terrain slope estimation (Zhu *et al.*, 2020), which was the specific application in this study. Nevertheless, to facilitate data integration, it is necessary to reproject all datasets into a shared local coordinate reference system (CRS). Using ArcGIS Pro, the SRTM data was transformed into the WGS 84 UTM zone 35S coordinate system, and subsequently, the scene was validated against a base map and masked to the area of study as illustrated in Figure *7*.

3.5.2 Soil types

The soil type dataset used in the study was acquired by applying a mask to the ESRI shapefile with its attribute database, limiting it to the study area. Subsequently, the dataset was reprojected to align with the WGS 84 UTM zone 35S coordinate system as shown in Figure 9. This was verified against a base map for accuracy prior to being saved to a locally shared storage location.

3.5.3 Precipitation

The spatial and temporal varying precipitation data collected from CHIRPS for the 20-year period was analysed in RStudio and plotted in ArcGIS Pro as shown in Figure 3. Initially, a time series spanning 20 years was generated to examine seasonal patterns, as illustrated in Figure 4. Subsequently, the data was further analysed by categorizing it based on monthly maximum precipitation, focusing on the maximum, average, and minimum precipitation for each year over the 20 years to identify trends in precipitation as shown Figure 5. Recognizing that precipitation exhibits a high parametric index, it was examined to identify instances of high precipitation that are likely to lead to flooding. This was achieved by statistically analyzing the R and P values for the 20-year period.

3.5.4 LULC

For this study, the LULC dataset from South Africa's Department of Forestry, Fisheries, and the Environment (DFFE) for the year 2020 was utilized. The dataset was imported into ArcGIS Pro to extract data specific to the study area. Subsequently, the data was projected to the WGS 84 UTM zone 35S coordinate system within ArcGIS Pro, and validation procedures were carried out to verify its accurate alignment with the new coordinate system as shown in Figure *8***Error! Reference source not found.**.

3.5.5 Ras Mapper and Ras Geometry

The pre-processing role of HEC-RAS Mapper for LULC, soil types, and Digital Elevation Model (DEM) in hydraulic modelling involved integrating various datasets to enhance detailed topographic information for improved precision, accuracy, and effectiveness of hydraulic analyses. Additionally, the model was configured in both HEC-RAS Mapper and Geometry by defining the study area, river network (reach), cross-sections, and banks. The incorporation of LULC and soil type data into the model accounts for land surface characteristics and soil properties, which are essential for computing Manning's n values. Regarding Manning's roughness value (n), there are numerous references available, including the HEC-RAS Mapper User's Manual, which provides suggested Manning's roughness values (n) for floodplain and stream analysis. However, for this study, the suggested Manning's n values according to factors that affect roughness are found in Chow's "Open Channel Hydraulics" (1959). The Jukskei River is a major river for this type of river Manning's roughness coefficient ranges from 0.025 – 0.050 (chow 1959) thus the model was run between these ranges (Soliman *et al*., 2022a). Manning's n-value formula is written in Equation 3.

Equation 3 Manning's N value

$$V = \frac{1.486}{n} R^{2/3} S_e^{1/2} \qquad \text{Equation 3}$$

Where *V* is the velocity of flow (ft), R is the hydraulic radius, S_e is the slope of the energy grade line and n is Manning's roughness coefficient.

3.6 Post-Processing

The HEC-RAS is a tool with a graphical user interface and GIS capabilities for 1D and 2D flood model processing using geospatial data. The 1D hydraulic modelling approach is known for its computational efficiency in determining floodplain and flood extents, particularly for higher flows, even when dealing with limited topographical datasets. As compared to 1D hydraulic model, the 2D hydraulic model offers improved accuracy, flexibility, and the ability to handle complex scenarios, making it suitable for detailed flood representation of flow behaviour in urban areas and regions with irregular topography.

3.6.1 1D Steady Flow

This involved specifying flow data under steady flow conditions, encompassing flow rates or water levels at the upstream boundary of the model domain (Chao *et al*., 2018; Okoli *et al*., 2019). To simulate a steady model, both the frictional average convergence method and the parabolic method for critical depth computation were utilized for a supercritical flow regime. The frictional average convergence method aims to achieve convergence by iteratively adjusting the frictional parameters until a stable and consistent solution is achieved (Lamichhane & Sharma, 2018). The parabolic method for critical depth computation involves employing the energy equation to determine the critical depth at which flow transitions from subcritical to supercritical. The energy equation takes into consideration energy losses due to friction to calculate water surface profiles along the river reach (Lamichhane & Sharma, 2018; Leon & Goodell, 2016). By solving the energy equation, HEC-RAS computes water surface profiles from one cross-section to another using an iterative procedure known as the standard step method (Lamichhane & Sharma, 2018).

Equation 4 Energy equation

$$Z_1 + Y_1 + \frac{a_1 V_1^2}{2g} + H_e = Z_2 + Y_2 + \frac{a_2 V_2^2}{2g} \qquad \text{Equation 4}$$

3.6.2 2D Unsteady Flow

Before initiating the simulation of 2D unsteady flow, it is essential to validate the input hydraulic parameters such as Manning's roughness coefficients, bed

elevations, and other factors (including LULC, soil types, DEM, and precipitation data) to accurately characterize flow behaviour within the model. The configuration of LULC, soil types, and DEM is performed in both HEC-RAS Mapper and HEC-RAS Geometry, as well as within the 2D flow area. Within the 2D editor, the boundary conditions for the 2D flow area are specified, and monthly precipitation data is uploaded to cover the entire duration of interest. During the analysis, the model equation employed for simulation is the diffusion wave equation with an initial time condition set to 5 hours. The execution of the 2D hydraulic simulation in HEC-RAS calculates various parameters such as water surface profiles, flow velocities, flood extents, and other hydraulic characteristics. The model results are calibrated by adjusting Manning's roughness (n) value and validated by comparing the simulated results with the output of a previous study conducted by Mawasha & Britz (2022) until the model achieves a satisfactory depiction of the scenario. The dynamic wave equations comprise equations for continuity and momentum.

Equation 5 Continuity Equation:

$$\frac{\partial y}{\partial t} + V\frac{\partial y}{\partial x} + y\frac{\partial V}{\partial x} = r - f \qquad \text{Equation 5}$$

(Kazezyilmaz-Alhan, 2012)

Equation 6 Momentum Equation:

$$\frac{\partial V}{\partial t} + V\frac{\partial V}{\partial x} + g\frac{\partial y}{\partial x} = g(S_0 - S_f) + \left[(r - f)\frac{V}{y}\right] \qquad \text{Equation 6}$$

(Kazezyilmaz-Alhan, 2012)

where y is the depth of water (L), S_f is friction slope (L/L), S_0 is bed slope (L/L), V is water velocity (L/T), r is rainfall intensity (L/T), f is infiltration rate (L/T), g is the acceleration of gravity (L/T^2), t is time (T), and x is distance (L).

3.6.3 Calibration And Validation

Calibration and validation of the HEC-RAS model is a critical aspect of ensuring the accuracy and reliability of its simulations. During the model calibration process, 40 events of dataset are used to adjust the model. The calibration process involved adjusting Manning's n value for this study to achieve the best fit between the model simulations. Due to the absence of satellite imagery on the day of the incident, the validation of the model relied on data from a study conducted by Mawasha and Britz (Mawasha & Britz, 2022). In their research, ground truthing was undertaken to determine the extent of flooding in 2006. This procedure entailed outlining the inundation utilizing Mawasha and Britz's model and then contrasting it with the model outcomes obtained in the current study following each variation in Manning's value and simulation.

3.6.4 Flood Mapping

Flood hazard and flood risk are very crucial aspects in understanding the areas, infrastructures and livelihoods that are likely to be affected in the event of precipitation with amounts as investigated. Flood depths, flood velocity and flood inundation were generated in HEC-RAS and exported into ArcGIS Pro. The modelled flood outputs were visualized on the terrain model to gain insight into potential areas prone to flood hazards. Additionally, a base map of street networks and buildings was superimposed on the DTM to further quantify the affected infrastructure within the flood risk zones alongside the water surface level (WSL), and channel profile.

CHAPTER 4: RESULTS AND DISCUSSION

4.1 Rainfall Data Analysis

The precipitation over Alexandra, Johannesburg was assessed in RStudio to evaluate the trend in the parameter. The assumption made was that high precipitations are the cause of floods. That said, the maximum precipitation recorded by the spatial in the watershed was applied in the analysis. The time series of rainfall for Alexandra, Johannesburg, is presented in Figure 4 with largely the contributing region being Johannesburg city. From the literature, Meissner & Nicolai, 2019 pointed out that precipitation is a very high matrix in accessing flood events. For the period 2000 to 2020, the results show that there have been random and spontaneous events in frequency and intensity of high precipitation. Henceforth, an evaluation was conducted regarding the climatic seasons within South Africa, namely Summer, Autumn, Winter, and Spring. This involved the spatial and temporal analysis to establish the correlation between precipitation and time over the years. The analysis revealed that among these seasons, only three Spring, Summer, and Autumn exhibited high levels of precipitation close to or above 20mm in Alexandra. During the period spanning from 1st June to 31st August, Winter typically experiences an average precipitation of 10mm or less. The trend analysis also revealed that months characterized by significantly elevated precipitation levels are January, February, and March, which coincide with the Summer and Autumn seasons, registering 60mm and above in precipitation having an average R-square value of 0.061 from the regression model Figure 5. As shown by the R^2 values in Figure 5, the average R^2 value of 0.061 indicates a weak positive correlation between time and rainfall.

For a better understanding, over the years the maximum precipitation data were statistically aggregated from monthly to annual bases into minimum, average and maximum annual values and then analysed for R-squared coefficients and P-values using the linear statistical regression model calculated using the optimisation technique within RStudio. The results are presented in Figure 6. The statistical evaluation of the maximum yearly precipitation in Figure 6 (A), indicates a positive R-value of 0.15 and P-value of 0.52. The R-value explains the strength and direction

of the precipitation as it increases from the year 2000 to 2020 whereas the P-value examines the data on a scale of 0 to 1, the quantity of the data (precipitation) that influenced the trend in the statistics. With the P value of 0.52 greater than the significance level of 0.05, it less strongly suggests that there is an increase in precipitation over the years. Likewise, statistics of the average precipitation across the years as shown in Figure 6 (B), indicates an R-value of -0.16. This explains a slight decrease in precipitation across the years. With a p-value of 0.48 in the context of 20 years of average precipitation data indicates that there is a high portion of the precipitation data (i.e. 48%) explains the trend in the results of precipitation statistics. This also implies that the observed precipitation patterns over the 20-year period are not statistically significant at the conventional significance level of 0.05. Finally, Figure 6 (C) is a plot of the minimum precipitation across 20-year period of observation. The statistics reveal an R-value of -0.42 and a p-value of 0.06. In this case, an R-value of -0.42 indicates a moderate negative correlation, suggesting that as years increase, precipitation tends to decrease. However, the magnitude of the correlation is not strong, indicating that the relationship is not highly linear. The p-value of 0.06 suggests that only 0.06 (6%) of observation in the data (precipitation) explains the decrease in trend of the analysis. While this p-value greater than the threshold of 0.05 for statistical significance, it suggests that there is no difference, and the null hypothesis is true for a decrease in precipitation.

In summary, the statistical evaluation of precipitation data reveals different patterns across the years. The maximum yearly precipitation shows a positive correlation, but the increase is less statistically significant, but the plot shows a few years with high sporadic precipitation. Average precipitation displays a slight negative correlation, but the observed patterns are not statistically significant. Minimum precipitation indicates a moderate negative correlation, but the relationship is not highly linear, and the statistical significance is close to the conventional threshold. As highlighted by (Akiyode *et al*., 2017) the impact of climate change is gradual yet significant, especially through alterations in precipitation and temperature patterns.

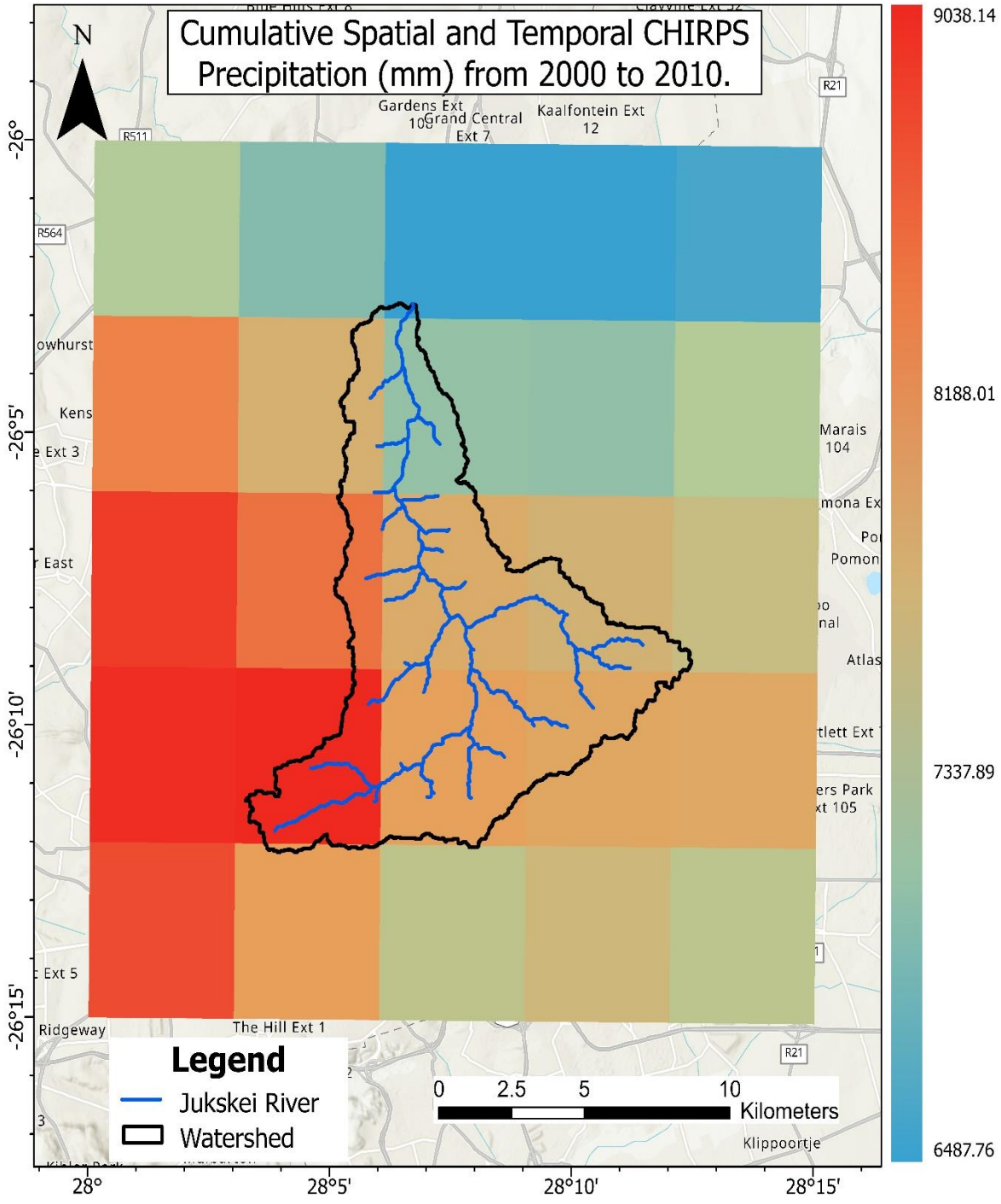
Cumulative Spatial and Temporal CHIRPS Precipitation (mm) from 2000 to 2010.
N
9038.14
8188.01
7337.89
6487.76
Legend
Jukskei River
Watershed
0 2.5 5 10
Kilometers
-26°
-26°5'
-26°10'
-26°15'
28°
28°5'
28°10'
28°15'
Gardens Ext 109
Grand Central Ext 7
Kaalfontein Ext 12
R21
R511
R564
Marais 104
Pomona
Atlas
Ridgeway
The Hill Ext 1
Klippoortje

A

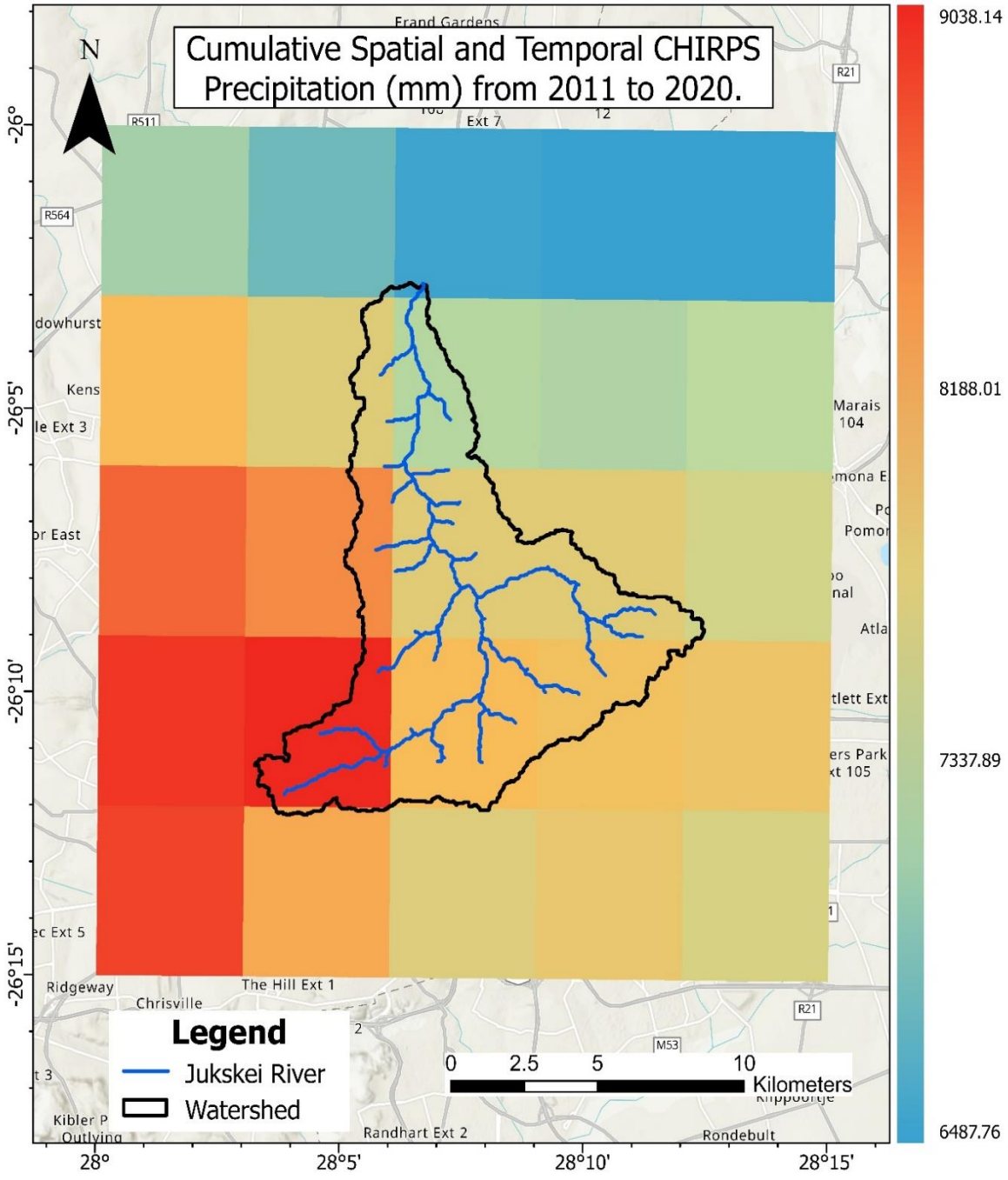

B

Figure 3. Spatial variation of precipitation (mm) over 10 years interval for **A** (2000-2010) and **B** (2011-2020).

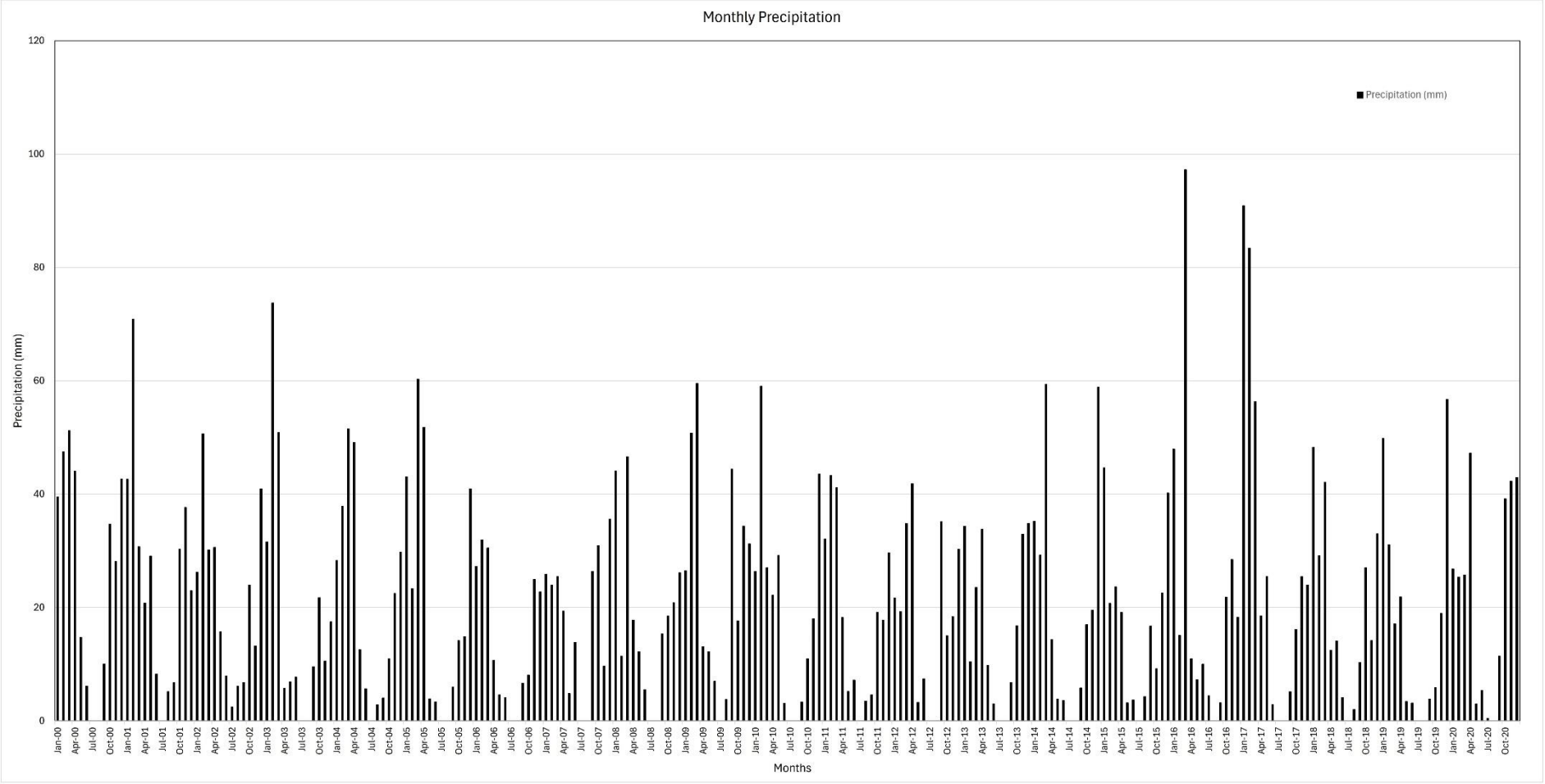

Figure 4. Maximum monthly precipitation from CHIRPS for a period of 20 years (2000-2020).

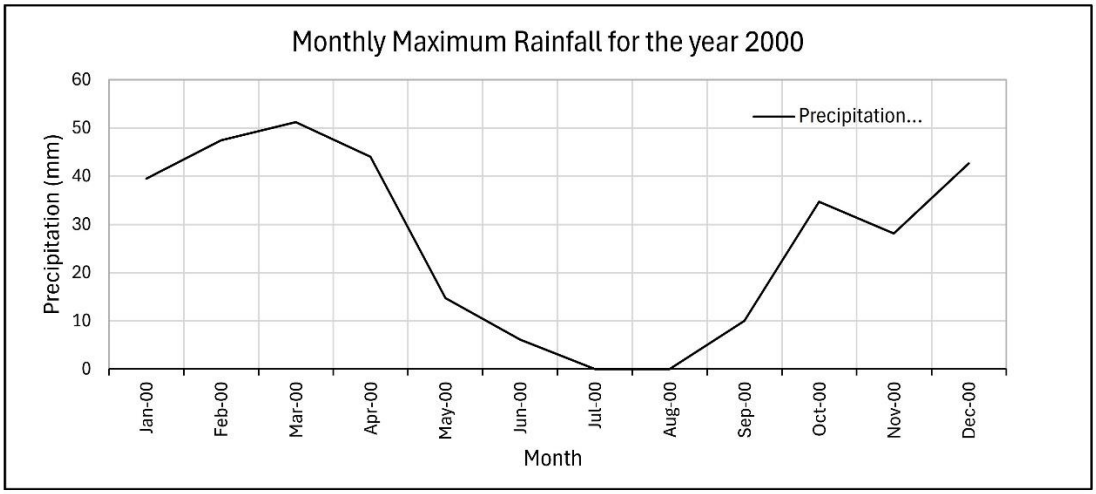
Monthly Maximum Rainfall for the year 2000
Precipitation (mm)
Precipitation...
Jan-00
Feb-00
Mar-00
Apr-00
May-00
Jun-00
Jul-00
Aug-00
Sep-00
Oct-00
Nov-00
Dec-00
Month

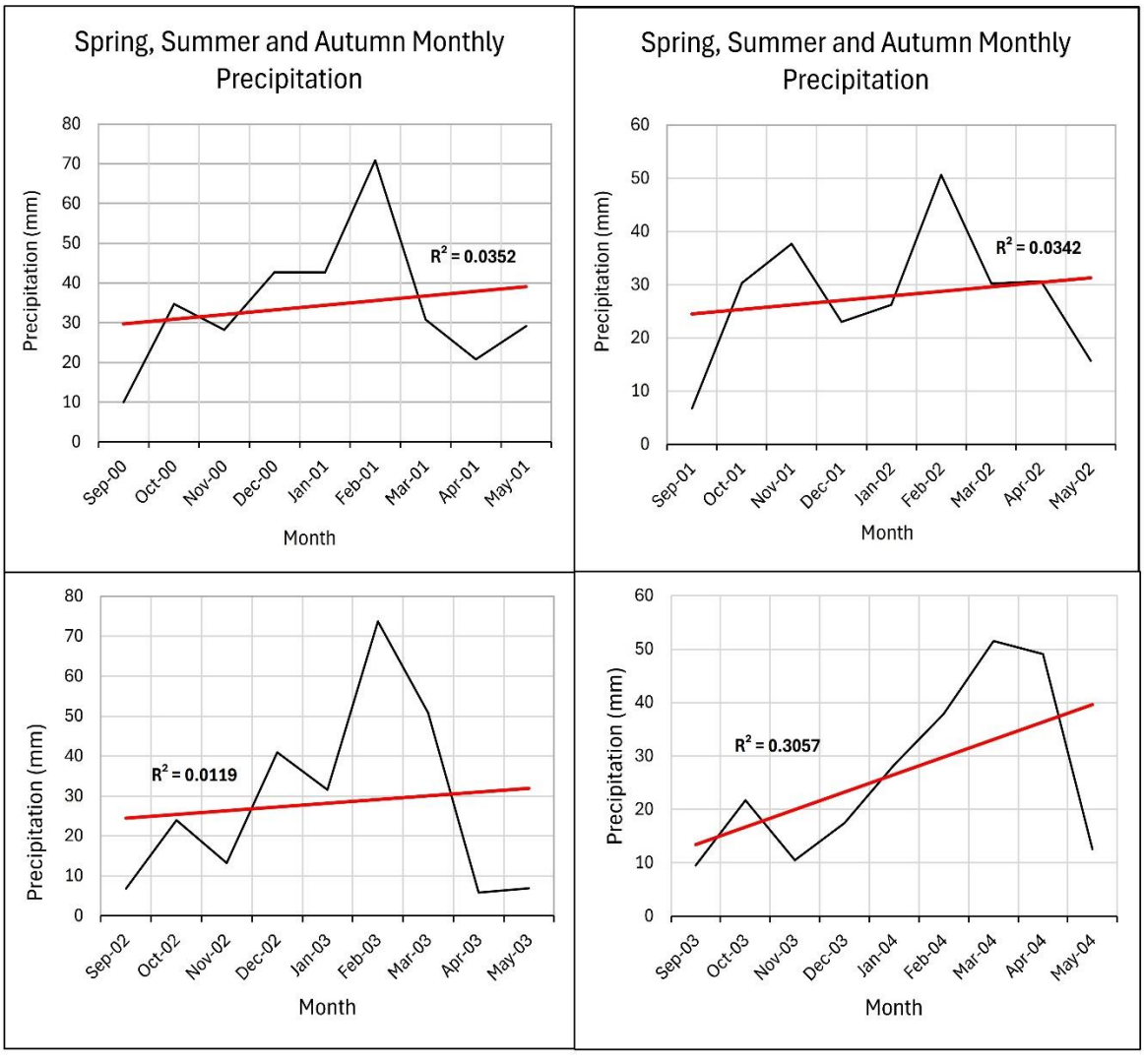
Spring, Summer and Autumn Monthly Precipitation
Precipitation (mm)
R² = 0.0352
Sep-00
Oct-00
Nov-00
Dec-00
Jan-01
Feb-01
Mar-01
Apr-01
May-01
Month
Spring, Summer and Autumn Monthly Precipitation
Precipitation (mm)
R² = 0.0342
Sep-01
Oct-01
Nov-01
Dec-01
Jan-02
Feb-02
Mar-02
Apr-02
May-02
Month
Precipitation (mm)
R² = 0.0119
Sep-02
Oct-02
Nov-02
Dec-02
Jan-03
Feb-03
Mar-03
Apr-03
May-03
Month
Precipitation (mm)
R² = 0.3057
Sep-03
Oct-03
Nov-03
Dec-03
Jan-04
Feb-04
Mar-04
Apr-04
May-04
Month

A

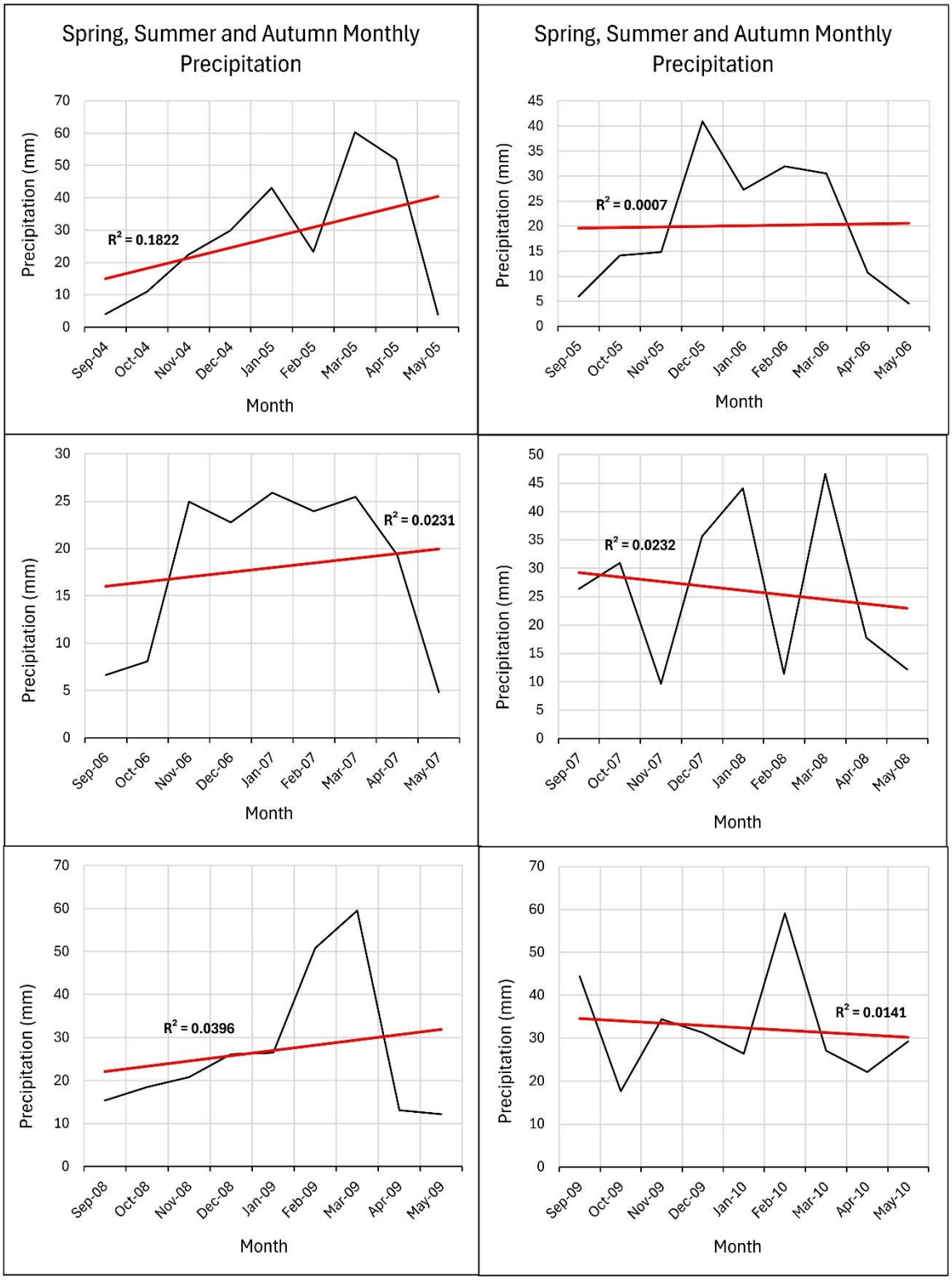
Spring, Summer and Autumn Monthly Precipitation
Precipitation (mm)
Month
R² = 0.1822
Sep-04
Oct-04
Nov-04
Dec-04
Jan-05
Feb-05
Mar-05
Apr-05
May-05
Spring, Summer and Autumn Monthly Precipitation
Precipitation (mm)
Month
R² = 0.0007
Sep-05
Oct-05
Nov-05
Dec-05
Jan-06
Feb-06
Mar-06
Apr-06
May-06
Precipitation (mm)
Month
R² = 0.0231
Sep-06
Oct-06
Nov-06
Dec-06
Jan-07
Feb-07
Mar-07
Apr-07
May-07
Precipitation (mm)
Month
R² = 0.0232
Sep-07
Oct-07
Nov-07
Dec-07
Jan-08
Feb-08
Mar-08
Apr-08
May-08
Precipitation (mm)
Month
R² = 0.0396
Sep-08
Oct-08
Nov-08
Dec-08
Jan-09
Feb-09
Mar-09
Apr-09
May-09
Precipitation (mm)
Month
R² = 0.0141
Sep-09
Oct-09
Nov-09
Dec-09
Jan-10
Feb-10
Mar-10
Apr-10
May-10

B

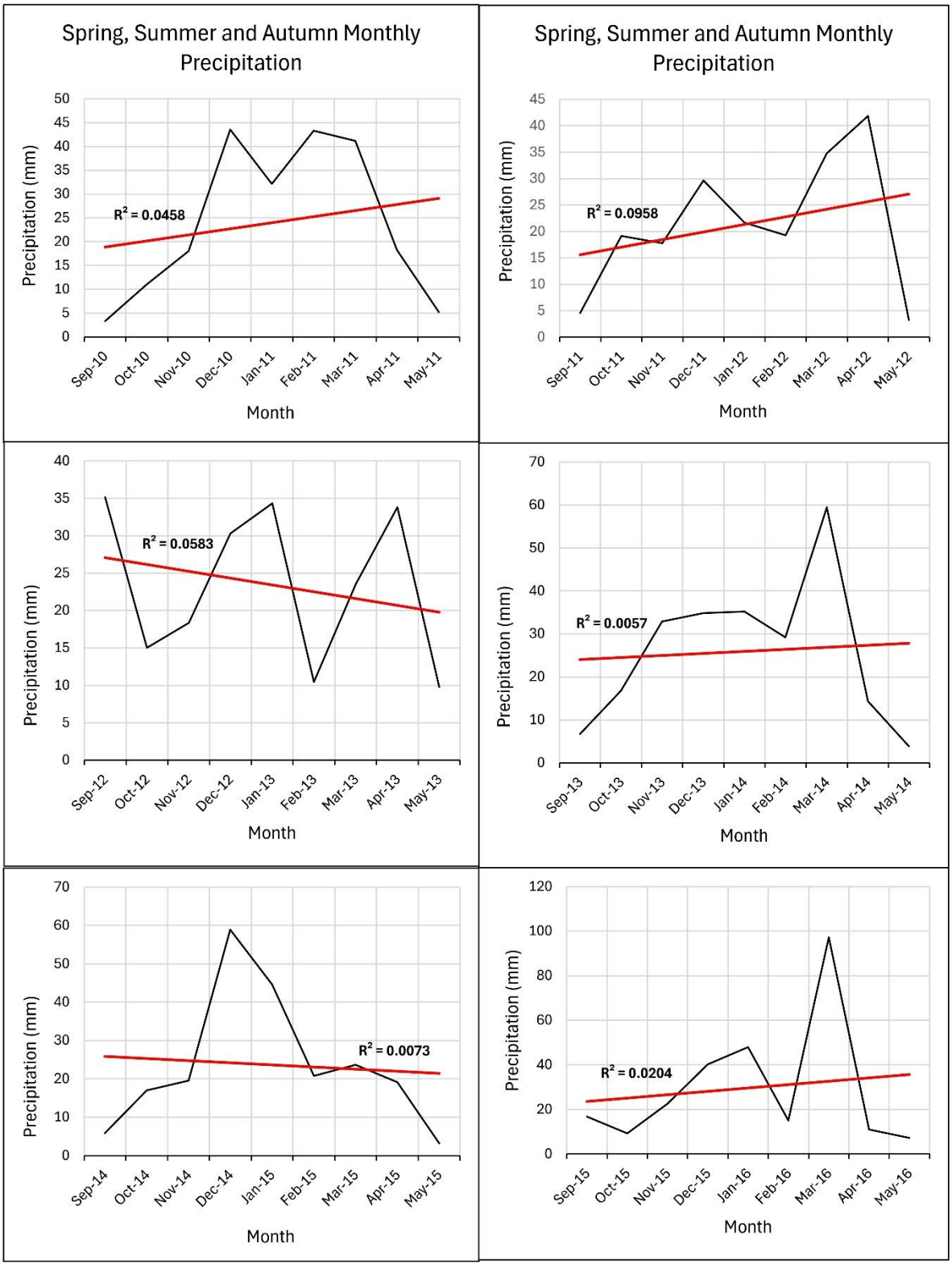
Spring, Summer and Autumn Monthly Precipitation
Precipitation (mm)
Month
R² = 0.0458
Sep-10
Oct-10
Nov-10
Dec-10
Jan-11
Feb-11
Mar-11
Apr-11
May-11
Spring, Summer and Autumn Monthly Precipitation
Precipitation (mm)
Month
R² = 0.0958
Sep-11
Oct-11
Nov-11
Dec-11
Jan-12
Feb-12
Mar-12
Apr-12
May-12
Precipitation (mm)
Month
R² = 0.0583
Sep-12
Oct-12
Nov-12
Dec-12
Jan-13
Feb-13
Mar-13
Apr-13
May-13
Precipitation (mm)
Month
R² = 0.0057
Sep-13
Oct-13
Nov-13
Dec-13
Jan-14
Feb-14
Mar-14
Apr-14
May-14
Precipitation (mm)
Month
R² = 0.0073
Sep-14
Oct-14
Nov-14
Dec-14
Jan-15
Feb-15
Mar-15
Apr-15
May-15
Precipitation (mm)
Month
R² = 0.0204
Sep-15
Oct-15
Nov-15
Dec-15
Jan-16
Feb-16
Mar-16
Apr-16
May-16

C

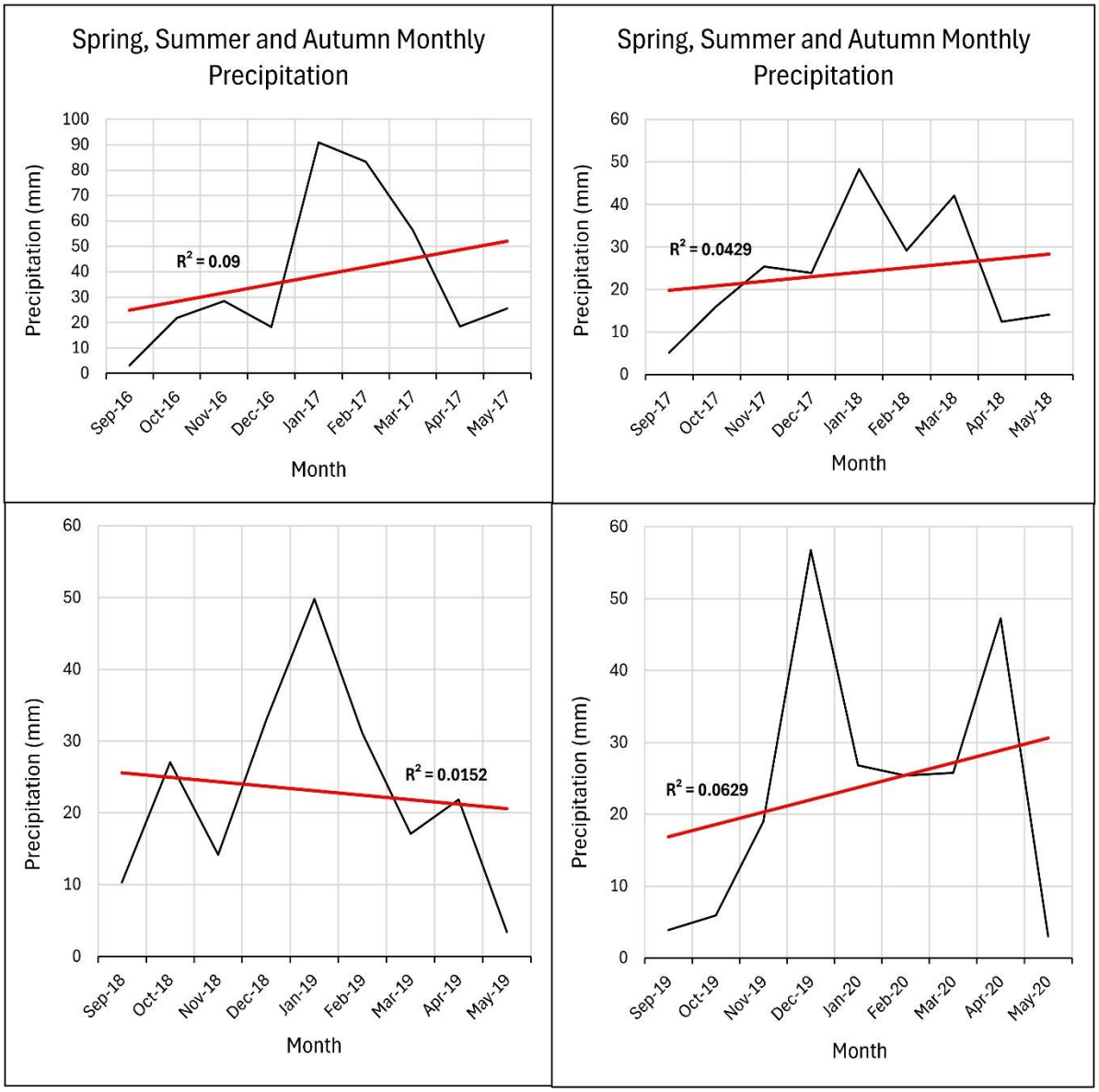

D

Figure 5. The three seasons (spring, summer, and winter) pattern with high rainfall in South Africa in A, B, C, and D.

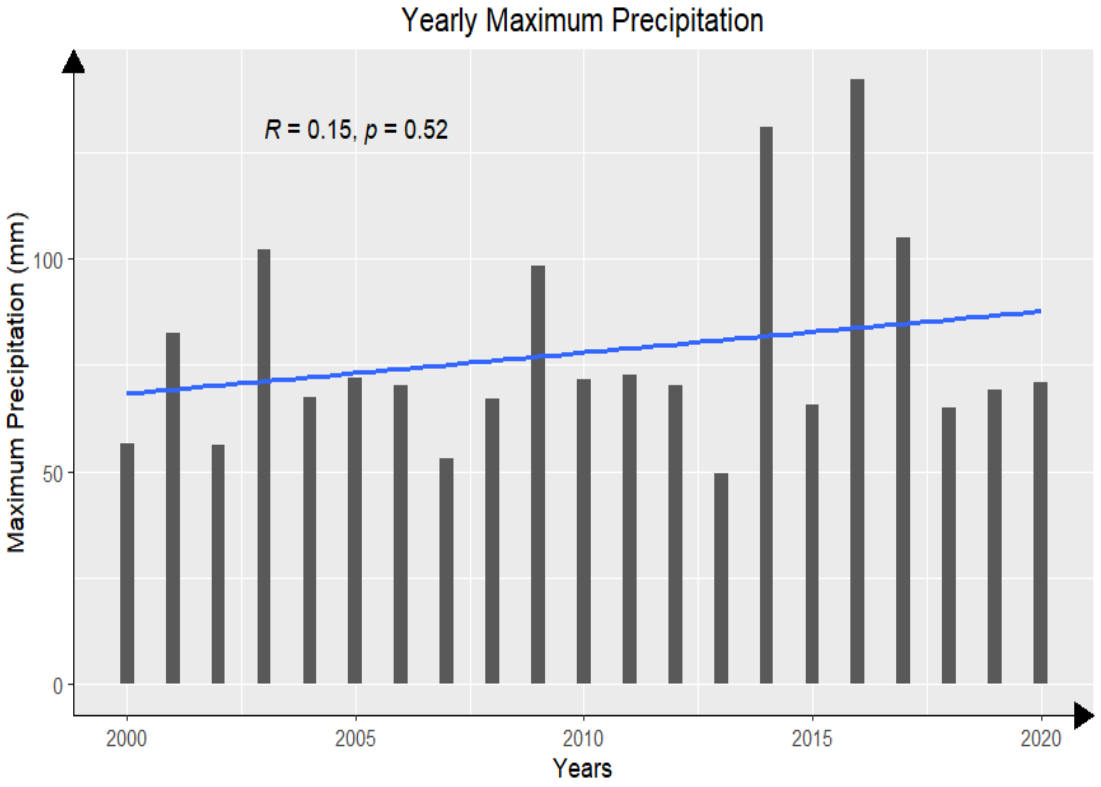
Yearly Maximum Precipitation
R = 0.15, p = 0.52
Maximum Precipitation (mm)
0
50
100
2000
2005
2010
2015
2020
Years

A

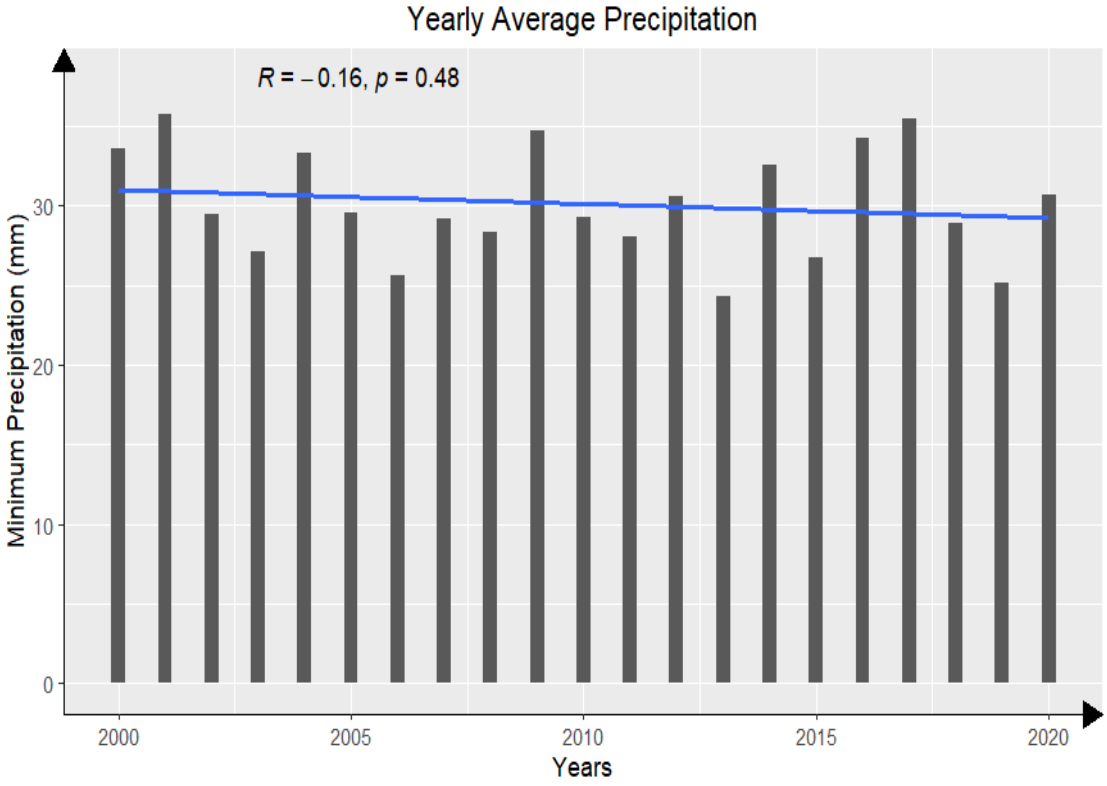
Yearly Average Precipitation
R = −0.16, p = 0.48
Minimum Precipitation (mm)
0
10
20
30
2000
2005
2010
2015
2020
Years

B

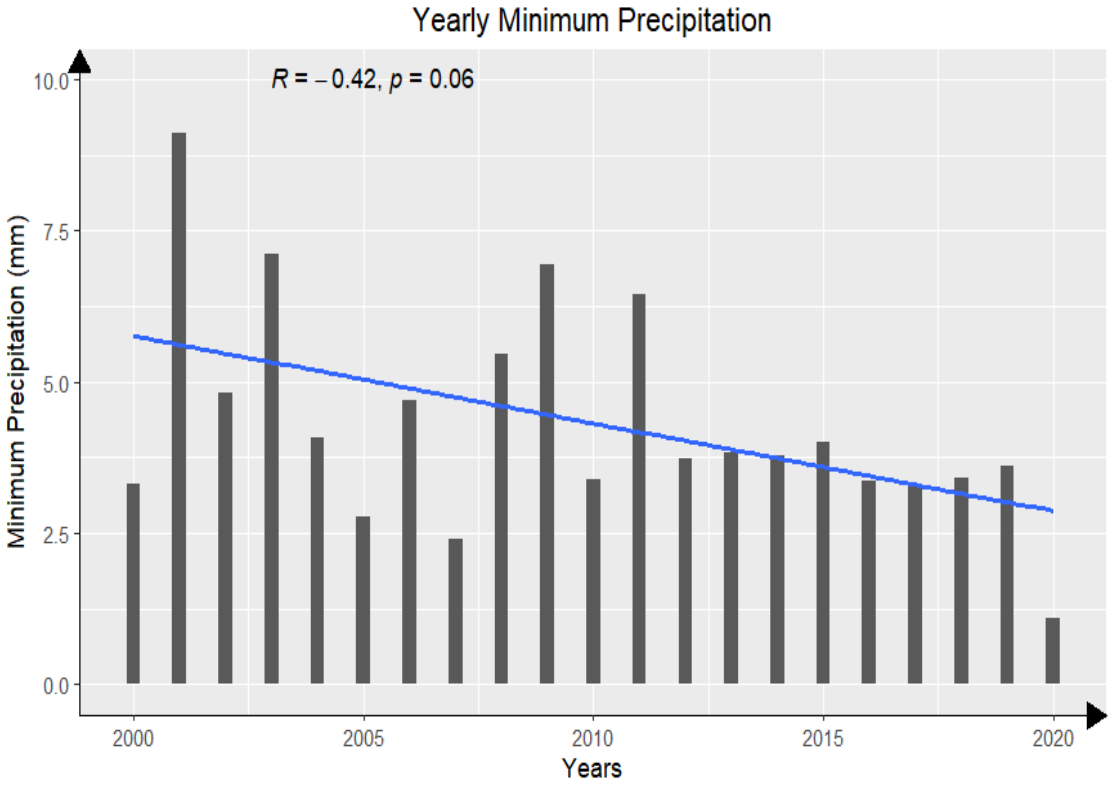

C

Figure 6. Yearly precipitation for (A) maximum, (B) average and (C) minimum period of 20 years (2000 to 2020).

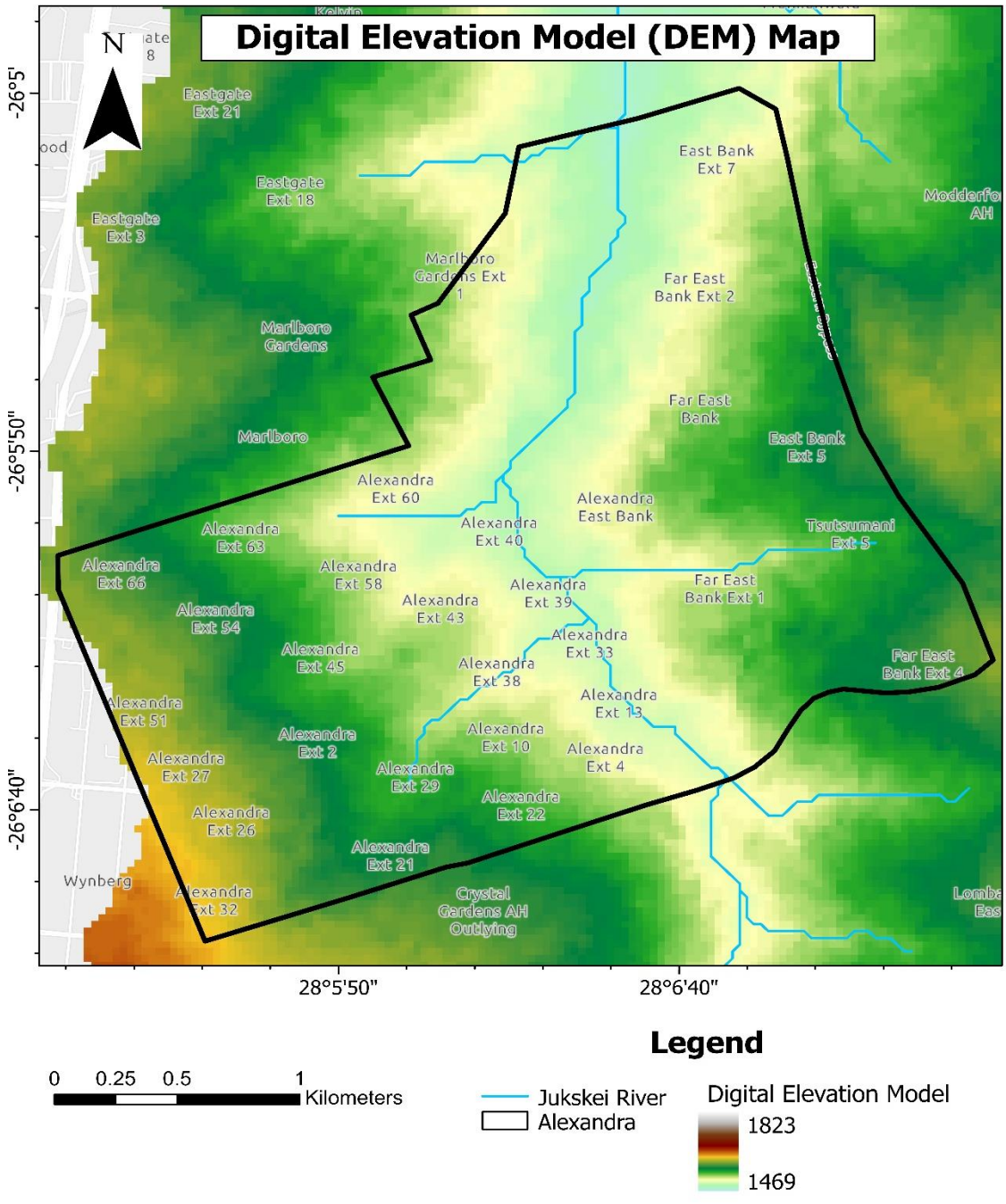

Figure 7. Map of DEM (SRTM) covering Alexandra.

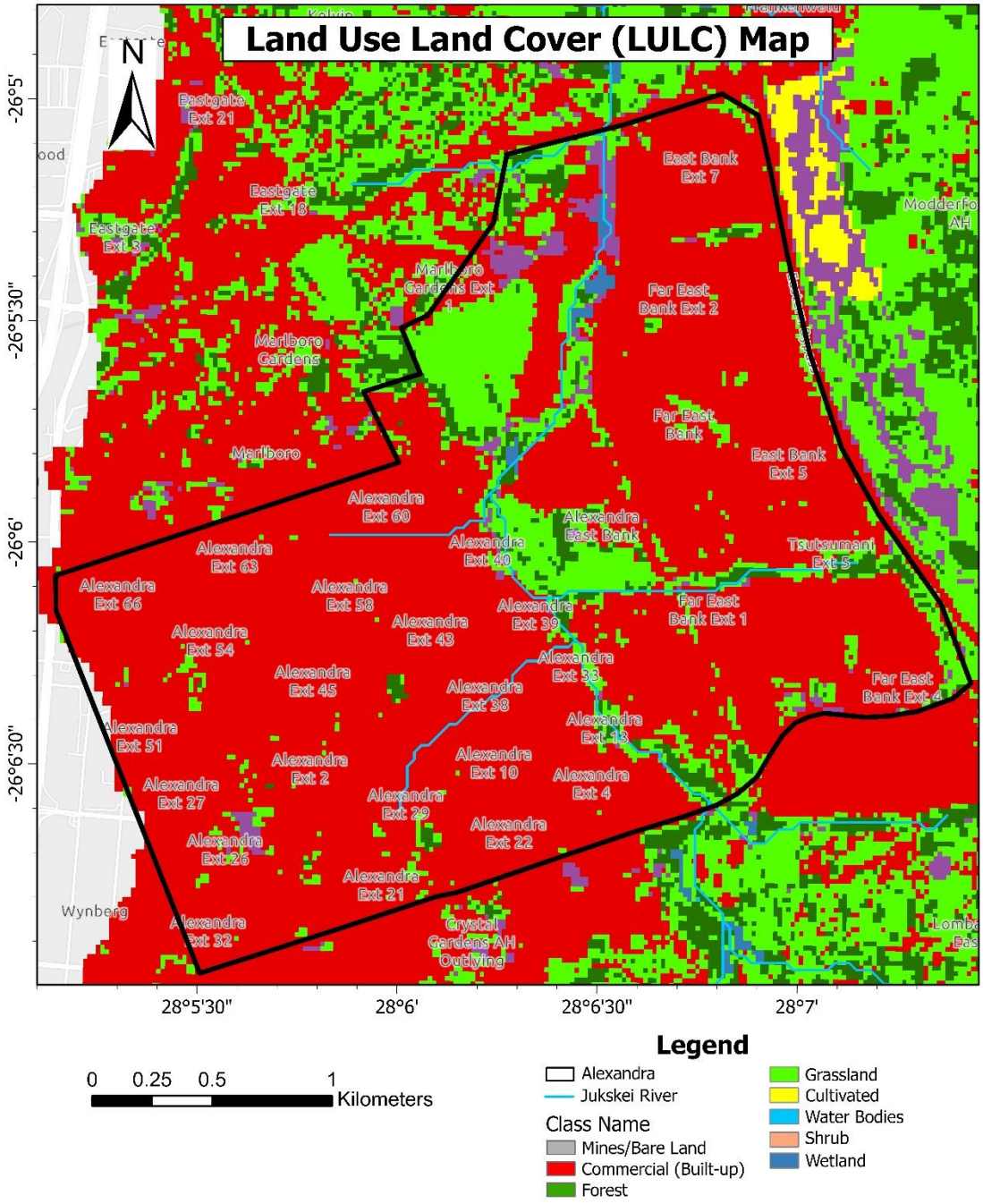

Figure 8. Map of LULC covering Alexandra.

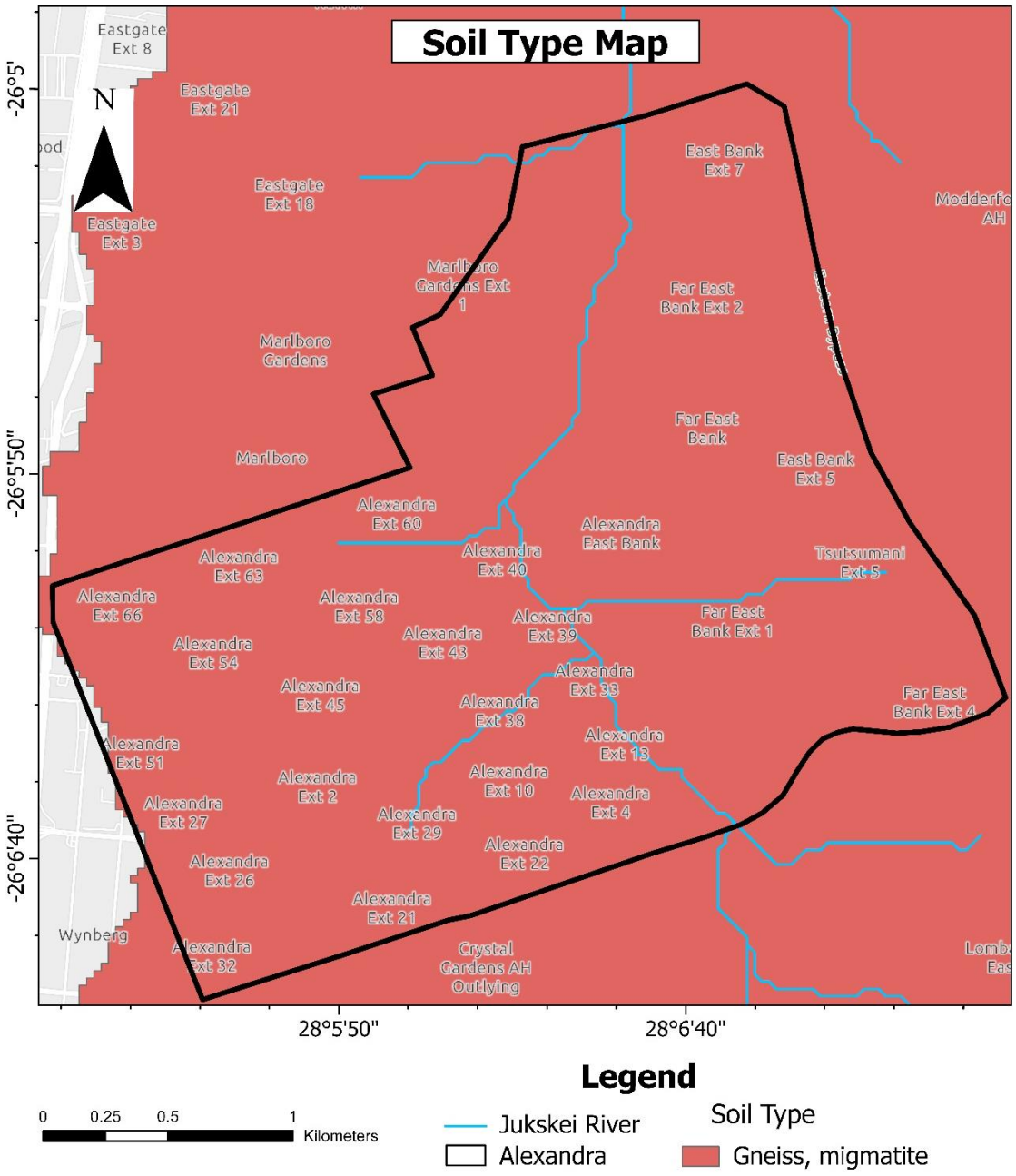

Figure 9. Map of soil types covering Alexandra.

4.2 Flood Area Mapping

A base map for Alexandra was established by utilizing digital satellite imagery showcasing crucial elements like cultivated areas, structures, roads, names of places, etc. as can be seen in Figure 1. The flood map displayed distinct features within the channel and along the banks, such as water surface elevation (WSE), volume, velocity, and depth, at monitoring stations traversing Alexandra, corresponding to different levels of precipitation. Prominent features include inundation occurrences corresponding to precipitation levels of 28mm, 49.43mm, and 142.03mm within the catchment area. Given the catchment area's average slope of 0.05 and Manning's n values in Table 5, at a precipitation level of 28mm, the model produced a water surface elevation (WSE) depth of 2.64 meters and a volume of 318.22 cubic meters within the reach. At the most severe location, cross-section CS_4 in Alexandra, the flood travelled 102.22 meters to the left and 44.77 meters to the right as shown in

Table *4*, impacting a total of 1,473 buildings (in Table 3) with a cumulative area coverage of 324,268 square meters (in Table 2). Notably, medium-risk and low-risk areas encompassed a larger area compared to high-risk areas, primarily situated within the reach. Additionally, it was noted that at a precipitation level of 49.429 mm, the flood depth escalated to 5.76 meters, accompanied by a volume of 5,743.5 cubic meters, which inundated an area totalling 526,216 square meters and impacted a total of 2,803 buildings within the catchment area. The flood extended 143.49 meters to the left and 85.76 meters to the right at the designated cross-section labelled CS_4. With a precipitation level of 142.03mm, the flood depth surged to 8.41 meters, accompanied by a volumetric flow rate of 29,844.87 cubic meters passing through the specified cross-section. The overall inundated area amounted to 1,137,908 square meters (approximately 1.138 square kilometres), impacting a total of 7,242 buildings. The flood travelled 421.73 meters to the left and 151.12 meters to the right from the reach.

Table 2. Precipitations against WSE, depth and water volume.

Precipitation (mm)	Water Surface Elevation (WSE) (m)	Depth (m)	Volume (1000 m^3)
14.00	1506.65	0.65	13.29
24.34	1507.49	1.47	63.29
28.00	1508.65	2.64	318.22
39.69	1509.25	3.24	891.21
45.00	1510.87	4.85	2,492.63
49.429	1511.79	5.76	5,743.50
88.00	1512.70	6.67	10,888.30
111.17	1513.69	7.65	18,775.41
142.03	1514.45	8.41	29,844.87

Table 3. Flood inundation and affected buildings.

Precipitation (mm)	Inundated Area (m^2)			Total Area (m^2)	Affected Buildings
	<1 (Low Risk)	1-5 (Medium Risk)	>5 (High Risk)		
28	149,448	168,436	6,384	324,268	1,473
49.429	182,812	278,024	65,380	526,216	2,803
142.03	595,172	334,408	208,328	1,137,908	7,242

Table 4. Distance travelled by flood from the reach along cross sections.

Horizontal travelled by flood from the reach (m)										
Precipitation (mm)	CS_1		CS_2		CS_3		CS_4		CS_5	
	Left	Right	Left	Right	Left	Right	Left	Right	Left	Right
28	70.96	95.01	56.38	55.9	93.36	71.19	102.22	44.77	32.39	44.77

49.429	88.52	129.08	92	91.24	112.97	96.64	143.49	85.76	56.8	64.91
142.03	117.26	174.1	180.1	109.89	154.35	113.79	421.73	151.12	75.58	87.19

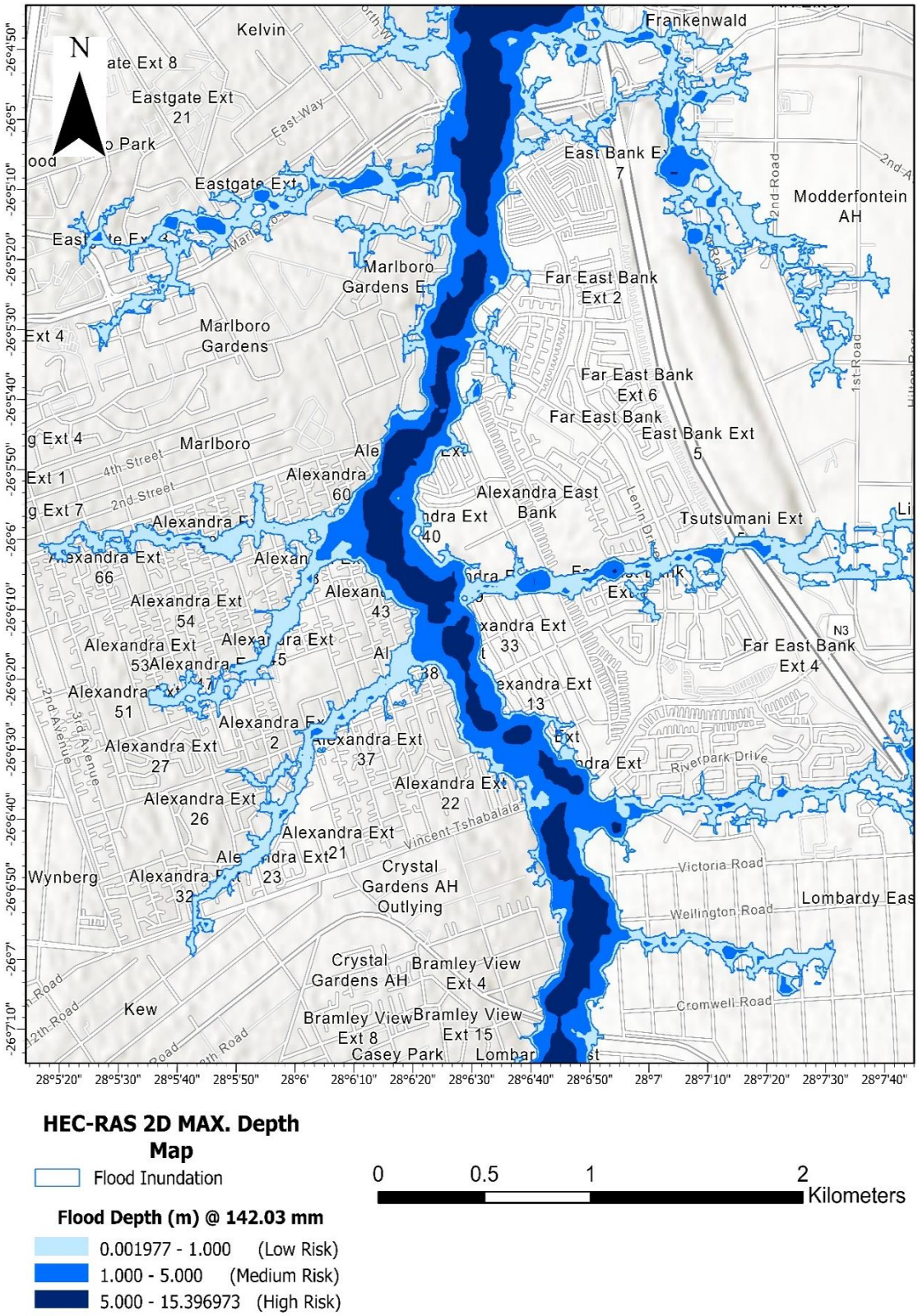

Figure 10. Maximum flood depth map of Alexandra.

4.3 Flood Hazard Maps

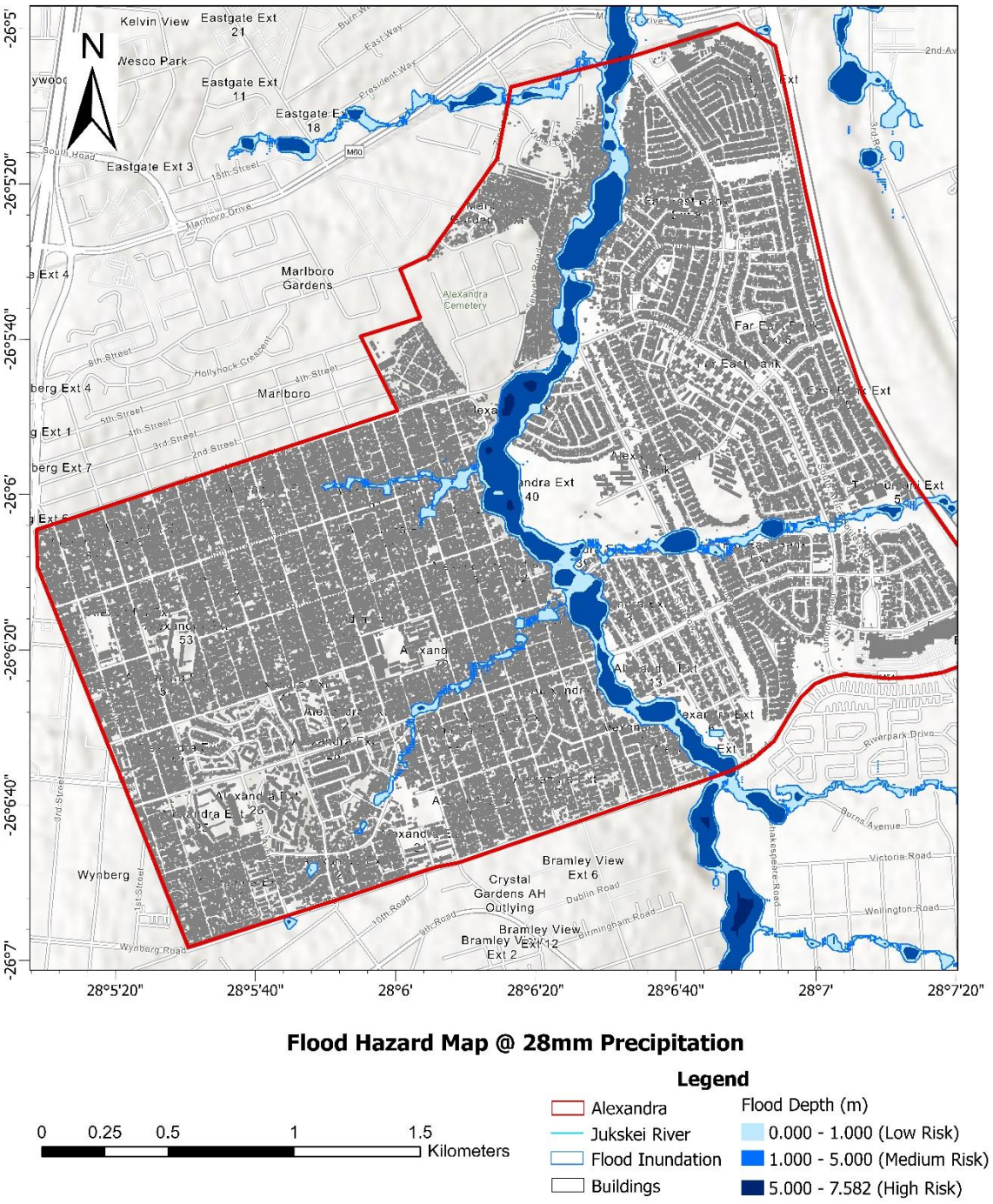

Figure 11. flood hazard map at 28mm of precipitation.

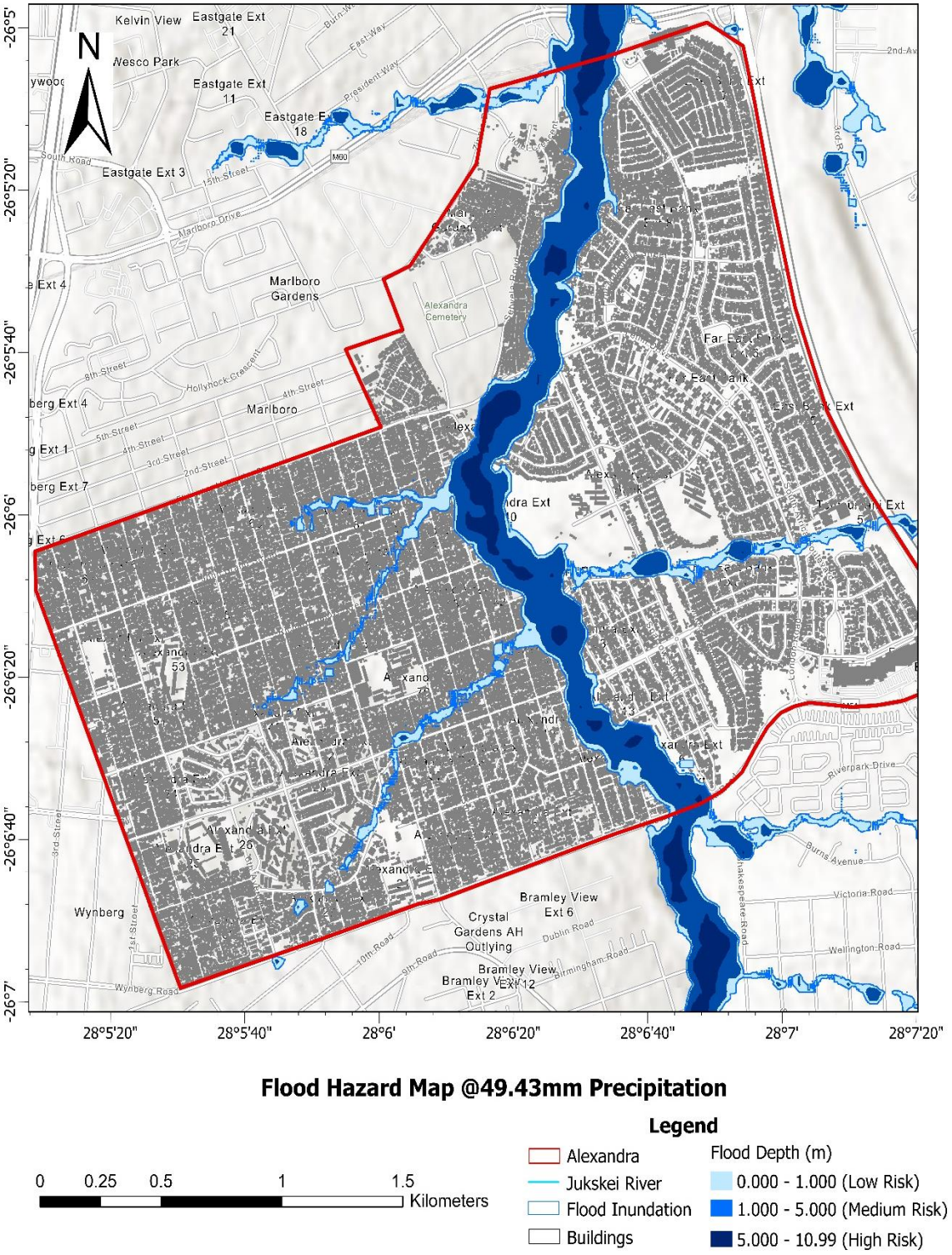

Figure 12. flood hazard map at 49.43mm of precipitation.

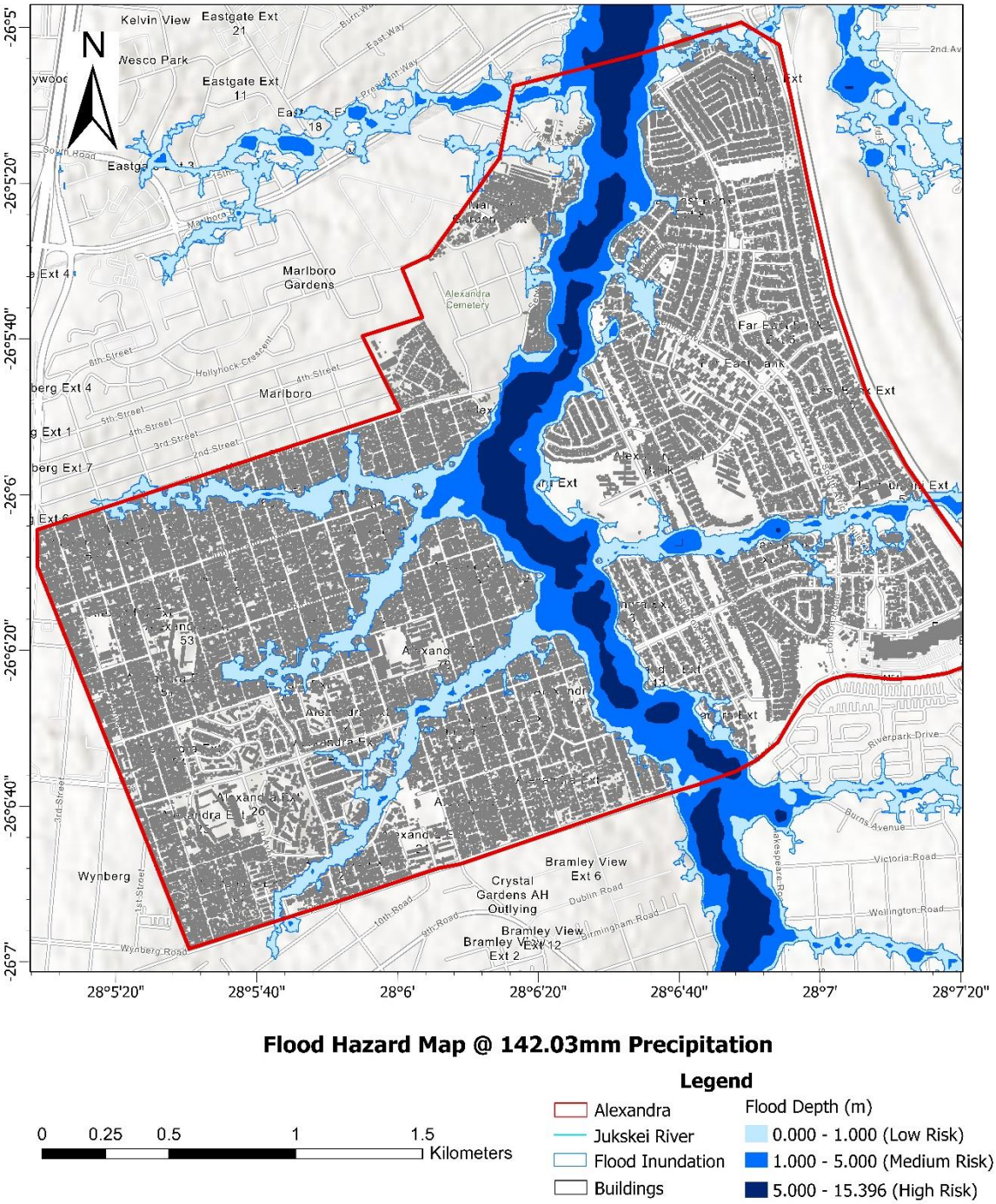

Figure 13. flood hazard map at 142.03mm of precipitation.

4.4 Flood Risk Map

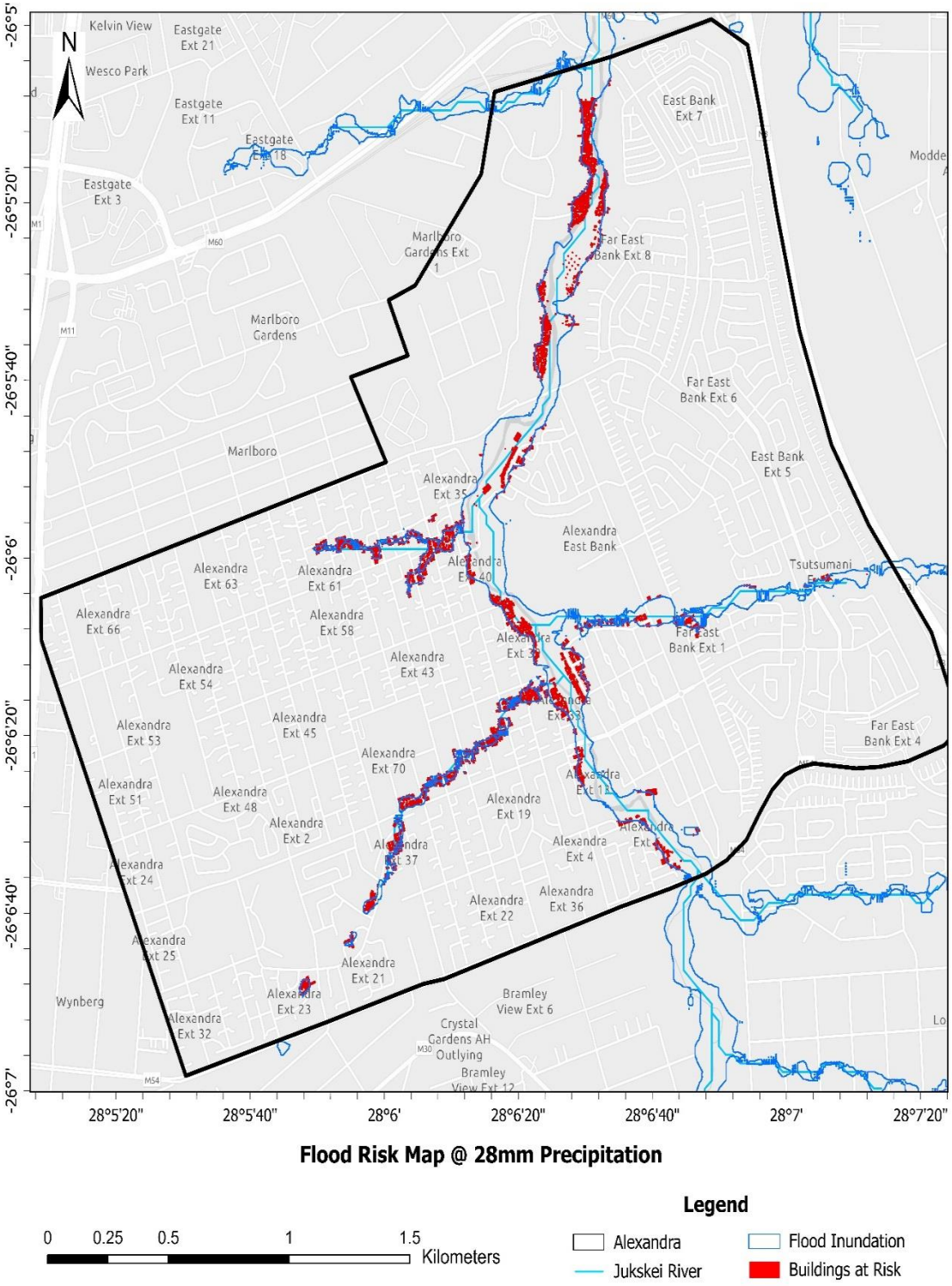

Figure 14. flood risk map at 28mm of precipitation.

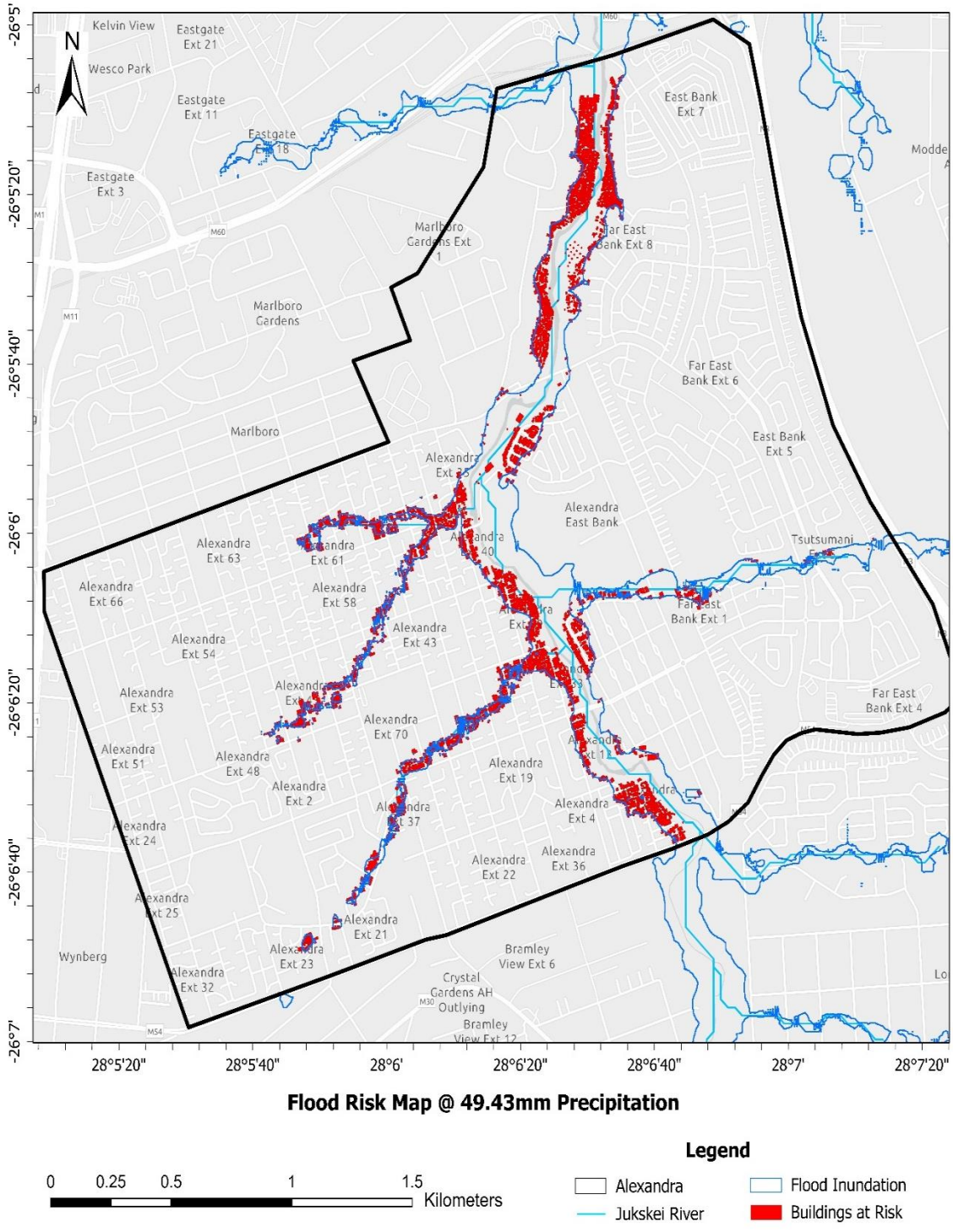

Figure 15. flood risk map at 49.43mm of precipitation.

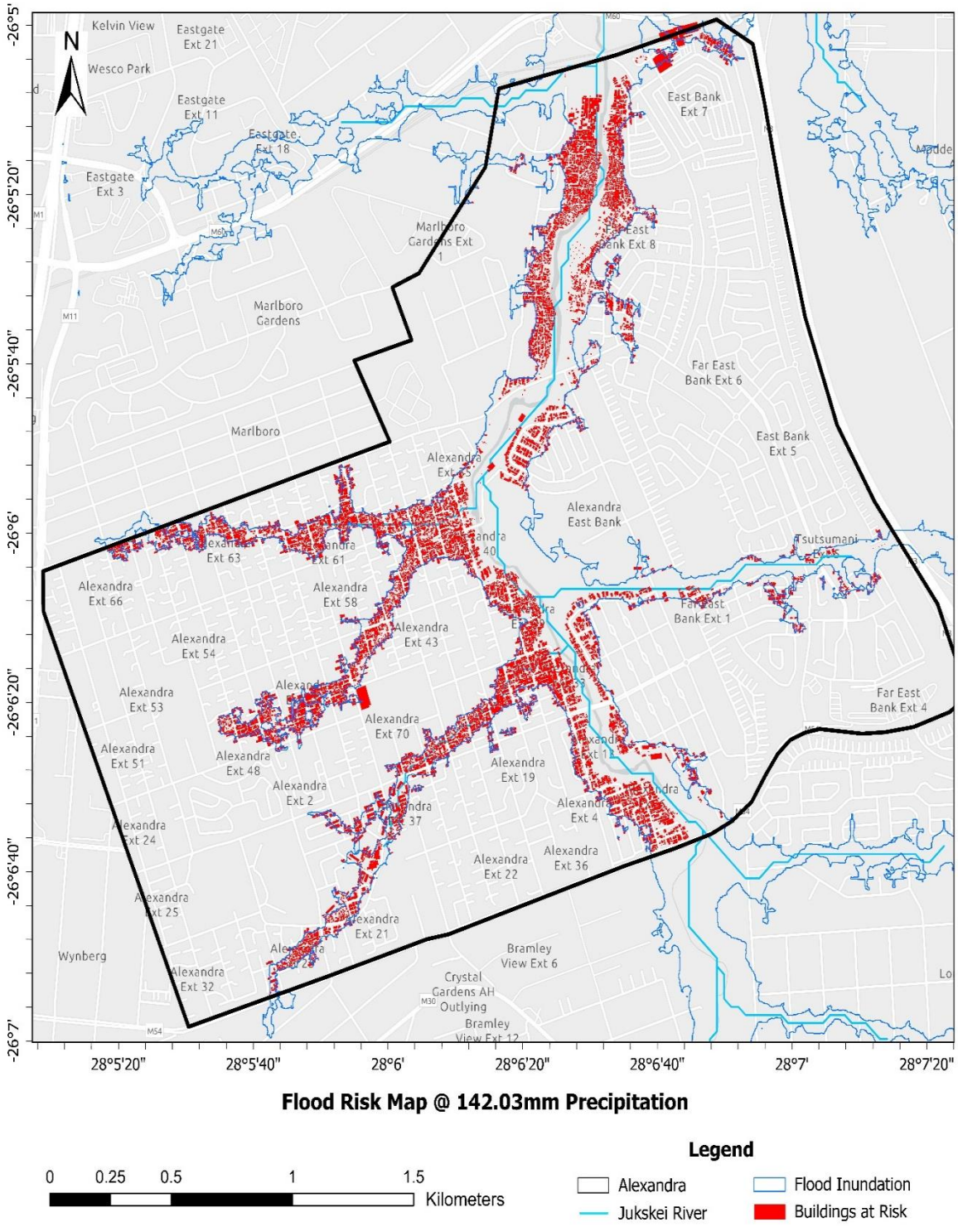

Figure 16. flood risk map at 142.03mm of precipitation.

4.5 Water Surface Elevational (WSE) Maps

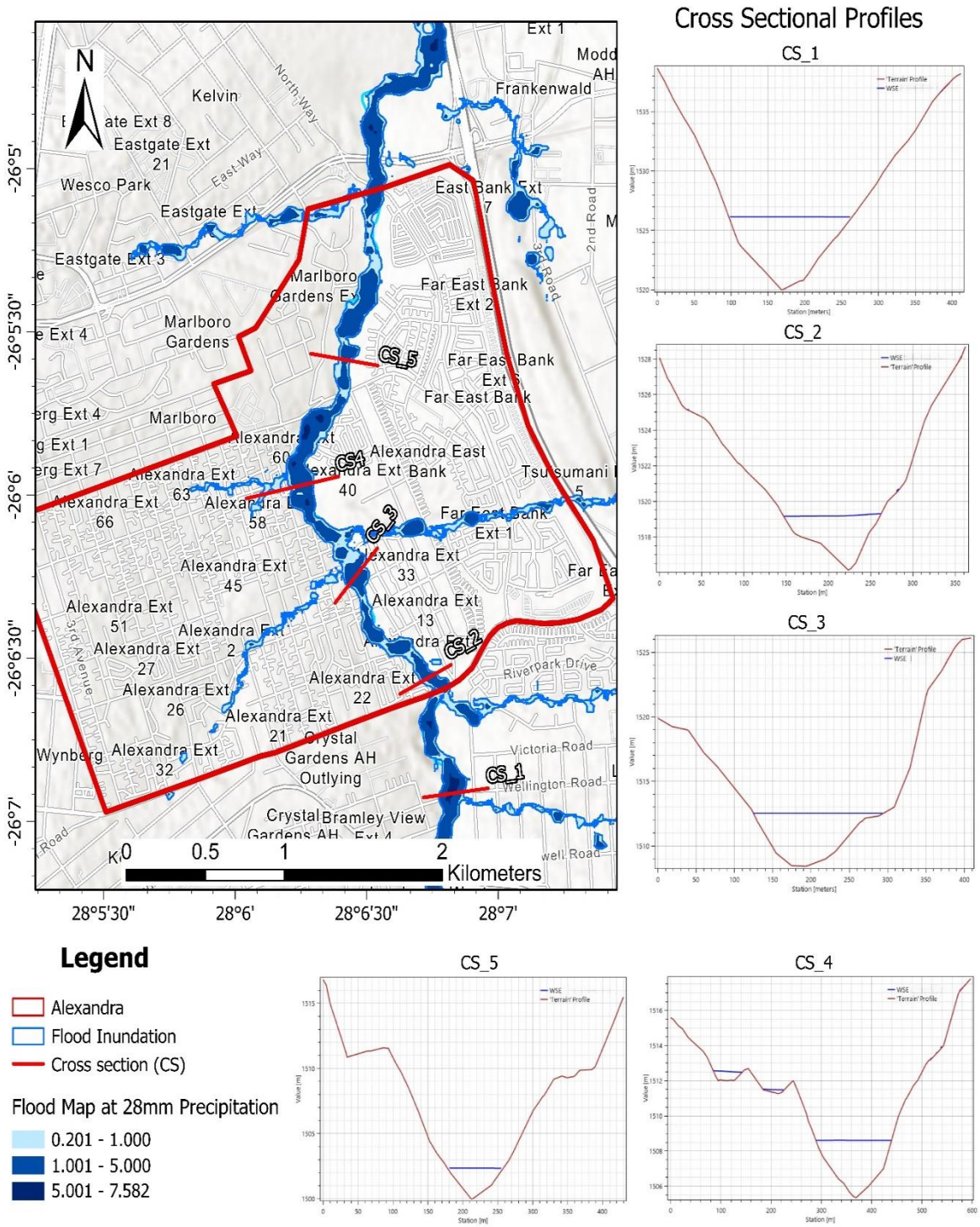

A

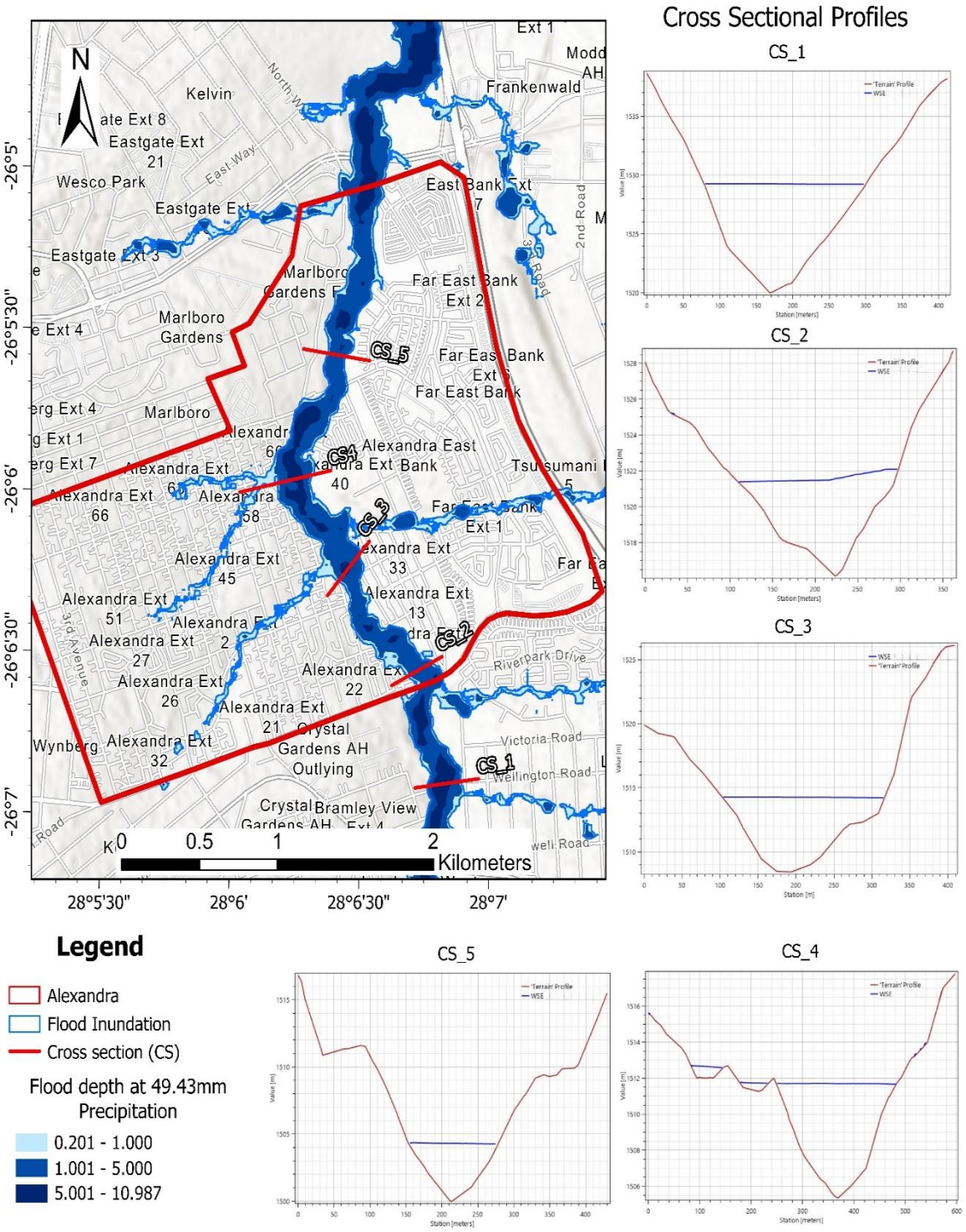
Cross Sectional Profiles
CS_1
CS_2
CS_3
CS_4
CS_5
Legend
Alexandra
Flood Inundation
Cross section (CS)
Flood depth at 49.43mm Precipitation
0.201 - 1.000
1.001 - 5.000
5.001 - 10.987
Kelvin
Eastgate Ext 21
Wesco Park
Eastgate Ext
Eastgate Ext 3
Marlboro Gardens
Marlboro
Alexandra East
Alexandra Ext 40
Alexandra Ext 66
Alexandra Ext 45
Alexandra Ext 51
Alexandra Ext 27
Alexandra Ext 26
Alexandra Ext 21
Alexandra Ext 32
Alexandra Ext 33
Alexandra Ext 13
Alexandra Ext 22
Crystal Gardens AH Outlying
Crystal Bramley View Gardens AH
Frankenwald
East Bank Ext 7
Far East Bank Ext 2
Far East Bank Ext 1
Tsunsumani
Riverpark Drive
Victoria Road
Wellington Road
North Way
East Way
3rd Avenue
2nd Road
3rd Road
CS_1
CS_2
CS_3
CS_4
CS_5
-26°5'
-26°5'30"
-26°6'
-26°6'30"
-26°7'
28°5'30"
28°6'
28°6'30"
28°7'
0
0.5
1
2
Kilometers

B

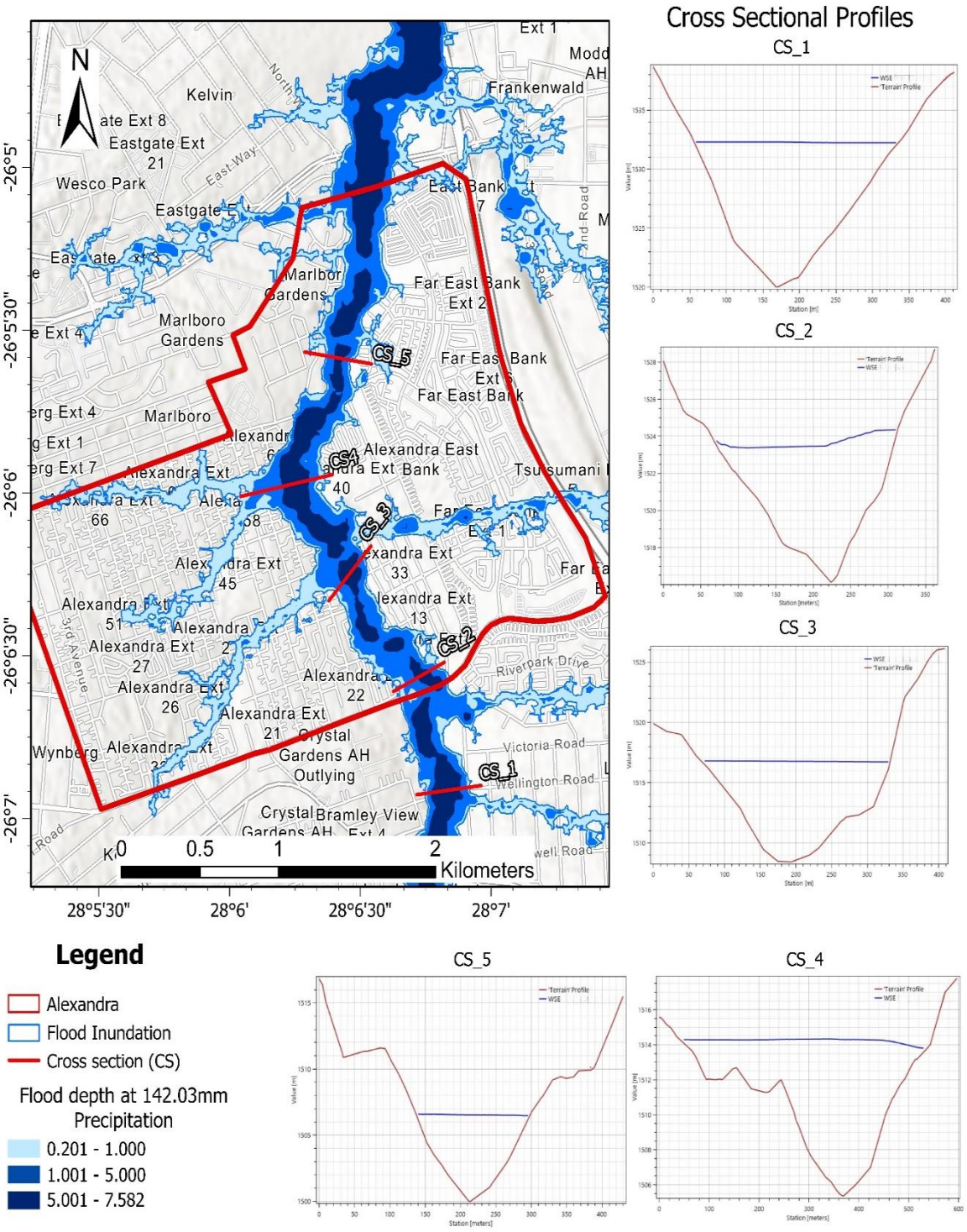

C

Figure 17. Cross-section showing depth at different amounts of precipitation at **A** (28mm), **B** (49.43mm) and **C** (142.03mm) at Alexandra.

4.6 Flood Velocity Map

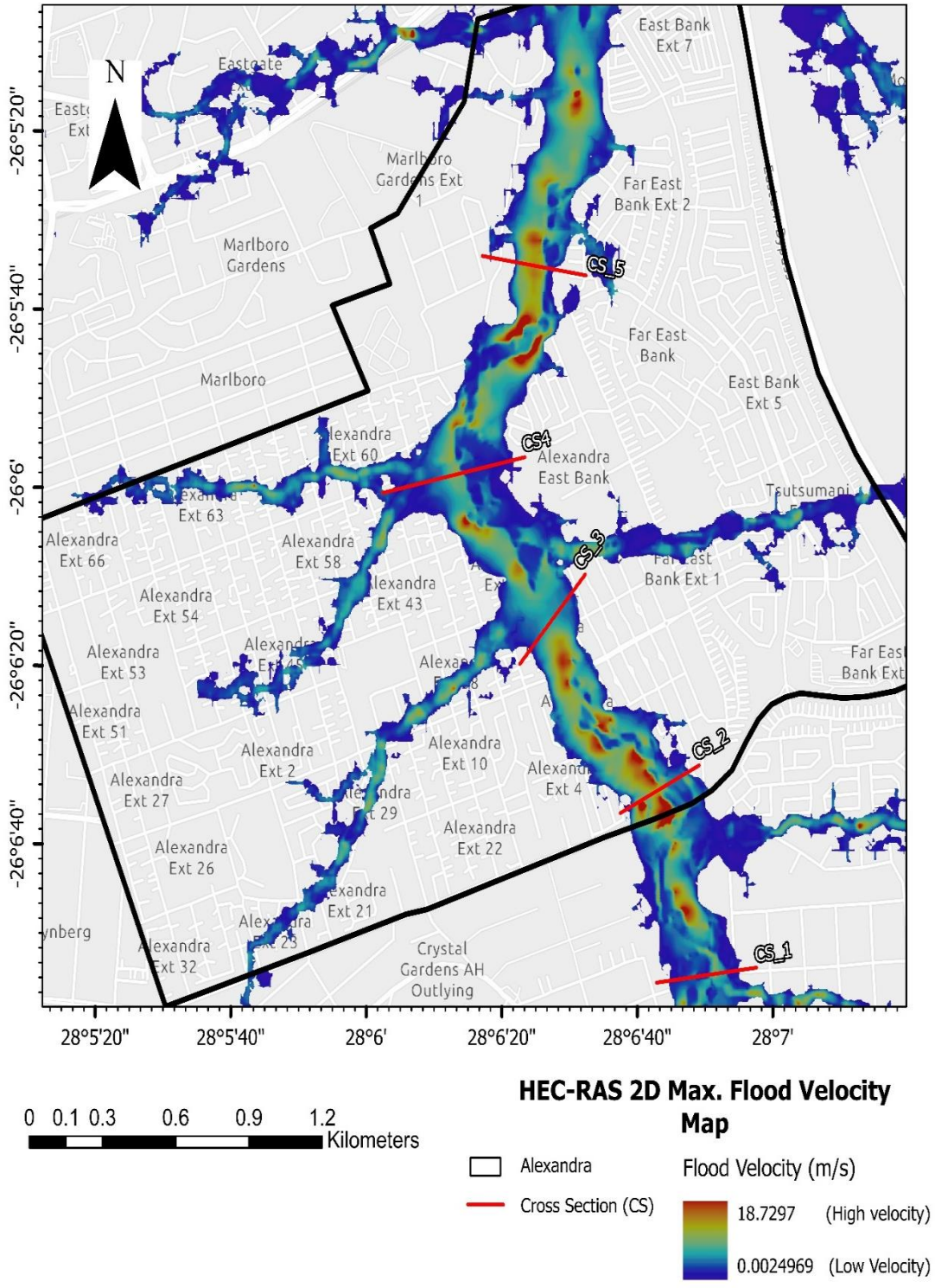

Figure 18. Flood hazard map of Alexandra, Johannesburg.

4.7 Model Calibration and Validation

During the calibration process, adjustments were continuously made to Manning's coefficient "n" until the disparities between observed and simulated inundations fell within acceptable limits. The validation involved a comparison between the model flood extent results at specific flow rates at a stage to observations. Since satellite imagery covering the day of the events was not available and where it was the imagery had a minimum of 70% cloud coverage, the results of the simulations were validated against findings from Mawasha and Britz (Mawasha & Britz, 2022). That was necessary because in a study undertaken by Mawasha and Britz, given the absence of satellite data during the specific days or weeks of the events, field validation was carried out within the catchment area to gather data for validating the flood model (Mawasha & Britz, 2022). Table 5 shows the list of LULC types with Chow's 1959 Manning's n values and the final Manning's n value for the dynamic flood model.

Table 5. Reference table for Manning roughness based on Chow-1959 (Soliman *et al*., 2022b).

Description	Manning's n Value Range	Final Manning's n Value
Grassland/Herbaceous	0.025 – 0.050	0.035
Barren Land (Rock/Sand/Clay)	0.023 – 0.030	0.270
Cultivated Land	0.020 – 0.050	0.035
Commercial/Developed, High Intensity	0.120 – 0.200	0.200
River/Open Water	0.025 – 0.050	0.035
Wetland/Open Water	0.045 – 0.150	0.025
Shrub/Scrub	0.070 – 0.160	0.115
Deciduous Forest	0.100 – 0.200	0.150

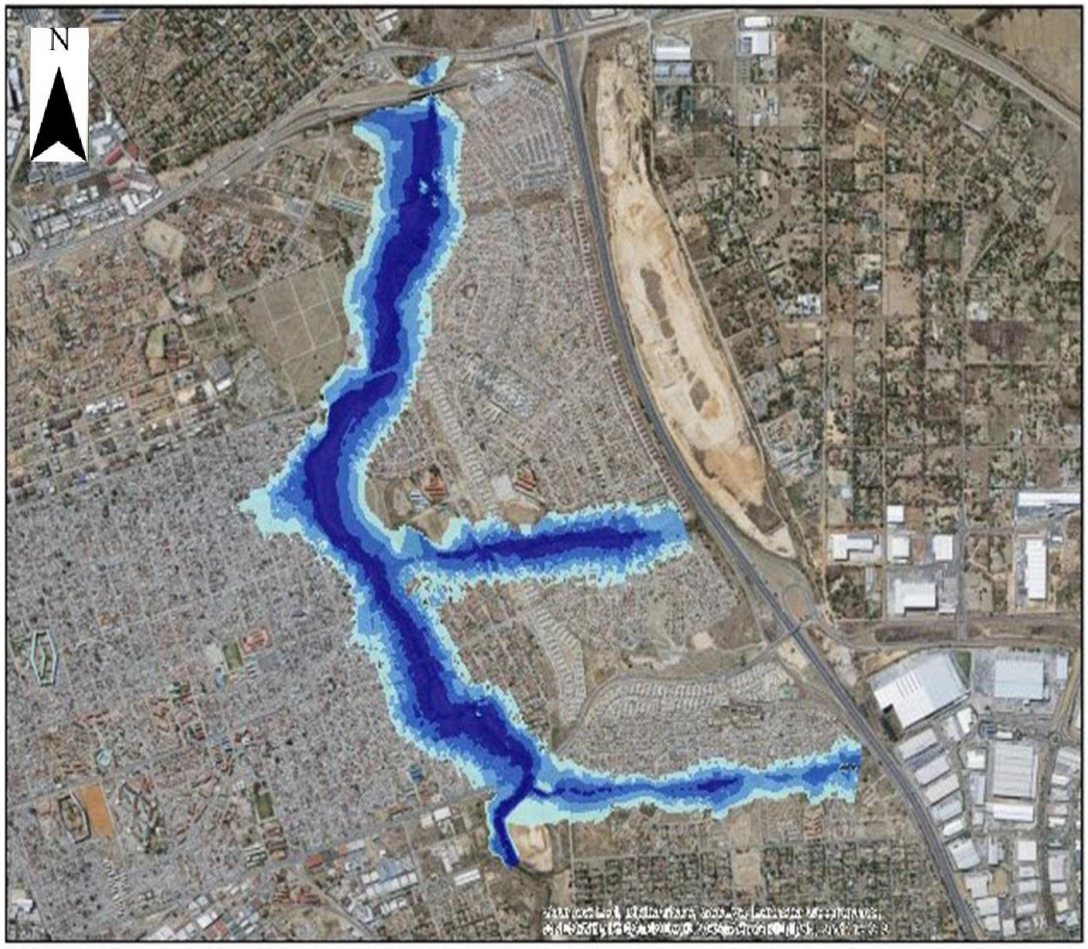

Figure 19. Validation imagery for the calibrated model. Source (Mawasha & Britz, 2022)

4.8 Discussion

There are various methods that can be employed to conduct flood analysis, including hydrological modelling, probabilistic analysis, geospatial analysis, statistical analysis, real-time monitoring, climate change impact assessment, and integrated approaches, among others. Most of these techniques rely on ground station datasets, real-time information, etc. This research presents a practical method for mapping flood hazards, aiming to assist informed management and decision-making for individuals with limited or no expertise in GIS and remote sensing, utilizing multiple factors such as precipitation, DEM, LULC and soil properties. Nevertheless, these influencing factors are interconnected, impacting flood inundation indirectly through chains of factors that contribute to disasters.

4.8.1 Effect of precipitation

The statistical results presented in Figure 5 and Figure 6 indicate that precipitation data has a notably more substantial effect on the catchment area. The maximum category is distinguished by irregularly elevated precipitation levels, constituting a trend identified with a 32% p-value and an R-value of 22%, confirming both the strength and the increase observed from the year 2000 to 2020. Conversely, the minimum category also demonstrated a decrease in precipitation, with 8.8% (p-value) of the data reflecting the underlying trend, and a -36% (R-value) confirming both the strength and direction of this decline. The average category exhibits a minimal difference in trend, with 8% (p-value) of the data elucidating the underlying trend, and a decrease of 5% (R-value) explaining the strength and direction. According to (Fischer *et al*., 2023), the interaction between severe dry land conditions over long durations followed by heavy rainfall events yields severe runoff which significantly influences flooding patterns and increases the risk of flood occurrence.

4.8.2 Effect of LULC

Research conducted by Tom and his colleagues in Nairobi highlighted that, despite the prevalence of city flooding, its impacts varied, with the informal settlements and urban poor bearing the brunt. This clearly illustrates the fundamental factors driving flood risk vulnerabilities throughout the urbanised poor. The ongoing and swift transformations in LULC, attributed to urbanisation, have played a role in the heightened runoff, leading to the occurrence of flooding in the city (Tom *et al*., 2022).

According to studies by Mawasha and Britz, the LULC increased by 22.5% between 1987 and 2015 resulting in an equivalent reduction of sparse and intact vegetation which is predominantly due to an increase in informal settlement driven by urbanisation into flood plains in Alexandra (Mawasha & Britz, 2022). The classified land use data involved the use of Sentinel-2 data obtained from the Department of Forestry, Fisheries, and the Environment (DFFE) in South Africa. The data showed about 96% built-up areas, with little to no vegetation in some parts

of Alexandra. The LULC dataset proved useful for assessing imperviousness and computing Manning's roughness coefficients for hydraulic modelling.

4.8.3 Effect of DEM (Topography)

The role of DEM in the delineation of watercourses in hydraulic flood models is essential to the accuracy and reliability of flood mapping. In this research, it was noted that using a 30-meter resolution Digital Elevation Model (DEM) caused water accumulation at the resolution's edges, in an effort to represent water flow between pixels, as pointed out by Saksena and Merwade (Saksena & Merwade, 2015). This effect was more pronounced with coarser resolution DEMs, leading to greater flood inundation areas (Saksena & Merwade, 2015). Again, the low resolution of the DEM hindered the accurate depiction of the River Jukskei during periods of low water levels following minimal precipitation in the simulation (Arash & Yasi, 2023).

4.8.4 Effect of Manning's roughness

From the hydraulic model calibration, the study found that the application of various Manning's roughness values can result in differences in inundation extent and travel times. Although the magnitude of this increase may not be significant, it was observed that lower Manning's roughness values in the floodplain led to a rise in travel times (Tuozzolo *et al*., 2019). According to Tuozzolo and colleagues, the variability of Manning's roughness coefficients, particularly with respect to channel depth, has a significant effect on river flow resistance, with riverbed resistance decreasing as river size increases (Tuozzolo *et al*., 2019).

4.8.5 Model Calibration and Validation

The research involved calibration and validation of HEC-RAS model to accurately simulate the flood. Despite variations in mathematical frameworks, complexity, and dimensionality, all flood models have their limitations and strengths. In that respect, a perfect model is almost impossible to simulate in isolating the natural hydrodynamic procedures and thus flooding of urban regions. The challenges of modelling urban floods are more pronounced in growing cities, where the physical processes and microenvironments play a substantial role in city flood dynamics. Consequently, it is crucial to accurately represent these factors in model simulations

(Tom *et al*., 2022). The calibration of models is an essential procedure that facilitates the use of present flood models in developing urban areas. Nevertheless, discussions regarding model calibration consistently emphasize the necessity of identifying and integrating uncertainties into the modelling process to guarantee that the results are sufficiently meaningful for the study area (Dottori *et al*., 2013). This was achieved by utilizing Manning's value based on the LULC data by DFFE of South Africa, along with precipitation data specific to Alexandra township. Consequently, Chow's Manning coefficients data was used for calibration of the hydraulic models in WMS, and HEC-RAS. The flooding pattern produced through the 1D and 2D hydraulic modelling approach using WMS and HEC-RAS in the Alexandra region of the basin closely resembles the findings reported in studies carried out by (Mawasha & Britz, 2022) as well in validation as shown in Figure 19.

4.8.6 Hydraulic Model

The results as shown in the flood hazard and flood risk maps as well as in Table 2, Table 3, and

Table *4* gives a breakdown of precipitation against water surface elevation (WSE), water depth and volume of water through a station in the model at Alexandra. According to the breakdown in Table 2, with a 39.69 mm increase in precipitation has a corresponding WSE of 1509.25 m, depth of 3.24 m and volume of 891.21 m^3. With the average slope on the left bank at 0.057 and on the right bank at 0.064, it distinctly illustrates how water inundates the banks leading to the settlement at Alexandra.

The outcome presents a summary of the research area, aiming to comprehend the difficulties encountered by those residing in high-risk areas. It is anticipated that this will strongly encourage city officials to recognize and implement effective countermeasures. These measures must factor in safe areas within the catchment area, away from the riverbanks which substantially exceeds the elevation covered by the flood model. In addition, since the catchment is low-lying with the meandering river channel, I suggest authorities and local government take steps to protect the riverbanks from excessive erosion. Furthermore, the

catchment will benefit from further studies to estimate silt and debris transport and deposits from dynamic floods.

CHAPTER 5: CONCLUSION AND RECOMMENDATIONS

5.1 Conclusion

In this study, various parameters including LULC, DEM, soil types, and precipitation data spanning a 20-year period were utilized to evaluate the effects of dynamic flooding in Alexandra, Johannesburg. Employing HEC-RAS and GIS techniques, these parameters proved effective in analysing flood impacts within the Alexandra catchment area. Precipitation statistics were employed to examine trends in rainfall fluctuations over the specified time frame. Additionally, dynamic modelling techniques were employed to identify inundation changes, with GIS facilitating the assessment of impacts within the catchment area. The dynamic flood analysis aimed to quantify flood impacts based on varying amounts of rainfall over time, categorized into two levels: (1) precipitation analysis over the 20-year period, and (2) assessing the flood's impact on community infrastructure for three levels of rainfall intensity. R and P value analyses were conducted to discern precipitation trends, while diffusion wave analysis was employed to model dynamic flooding in Alexandra. The research effectively achieved its objectives, leading to the following conclusion:

In this study, various parameters including LULC, DEM, soil types, and precipitation. The precipitation data spanning a 20-year period were utilized to evaluate the effects of climate change in Alexandra, Johannesburg, whereas the other parameters including precipitation for the month of November 2016 was used in modelling the dynamic flood modelling. From the study, it was proven that Geographical Information Systems (GIS) and remote sensing are valuable tools for identifying environmental hazards, particularly floods. By integrating remote sensing data with field studies and software like HEC-RAS, it is possible to determine flood-prone areas, establish construction limits, and set criteria for flood zoning. The primary benefits of using GIS in flood management lies not only in its ability to visualize flooding but also in its capacity to further analyze this data to estimate potential flood damage. These advancements offer a more efficient and accurate alternative to traditional methods of studying riverine floods. The dynamic flood analysis aimed to quantify flood impacts based on varying amounts of rainfall

over time, categorized into two levels: (1) precipitation analysis over a month, and (2) assessing the flood's impact on community infrastructure for three levels of rainfall intensity. R and P value analyses were conducted to discern precipitation trends, while diffusion wave analysis was employed to model dynamic flooding in Alexandra. The research effectively achieved its objectives, leading to the following conclusion:

I. The precipitation data spanning 20 years from 2000 to 2020 in Alexandra was collected for this study. Analysis of the precipitation data revealed varying amounts of rainfall across the four seasons, with Spring, Summer, and Autumn exhibiting higher records of rainfall. The highest average rainfall of 142.03 mm was observed during the Autumn season in March 2016, while the lowest average of 35.23 mm occurred during the summer season in November 2006. The average R-square value for these three seasons was determined to be 0.0638. Additionally, an increasing trend in overall rainfall was noted, with an R-value of 0.15 for the yearly maximum precipitation over the 20-year period which was largely influenced by irregular high rainfall. Conversely, a decreasing trend was observed in the yearly minimum precipitation over the same period, with an R-value of 0.42.

II. In this study, the effect of flooding on the catchment area of Alexandra was examined. The hazards and inundations observed following rainfall events of 28 mm, 49.43 mm, and 142.03 mm indicated instances of flooding in Alexandra, posing risks to property and livelihoods across the three categories. Specifically, the number of buildings affected by 28 mm of rainfall was determined to be 1,473, covering an area of 324,268 square meters. This number increased by 47.45%, reaching a total inundation area of 526,216 square meters, when precipitation levels rose to 49.43 mm. Subsequently, with a precipitation level of 142.03 mm, the percentage increase in affected buildings surged by 61.3%, resulting in a total inundation area of 1,137,908 square meters.

5.2 Recommendations

Based on the findings and considerations of this thesis, it is strongly recommended to enhance the accuracy and precision of future studies in hydraulic analysis and environmental modelling through the following measures:

Misrepresentation of LULC classes by low multispectral resolution analysis in hydraulic modelling within HEC-RAS can present several implications. The limited spectral information hampers the discrimination of diverse land cover types, leading to oversimplified classifications and potential loss of fine-scale features. Mixed pixels and inaccuracies in surface roughness representation may arise, impacting the precision of hydraulic modelling. Particularly in urban areas, challenges in distinguishing impervious surfaces, vegetation, and water bodies may compromise the accuracy of flood simulations. A LULC with a high spatial resolution of 0.5 meters is recommended for better replication of surface roughness.

With accurate daily precipitation data, the hydraulic model will yield a better representation of the flood event. Higher temporal resolution enables the precise representation of individual rainfall events, capturing short-duration, intense rainfalls crucial for modelling flash floods. Detailed temporal data facilitates the realistic simulation of rainfall patterns, contributing to accurate predictions of peak flow rates during flood events. Additionally, fine temporal resolution enhances the understanding of hydrological processes such as surface runoff and infiltration, leading to improved insights into how precipitation interacts with the watershed. This level of detail aids in better-representing storm duration, essential for estimating total rainfall volume and its impact on flooding. Furthermore, the availability of high temporal resolution data supports improved calibration and validation of hydraulic models, enhancing their accuracy by aligning simulated hydrographs with observed data at small time intervals. If available, a precise daily or hourly representation of precipitation is recommended for improving the reliability and effectiveness of hydraulic flood models.

Due to a lack of high-resolution DEM (1-5m) not available for the conducted studies, stagnant water pools were observed in concealed areas within the catchment, and water flow was impeded at specific precipitation levels in the designated reach. High spatial resolution ensures a detailed representation of the

Earth's surface, capturing subtle variations in elevation that are essential for accurate modelling of flow paths and inundation patterns during floods. This level of detail is particularly crucial in urban areas, where complex topography requires precise representation for modelling flood scenarios with accuracy. Additionally, fine spatial resolution aids in the identification of small-scale features, such as channels and depressions, contributing to a more realistic simulation of water flow and the prediction of flood-prone areas. High-resolution DEMs also improve the modelling of small water bodies, enhance the representation of river and stream channel networks, and enable more accurate mapping of floodplains. Ultimately, the spatial resolution of DEMs plays a crucial role in improving the reliability of hydraulic flood models, providing crucial insights for flood risk assessment and mitigation strategies. As discussed by (Annis *et al*., 2020; Hawker *et al*., 2018; Thomas Steven Savage *et al*., 2016). Considering the widest portion of the river in the study area is 25m, it is recommended that a higher-resolution DEM to describe the river channel be used for real replication of terrain and more effective model performance.

Implementing these recommendations will contribute to the advancement of research in environmental science and hydraulic modelling, fostering a more comprehensive assessment of the dynamics influencing LULC, precipitation patterns, and river channels.

REFERENCES

A Web-GIS Platform for Floods Risk Mapping Case Study: The Floodplain of Khartoum State. (2022). A WEB-GIS PLATFORM FOR FLOODS RISK MAPPING CASE STUDY: THE FLOODPLAIN OF KHARTOUM STATE. *International Research Journal of Modernization in Engineering Technology and Science*. https://doi.org/10.56726/irjmets29456

Addison-Atkinson, W., Chen, A. S., Memon, F. A., & Chang, T. J. (2022). Modelling urban sewer flooding and quantitative microbial risk assessment: A critical review. In *Journal of Flood Risk Management* (Vol. 15, Issue 4). John Wiley and Sons Inc. https://doi.org/10.1111/jfr3.12844

Ahmad, B., Alam, A., Bhat, M. S., Bhat, K. A., Haq, J. I. ul, Ahmad, H. F., & Qadir, J. (2021). Retracing Realistic Disaster Scenarios from Archival Sources: A Key Tool for Disaster Risk Reduction. *International Journal of Disaster Risk Science*, *12*(5), 635–648. https://doi.org/10.1007/s13753-021-00363-5

Ahmadisharaf, E., & Kalyanapu, A. J. (2019). A coupled probabilistic hydrologic and hydraulic modelling framework to investigate the uncertainty of flood loss estimates. *Journal of Flood Risk Management*, *12*. https://doi.org/10.1111/jfr3.12536

Ahmadisharaf, E., Kalyanapu, A. J., & Chung, E. S. (2017). Sustainability-based flood hazard mapping of the Swannanoa River watershed. *Sustainability (Switzerland)*, *9*(10). https://doi.org/10.3390/su9101735

Akiyode, O., Tumushabe, A., Hadijjah, K., & Onu, P. (2017). Climate Change, Food Security and Environmental Securi-Ty : A Conflict Inclination Assessment of Karamoja Region of Uganda. In *International Journal of Scientific World*. https://doi.org/10.14419/ijsw.v5i2.8458

Aldardasawi, A. F. M., & Eren, B. (2021). Floods and Their Impact on the Environment. *Academic Perspective Procedia*, *4*(2), 42–49. https://doi.org/10.33793/acperpro.04.02.24

Alexandra, South Africa - Wikipedia. (n.d.). Retrieved March 8, 2024, from https://en.wikipedia.org/wiki/Alexandra,_South_Africa.

Alhassan, H. (2020). Farm households' flood adaptation practices, resilience and food security in the Upper East region, Ghana. *Heliyon*, *6*(6). https://doi.org/10.1016/j.heliyon.2020.e04167

Alsilibe, F., & Bene, K. (2022). Watershed subdivision and weather input effect on streamflow simulation using SWAT model. *Pollack Periodica*, *17*(1), 88–93. https://doi.org/10.1556/606.2021.00349

Amarnath, C. R., & Thatikonda, S. (2020). Study on backwater effect due to Polavaram Dam Project under different return periods. *Water (Switzerland)*, *12*(2). https://doi.org/10.3390/w12020576

Annis, A., Nardi, F., Petroselli, A., Apollonio, C., Arcangeletti, E., Tauro, F., Belli, C., Bianconi, R., & Grimaldi, S. (2020). UAV-DEMs for small-scale flood hazard mapping. *Water (Switzerland)*, *12*(6). https://doi.org/10.3390/w12061717

Anuruddhika, M. L. P., Perera, K. K. K. R., Premarathna, L. P. N. D., Hansameenu, W. P. T., & Weerasinghe, V. P. A. (2022). Forecasting flood inundation areas of Attanagalu Oya. *Ceylon Journal of Science*, *51*(3), 217. https://doi.org/10.4038/cjs.v51i3.8030

Arafat, Y., Tunas, I., Amaliah, T., & Amiruddin, A. (2020). Hydrograph Study of Palu River Watershed. *MATEC Web of Conferences*, *331*, 04001. https://doi.org/10.1051/matecconf/202033104001

Arash, A. M., & Yasi, M. (2023). The assessment for selection and correction of RS-based DEMs and 1D and 2D HEC-RAS models for flood mapping in different river types. *Journal of Flood Risk Management*, *16*(1), e12871. https://doi.org/10.1111/JFR3.12871

Armain, M. Z. S., Hassan', Z., Mohd Remy Rozainy, M. A. Z., & Kamarudzaman, A. N. (2021). Hydrodynamic modelling of historical flood event using one dimensional HEC-RAS in Kelantan basin, Malaysia. *IOP Conference Series: Earth and Environmental Science*, *920*(1). https://doi.org/10.1088/1755-1315/920/1/012031

Bailey, R., Rathjens, H., Bieger, K., Chaubey, I., & Arnold, J. (2017). SWATMOD-Prep: Graphical User Interface for Preparing Coupled SWAT-MODFLOW Simulations. *Journal of the American Water Resources Association*, *53*(2), 400–410. https://doi.org/10.1111/1752-1688.12502

Baudoin, M. A., Henly-Shepard, S., Fernando, N., Sitati, A., & Zommers, Z. (2016). From Top-Down to "Community-Centric" Approaches to Early Warning Systems: Exploring Pathways to Improve Disaster Risk Reduction Through Community Participation. *International Journal of Disaster Risk Science*, *7*(2), 163–174. https://doi.org/10.1007/s13753-016-0085-6

Beck, Zammit-Mangion, Fry, Smith, & Gabbe. (2021). Spatiotemporal mapping of major trauma in Victoria, Australia. *PLoS ONE*.

Bezak, N., Šraj, M., Rusjan, S., & Mikoš, M. (2018). Impact of the rainfall duration and temporal rainfall distribution defined using the Huff curves on the hydraulic flood modelling results. *Geosciences (Switzerland)*, *8*(2). https://doi.org/10.3390/geosciences8020069

Bhardwaj, J., Asghari, A., Aitkenhead, I., Jackson, M., & Kuleshov, Y. (2021). Climate Risk and Early Warning Systems: Adaptation Strategies for the Most Vulnerable Communities. *Journal of Science Policy & Governance*, *18*(02). https://doi.org/10.38126/jspg180201

Brunner, M. I., Slater, L., Tallaksen, L. M., & Clark, M. (2021). Challenges in modeling and predicting floods and droughts: A review. In *Wiley Interdisciplinary Reviews: Water* (Vol. 8, Issue 3). John Wiley and Sons Inc. https://doi.org/10.1002/wat2.1520

Chao, Y. C., Chen, C. W., Li, H. C., & Chen, Y. M. (2018). Riverbed Migrations in Western Taiwan under Climate Change. *Water 2018, Vol. 10, Page 1631*, *10*(11), 1631. https://doi.org/10.3390/W10111631

Chen, L.-L., & Tseng, d C.-H. (2019). Climate Change Adaptation and Disaster Reduction Risk Applying Method in Industrial Supply Chain Process. *Passive Remote Study of the Aerosol in the Upper Atmosphere of the Earth*, 1–6. https://doi.org/10.47363/JEESR/2019(1)108

Chen, W., Xu, J., & Li, S. (2020). Prediction of Meteorological Drought in the Lower Nu River by Statistical Model. *American Journal of Climate Change*, *09*(02), 87–99. https://doi.org/10.4236/ajcc.2020.92007

Ciullo, A., Viglione, A., Castellarin, A., Crisci, M., & Di Baldassarre, G. (2017). Socio-hydrological modelling of flood-risk dynamics: comparing the resilience of green and technological systems. *Hydrological Sciences Journal*, *62*(6), 880–891. https://doi.org/10.1080/02626667.2016.1273527

CIWEM. (2020). Flood risk management in Africa. *Journal of Flood Risk Management*, *13*(3). https://doi.org/10.1111/jfr3.12612

Cordell, D., Unsworth, M. J., Lee, B., Díaz, D., Bennington, N. L., & Thurber, C. H. (2020). Integrating Magnetotelluric and Seismic Images of Silicic Magma Systems: A Case Study From the Laguna del Maule Volcanic Field, Central Chile. *Journal of Geophysical Research: Solid Earth*, *125*(11). https://doi.org/10.1029/2020JB020459

Costabile, P., Costanzo, C., Ferraro, D., Macchione, F., & Petaccia, G. (2020). Performances of the new HEC-RAS version 5 for 2-D hydrodynamic-based rainfall-runoff simulations at basin scale: Comparison with a state-of-the art model. *Water (Switzerland)*, *12*(9). https://doi.org/10.3390/W12092326

Cui, Y., Liang, Q., Wang, G., Zhao, J., Hu, J., Wang, Y., & Xia, X. (2019). Simulation of hydraulic structures in 2D high-resolution urban flood modeling. *Water (Switzerland)*, *11*(10). https://doi.org/10.3390/w11102139

Dang, A. T. N., & Kumar, L. (2017). Application of remote sensing and GIS-based hydrological modelling for flood risk analysis: a case study of District

8, Ho Chi Minh city, Vietnam. *Geomatics, Natural Hazards and Risk*, *8*(2), 1792–1811. https://doi.org/10.1080/19475705.2017.1388853

Das, G., & Lepcha, K. (2019). Application of logistic regression (LR) and frequency ratio (FR) models for landslide susceptibility mapping in Relli Khola river basin of Darjeeling Himalaya, India. *SN Applied Sciences*, *1*(11). https://doi.org/10.1007/s42452-019-1499-8

Dept. of Transport and Main Roads, & State of QLD. (2019). *Technical Guideline Hydrologic and Hydraulic Modelling*. Queensland Government, Dept. of Transport and Main Roads. https://www.tmr.qld.gov.au/business-industry/Technical-standards-publications/Hydro\logic-and-Hydraulic-Modelling

Deshays, R., Segovia, P., & Duviella, E. (2021). Design of a matlab hec-ras interface to test advanced control strategies on water systems. *Water (Switzerland)*, *13*(6). https://doi.org/10.3390/w13060763

Dhungel, S., Barber, M. E., & Mahler, R. L. (2019). Comparison of one- And two-dimensional flood modeling in urban environments. *International Journal of Sustainable Development and Planning*, *14*(4), 356–366. https://doi.org/10.2495/SDP-V14-N4-356-366

Didier, D., Baudry, J., Bernatchez, P., Dumont, D., Sadegh, M., Bismuth, E., Bandet, M., Dugas, S., & Sévigny, C. (2019). Multihazard simulation for coastal flood mapping: Bathtub versus numerical modelling in an open estuary, Eastern Canada. *Journal of Flood Risk Management*, *12*(S1). https://doi.org/10.1111/jfr3.12505

Diogo, A. F., & do Carmo, J. A. (2019). Peak flows and stormwater networks design-current and future management of urban surface watersheds. *Water (Switzerland)*, *11*(4). https://doi.org/10.3390/w11040759

Do, V. Q., Phung, M. L., Truong, D. T., Pham, T. T. T., Dang, V. T., & Nguyen, T. K. (2021). The impact of extreme events and climate change on agricultural and fishery enterprises in central Vietnam. *Sustainability (Switzerland)*, *13*(13). https://doi.org/10.3390/su13137121

Dottori, F., Di Baldassarre, G., & Todini, E. (2013). Detailed data is welcome, but with a pinch of salt: Accuracy, precision, and uncertainty in flood inundation modeling. *Water Resources Research*, *49*(9), 6079–6085. https://doi.org/10.1002/wrcr.20406

Dube, E., Mtapuri, O., & Matunhu, J. (2018). *Managing flood disasters on the built environment in the rural communities of Zimbabwe: Lessons learnt*. https://doi.org/10.4102/jamba

Dysarz, T. (2018). Application of python scripting techniques for control and automation of HEC-RAS simulations. *Water (Switzerland)*, *10*(10). https://doi.org/10.3390/w10101382

Echendu, A. J. (2020). The impact of flooding on Nigeria's sustainable development goals (SDGs). *Ecosystem Health and Sustainability*, *6*(1). https://doi.org/10.1080/20964129.2020.1791735

Echogdali, F. Z., Boutaleb, S., Elmouden, A., & Ouchchen, M. (2018). Assessing Flood Hazard at River Basin Scale: Comparison between HECRAS-WMS and Flood Hazard Index (FHI) Methods Applied to El Maleh Basin, Morocco. *Journal of Water Resource and Protection*, *10*(09), 957–977. https://doi.org/10.4236/jwarp.2018.109056

Edmonds, D. A., Caldwell, R. L., Brondizio, E. S., & Siani, S. M. O. (2020). Coastal flooding will disproportionately impact people on river deltas. *Nature Communications*, *11*(1). https://doi.org/10.1038/s41467-020-18531-4

Environmental Modeling Research Laboratory of Brigham Young University, & Aquaveo LLC. (2016). *WMS User Manual (v10.1) The Watershed Modeling System*.

Everett, J. D., Baird, M. E., Buchanan, P., Bulman, C., Davies, C., Downie, R., Griffiths, C., Heneghan, R., Kloser, R. J., Laiolo, L., Lara-Lopez, A., Lozano-Montes, H., Matear, R. J., McEnnulty, F., Robson, B., Rochester, W., Skerratt, J., Smith, J. A., Strzelecki, J., … Richardson, A. J. (2017). Modeling what we sample and sampling what we model: Challenges for zooplankton model assessment. In *Frontiers in Marine Science* (Vol. 4, Issue MAR). Frontiers Media S. A. https://doi.org/10.3389/fmars.2017.00077

Fang, J., Lau, C. K. M., Lu, Z., Wu, W., & Zhu, L. (2019). Natural disasters, climate change, and their impact on inclusive wealth in G20 countries. *Environmental Science and Pollution Research*, *26*(2), 1455–1463. https://doi.org/10.1007/s11356-018-3634-2

Fang, S., Ji, Y., & Zhang, M. (2022). Numerical Modeling the Flood and Pollutant Transport Processes in Residential Areas with Different Land Use Types. *Advances in Meteorology*, *2022*. https://doi.org/10.1155/2022/9320089

Farooq, M. S., Tehseen, R., Qureshi, J. N., Omer, U., Yaqoob, R., Tanweer, H. A., & Atal, Z. (2023). FFM: Flood Forecasting Model Using Federated Learning. *IEEE Access*, *11*, 24472–24483. https://doi.org/10.1109/ACCESS.2023.3252896

Fischer, S., Lun, D., Schumann, A. H., & Blöschl, G. (2023). Detecting flood-type-specific flood-rich and flood-poor periods in peaks-over-threshold series with application to Bavaria (Germany). *Stochastic Environmental Research and Risk Assessment*, *37*(4), 1395–1413. https://doi.org/10.1007/s00477-022-02350-8

Frongia, S., Sechi, G. M., & Davison, M. (2016). *Tangible and Intangible Flood damage evaluation*. https://doi.org/10.1051/05007

Garvelmann, J., Pohl, S., & Weiler, M. (2015). Spatio-temporal controls of snowmelt and runoff generation during rain-on-snow events in a mid-latitude mountain catchment. *Hydrological Processes*, *29*(17), 3649–3664. https://doi.org/10.1002/hyp.10460

Ghobadian, & Khalaj. (2015). Incorporating seepage losses into a 1D unsteady model of floods in an ephemeral stream. *African Journals Online*, *14*.

Gillies, M. H., & Smith, R. J. (2015a). SISCO: surface irrigation simulation, calibration and optimisation. *Irrigation Science*, *33*(5), 339–355. https://doi.org/10.1007/s00271-015-0470-8

Gillies, M. H., & Smith, R. J. (2015b). SISCO: surface irrigation simulation, calibration and optimisation. *Irrigation Science*, *33*(5), 339–355. https://doi.org/10.1007/S00271-015-0470-8

Goswami, G., Prasad, R. K., & Kumar, D. (2023). Hydrodynamic flood modeling of Dikrong River in Arunachal Pradesh, India: a simplified approach using HEC-RAS 6.1. *Modeling Earth Systems and Environment*, *9*(1), 331–345. https://doi.org/10.1007/s40808-022-01507-2

Greenland, S., Senn, S. J., Rothman, K. J., Carlin, J. B., Poole, C., Goodman, S. N., & Altman, D. G. (2016). Statistical tests, P values, confidence intervals, and power: a guide to misinterpretations. *European Journal of Epidemiology*, *31*(4), 337–350. https://doi.org/10.1007/s10654-016-0149-3

Gude, V., Corns, S., & Long, S. (2020). Flood Prediction and Uncertainty Estimation Using Deep Learning. *Water (Switzerland)*, *12*(3). https://doi.org/10.3390/w12030884

Gurung, N., Fort, M., Bell, R., Arnaud-Fassetta, G., & Maharjan, N. R. (2021). Hydro-torrential hazard vs. anthropogenic activities along the Seti valley, Kaski, Nepal: Assessment and recommendations from a risk perspective. *Journal of Nepal Geological Society*, *62*, 58–87. https://doi.org/10.3126/jngs.v62i0.38695

Haba, Z. (2020). Power spectrum of stochastic wave and diffusion equations in the warm inflation models. *European Physical Journal C*, *80*(6). https://doi.org/10.1140/epjc/s10052-020-8135-z

Haddad, K., & Rahman, A. (2023). Dimensionality reduction for regional flood frequency analysis: Linear versus nonlinear methods. *Hydrological Processes*, *37*(4). https://doi.org/10.1002/hyp.14864

Hagg, W., Ram, S., Klaus, A., Aschauer, S., Babernits, S., Brand, D., Guggemoos, P., & Pappas, T. (2021). Hazard assessment for a glacier lake outburst flood in the mo chu river basin, bhutan. *Applied Sciences (Switzerland)*, *11*(20). https://doi.org/10.3390/app11209463

Hai, Z., & Perlman, R. L. (2022). *Extreme weather events and the politics of climate change attribution*. *8*, 2190. https://doi.org/10.17605/OSF.IO/5Q3AU

Hannum, R. M. F., Santikayasa, I. P., & Dasanto, B. D. (2022). Evaluation of Flood Hazard Potency in Jakarta based on Multi-criteria Analysis. *Agromet*, *36*(2), 101–111. https://doi.org/10.29244/j.agromet.36.2.101-111

Hawker, L., Rougier, J., Neal, J., Bates, P., Archer, L., & Yamazaki, D. (2018). Implications of Simulating Global Digital Elevation Models for Flood Inundation Studies. *Water Resources Research*, *54*(10), 7910–7928. https://doi.org/10.1029/2018WR023279

Hegger, D. L. T., Driessen, P. P. J., Wiering, M., Van Rijswick, H. F. M. W., Kundzewicz, Z. W., Matczak, P., Crabbé, A., Raadgever, G. T., Bakker, M. H. N., Priest, S. J., Larrue, C., & Ek, K. (2016). Toward more flood resilience: Is a diversification of flood risk management strategies the way forward? *Ecology and Society*, *21*(4). https://doi.org/10.5751/ES-08854-210452

HIRCA, T., & SÖNMEZ, O. (2019). Determination of Flood Inundation Maps: A Case Study of Akyazi Industrial Zone. *Sakarya University Journal of Science*, *23*(2), 301–307. https://doi.org/10.16984/saufenbilder.475974

Hoseini, Y. (2022). Evaluation of WMS model in basins without statistical data in southwestern Iran using Dicken's experimental method (case study: Kuhgel Basin of Khuzestan Province). *Applied Water Science*, *12*(7). https://doi.org/10.1007/s13201-022-01685-5

Hoseini, Y., Azari, A., & Pilpayeh, A. (2017). Flood modeling using WMS model for determining peak flood discharge in southwest Iran case study: Simili basin in Khuzestan Province. *Applied Water Science*, *7*(6), 3355–3363. https://doi.org/10.1007/s13201-016-0482-4

Huang, S., Wang, H., Xu, Y., She, J., & Huang, J. (2021). Key disaster-causing factors chains on urban flood risk based on bayesian network. *Land*, *10*(2), 1–21. https://doi.org/10.3390/land10020210

Huang, X. D., Wang, L., Han, P. P., & Wang, W. C. (2018). Spatial and temporal patterns in nonstationary flood frequency across a forest watershed: Linkage with rainfall and land use types. *Forests*, *9*(6). https://doi.org/10.3390/f9060339

Irwin, S., Schardong, A., Simonovic, S. P., & Nirupama, N. (2016). ResilSIM-A decision support tool for estimating resilience of urban systems. *Water (Switzerland)*, *8*(9). https://doi.org/10.3390/w8090377

Ishikawa, S., Todo, M., Taki, M., Uchiyama, Y., Matsunaga, K., Lin, P., Ogihara, T., & Yasui, M. (2023). *Example-Based Explainable AI and its Application for Remote Sensing Image Classification*. http://arxiv.org/abs/2302.01526

Kalbani, K. Al, & Rahman, A. A. (2022). 3D city model for monitoring flash flood risks in Salalah, Oman. *International Journal of Engineering and Geosciences*, *7*(1), 17–23. https://doi.org/10.26833/ijeg.857971

Kao, L. S., Chiu, Y. H., & Tsai, C. Y. (2017). An evaluation study of urban development strategy based on of extreme climate conditions. *Sustainability (Switzerland)*, *9*(2). https://doi.org/10.3390/su9020284

Kay, A. D., Lager, Z., Bhebheza, L., & Heinen-Kay, J. L. (2023). Integrating remote international experience and community engagement into course-based animal behavior research. *Ecology and Evolution*, *13*(1). https://doi.org/10.1002/ece3.9721

Kazezyilmaz-Alhan, C. M. (2012). An improved solution for diffusion waves to overland flow. *Applied Mathematical Modelling*, *36*(9), 4165–4172. https://doi.org/10.1016/j.apm.2011.11.045

Kelman, I. (2017). Linking disaster risk reduction, climate change, and the sustainable development goals. *Disaster Prevention and Management*, *26*(3), 254–258. https://doi.org/10.1108/DPM-02-2017-0043

Kelman, I., Gaillard, J. C., & Mercer, J. (2015). Climate Change's Role in Disaster Risk Reduction's Future: Beyond Vulnerability and Resilience. *International Journal of Disaster Risk Science*, *6*(1), 21–27. https://doi.org/10.1007/s13753-015-0038-5

Kemter, M., Merz, B., Marwan, N., Vorogushyn, S., & Blöschl, G. (2020). Joint Trends in Flood Magnitudes and Spatial Extents Across Europe. *Geophysical Research Letters*, *47*(7). https://doi.org/10.1029/2020GL087464

Khadraoui, N., Dahri, N., Bouamrane, A., Pham, Q. B., & Abida, H. (2023). Flood susceptibility mapping using qualitative and statistical methods in a semi-arid basin: case of the Manouba–Sijoumi watershed, Northeastern Tunisia. *Acta Geophysica*, *71*(5), 2307–2323. https://doi.org/10.1007/s11600-022-00966-6

Khan, I., Lei, H., Ashfaq, &, Shah, A., Khan, I., & Muhammad, I. (2021). *Climate change impact assessment, flood management, and mitigation strategies in Pakistan for sustainable future*. https://doi.org/10.1007/s11356-021-12801-4/Published

Khaskhelly, N., Sindh, A. T., Mughal, S., & Khushnood, E. (2021). VULNERABILITY OF WOMEN IN DISASTERS: A CASE STUDY OF DISTRICT BADIN. In *Biannual Research Journal Grassroots* (Vol. 55, Issue I).

Kim, V., Tantanee, S., & Suparta, W. (2020). Gis-based flood hazard mapping using hec-ras model: A case study of lower mekong river, cambodia. *Geographia Technica*, *15*(1), 16–26. https://doi.org/10.21163/GT_2020.151.02

Kirana, A., & Sufyan Bature, S. (2022). Socialization of Natural Disaster Mitigation to Minimize the Impact of the Risk of Economic Loss in the Citarum River Basin (DAS) West Bandung Regency. *International Journal of Research in Community Service*, *3*(4), 120–126.

Kiss, R., Schedler, S., & Muehlbauer, T. (2018). Associations Between Types of Balance Performance in Healthy Individuals Across the Lifespan: A Systematic Review and Meta-Analysis. In *Frontiers in Physiology* (Vol. 9). Frontiers Media S.A. https://doi.org/10.3389/fphys.2018.01366

Klijn, F., Kreibich, H., de Moel, H., & Penning-Rowsell, E. (2015). Adaptive flood risk management planning based on a comprehensive flood risk conceptualisation. *Mitigation and Adaptation Strategies for Global Change*, *20*(6), 845–864. https://doi.org/10.1007/s11027-015-9638-z

Kougkoulos, I., Cook, S. J., Edwards, L. A., Clarke, L. J., Symeonakis, E., Dortch, J. M., & Nesbitt, K. (2018). Modelling glacial lake outburst flood impacts in the Bolivian Andes. *Natural Hazards*, *94*(3), 1415–1438. https://doi.org/10.1007/s11069-018-3486-6

Książek, L., Woś, A., Florek, J., Wyrębek, M., Młyński, D., & Wałęga, A. (2019). Combined use of the hydraulic and hydrological methods to calculate the environmental flow: Wisloka river, Poland: case study. *Environmental Monitoring and Assessment*, *191*(4). https://doi.org/10.1007/s10661-019-7402-7

Lamichhane, N., & Sharma, S. (2018). Effect of input data in hydraulic modeling for flood warning systems. *Hydrological Sciences Journal*, *63*(6), 938–956. https://doi.org/10.1080/02626667.2018.1464166

Leon, A. S., & Goodell, C. (2016). Controlling HEC-RAS using MATLAB. *Environmental Modelling & Software*, *84*, 339–348. https://doi.org/10.1016/J.ENVSOFT.2016.06.026

Li, H., Huang, W., Zha, Z., & Yang, J. (2021). Application and platform design of geospatial big data. *International Archives of the Photogrammetry, Remote Sensing and Spatial Information Sciences - ISPRS Archives*, *43*(B4-2021), 293–300. https://doi.org/10.5194/isprs-archives-XLIII-B4-2021-293-2021

Lindner, R., Lückerath, D., Milde, K., Ullrich, O., Maresch, S., Peinhardt, K., Latinos, V., Hernantes, J., & Jaca, C. (2021). The standardization process as a chance for conceptual refinement of a disaster risk management framework: The arch project. *Sustainability (Switzerland)*, *13*(21). https://doi.org/10.3390/su132112276

Luu, C., Tran, H. X., Pham, B. T., Al-Ansari, N., Tran, T. Q., Duong, N. Q., Dao, N. H., Nguyen, L. P., Nguyen, H. D., Ta, H. T., Le, H. Van, & von Meding, J. (2020). Framework of spatial flood risk assessment for a case study in quang binh province, Vietnam. *Sustainability (Switzerland)*, *12*(7). https://doi.org/10.3390/su12073058

Mahapatra, A., Mahammood, V., & Venkatesh, K. (2022). Unsteady flow analysis using hydrological and hydraulic models for real-time flood forecasting in the Vamsadhara river basin. *Journal of Hydroinformatics*, *24*(6), 1207–1233. https://doi.org/10.2166/hydro.2022.065

Marr, S. M., & Swemmer, A. M. (2023). Hydrological characteristics of extreme floods in the Klaserie River, a headwater stream in southern Africa. *Journal of Limnology*, *82*. https://doi.org/10.4081/jlimnol.2023.2102

Marselina, M., Nurhayati, S. A., & Pandia, S. L. (2022). Flood Analysis and Estimating Economic Losses in an Affected Area (Case Study: Cikapundung Watershed). *Air, Soil and Water Research*, *15*. https://doi.org/10.1177/11786221221131277

Mawasha, T. S., & Britz, W. (2022). Hydrological impacts of land use - land cover change on urban flood hazard: A case study of the Jukskei River in Alexandra Township, Johannesburg, South Africa. *South African Journal of Geomatics*, *10*(2), 139–162. https://doi.org/10.4314/sajg.v10i2.11

Mcknight, C. J., Loney, D., & Winters, K. (2019). *Watershed and Catchment Meshing Python Tool Utilizing the XmsMesh Meshing Software*.

Mehring, P., Geoghegan, H., Cloke, H. L., & Clark, J. M. (2022). Going home for tea and medals: How members of the flood risk management authorities in England construct flooding and flood risk management. *Journal of Flood Risk Management*, *15*(1). https://doi.org/10.1111/jfr3.12768

Meissner, K. A., & Nicolai, H. (2019). Superheavy gravitinos and ultra-high energy cosmic rays. *Journal of Cosmology and Astroparticle Physics*, *2019*(09), 041–041. https://doi.org/10.1088/1475-7516/2019/09/041

Monty, F., Murti, R., Miththapala, S., & Buyck, C. (n.d.). *Ecosystems protecting infrastructure and communities Lessons learned and guidelines for implementation*. https://twitter.com/IUCN/

Morote, Á. F., & Hernández, M. (2020). Social representations of flooding of future teachers of primary education (social sciences): A geographical approach in the Spanish Mediterranean region. *Sustainability (Switzerland)*, *12*(15). https://doi.org/10.3390/su12156065

Mosavi, A., Ozturk, P., & Chau, K. W. (2018). Flood prediction using machine learning models: Literature review. In *Water (Switzerland)* (Vol. 10, Issue 11). MDPI AG. https://doi.org/10.3390/w10111536

Muthusamy, M., Casado, M. R., Salmoral, G., Irvine, T., & Leinster, P. (2019). A remote sensing based integrated approach to quantify the impact of fluvial and pluvial flooding in an urban catchment. *Remote Sensing*, *11*(5). https://doi.org/10.3390/rs11050577

Nakatani, R. (2019). *A Possible Approach to Fiscal Rules in Small Islands-Incorporating Natural Disasters and Climate Change*.

Nastos, P. T., & Dalezios, N. R. (2016). Preface: Advances in meteorological hazards and extreme events. In *Natural Hazards and Earth System Sciences* (Vol. 16, Issue 5, pp. 1259–1268). Copernicus GmbH. https://doi.org/10.5194/nhess-16-1259-2016

Nemakonde, L. D., & Van Niekerk, D. (2023). Enabling conditions for integrating government institutions for disaster risk reduction and climate change adaptation in the SADC region and beyond. *Risk, Hazards and Crisis in Public Policy*, *14*(1), 6–26. https://doi.org/10.1002/rhc3.12246

Nematollahi, B., Bakhtiari, P. H., Talebbeydokhti, N., Rakhshandehroo, G. R., Nikoo, M. R., & Gandomi, A. H. (2022). A Stochastic Conflict Resolution Optimization Model for Flood Management in Detention Basins: Application of Fuzzy Graph Model. *Water (Switzerland)*, *14*(5). https://doi.org/10.3390/w14050774

Nikitin, A. V., Klimentova, E. A., Dubovitski, A. A., Kastornov, N. P., Rogov, M. A., & Sukhareva, T. N. (2022). *Adaptive Management Of Climate Risk In Agricutual Enterprises*. 414–419. https://doi.org/10.15405/epsbs.2022.02.53

Ntakiyimana, C., Zhang, Y., & Twagirayezu, G. (2022). Road Flooding in Kigali City, Rwanda: Causes, Effects on Road Transportation and Mitigation Measures. *Polish Journal of Environmental Studies*, *31*(4), 3735–3744. https://doi.org/10.15244/pjoes/146215

Odm, L., Erzagian, E., & Wilopo, W. (2022). Flood assessment after Cempaka Cyclone 2019 in Imogiri District, Bantul Regency of Yogyakarta, Indonesia. *IOP Conference Series: Earth and Environmental Science*, *1071*(1). https://doi.org/10.1088/1755-1315/1071/1/012008

OECD. (2016). *Financial Management of Flood Risk PReliMinaRy VeRsion Financial Management of Flood Risk Financial Management of Flood Risk*.

Okoli, K., Breinl, K., Mazzoleni, M., & Di Baldassarre, G. (2019). Design Flood Estimation: Exploring the Potentials and Limitations of Two Alternative Approaches. *Water 2019, Vol. 11, Page 729*, *11*(4), 729. https://doi.org/10.3390/W11040729

Oladotun, O. M. (2022). Assessment of runoff potential for disaster risk reduction using geospatial technology in Opa watershed, Southwestern Nigeria. *South*

African Journal of Geomatics, *10*(2), 90–100. https://doi.org/10.4314/sajg.v10i2.8

Paul, A., Dutta, D., & Jha, C. S. (2022). *Open-Source Geospatial Technology for Coastal Asset Mapping and Management*. www.intechopen.com

Pekárová, P., Pramuk, B., Halmová, D., Miklánek, P., Prohaska, S., & Pekár, J. (2016). Identification of long-term high-flow regime changes in selected stations along the Danube River. *Journal of Hydrology and Hydromechanics*, *64*(4), 393–403. https://doi.org/10.1515/johh-2016-0045

Phillips, M. C. K., Cinderich, A. B., Burrell, J. L., Ruper, J. L., Will, R. G., & Sheridan, S. C. (2015). The effect of climate change on natural disasters: A college student perspective. *Weather, Climate, and Society*, *7*(1), 60–68. https://doi.org/10.1175/WCAS-D-13-00038.1

Prastica, R. M. S., Maitri, C., Hermawan, A., Nugroho, P. C., Sutjiningsih, D., & Anggraheni, E. (2018). Estimating design flood and HEC-RAS modelling approach for flood analysis in Bojonegoro city. *IOP Conference Series: Materials Science and Engineering*, *316*(1). https://doi.org/10.1088/1757-899X/316/1/012042

Priya, R., Kumar, R. S., Naiklal, S. K., & Kumar, A. (2020). FLOOD INUNDATION MODELLING FOR TUNGABHADRA BASIN USING HEC-RAS: A CASE STUDY OF HARALAHALLI DISCHARGE SITE. *Geographical Analysis*, *9*(2), 33–41. https://doi.org/10.53989/bu.ga.v9i2.8

Psomiadis, E., Diakakis, M., & Soulis, K. X. (2020a). Combining SAR and optical earth observation with hydraulic simulation for flood mapping and impact assessment. *Remote Sensing*, *12*(23), 1–29. https://doi.org/10.3390/rs12233980

Psomiadis, E., Diakakis, M., & Soulis, K. X. (2020b). Combining SAR and optical earth observation with hydraulic simulation for flood mapping and impact assessment. *Remote Sensing*, *12*(23), 1–29. https://doi.org/10.3390/rs12233980

Quintero, F., Mantilla, R., Anderson, C., Claman, D., & Krajewski, W. (2018). Assessment of changes in flood frequency due to the effects of climate change: Implications for engineering design. *Hydrology*, *5*(1). https://doi.org/10.3390/hydrology5010019

Qumba, B., Nkhonjera, G. K., & Alowo, R. (2022). An investigation of past and present stormwater management practices within the City of Johannesburg. *IOP Conference Series: Earth and Environmental Science*, *1087*(1), 012024. https://doi.org/10.1088/1755-1315/1087/1/012024

Rahmati, O., Zeinivand, H., & Besharat, M. (2016). Flood hazard zoning in Yasooj region, Iran, using GIS and multi-criteria decision analysis.

Geomatics, Natural Hazards and Risk, *7*(3), 1000–1017. https://doi.org/10.1080/19475705.2015.1045043

Ramirez, J. A., Lichter, M., Coulthard, T. J., & Skinner, C. (2016). Hyper-resolution mapping of regional storm surge and tide flooding: comparison of static and dynamic models. *Natural Hazards*, *82*(1), 571–590. https://doi.org/10.1007/s11069-016-2198-z

Rauf, I., Imran, & Sahdar, I. (2021). Simulation Of Flood Mapping in Amasing Kali Village Using HEC-RAS 2D. *E3S Web of Conferences*, *328*. https://doi.org/10.1051/e3sconf/202132810003

Raufu, I. O., Mukaila, I., Olaniyan, K., & Awodele, Z. (n.d.). *Application of Remote Sensing and Geographical Information System (GIS) in Flood Vulnerability Mapping: A Scenario of Akure South, Nigeria*. https://doi.org/10.30897/ijegeo

Razi, M. A. M., Adnan, M. S., Abustan, M. S. H., Uma, M. H. A., Anuar, N. D., & Jamal, M. H. (2023). Flood modelling at Bandar Batu Pahat, Johor using HEC-RAS software. *IOP Conference Series: Earth and Environmental Science*, *1205*(1). https://doi.org/10.1088/1755-1315/1205/1/012023

Razi, M. A. M., Deli, M. A. Z., Yusoff, M. A. M., Ahmad, M. A., & Adnan, M. S. (2022). Flood Modelling Studies Using River Analysis System (HEC-RAS) For Flood Plain Area in Muar City. *International Journal of Integrated Engineering*, *14*(9), 38–47. https://doi.org/10.30880/ijie.2022.14.09.006

Rebally, A., Valeo, C., He, J., & Saidi, S. (2021). Flood Impact Assessments on Transportation Networks: A Review of Methods and Associated Temporal and Spatial Scales. In *Frontiers in Sustainable Cities* (Vol. 3). Frontiers Media S.A. https://doi.org/10.3389/frsc.2021.732181

Riswanto, S., & Nanda, M. P. (2023). Use of Hec-Ras Software to Analyze Floods in Joyoakan Urban Village, Surakarta City, Central Java. *Journal of Advanced Civil and Environmental Engineering*, *6*(1), 33. https://doi.org/10.30659/jacee.6.1.33-41

Roy, B., Khan, M. S. M., Saiful Islam, A. K. M., Khan, M. J. U., & Mohammed, K. (2021). Integrated flood risk assessment of the arial khan river under changing climate using ipcc ar5 risk framework. *Journal of Water and Climate Change*, *12*(7), 3421–3447. https://doi.org/10.2166/wcc.2021.341

Rucker, C. A., Tull, N., Dietrich, J. C., Langan, T. E., Mitasova, H., Blanton, B. O., Fleming, J. G., & Luettich, R. A. (2021). Downscaling of real-time coastal flooding predictions for decision support. *Natural Hazards*, *107*(2), 1341–1369. https://doi.org/10.1007/s11069-021-04634-8

Saksena, S., & Merwade, V. (2015). Incorporating the effect of DEM resolution and accuracy for improved flood inundation mapping. *Journal of Hydrology*, *530*, 180–194. https://doi.org/10.1016/J.JHYDROL.2015.09.069

Saleh, A., & Bba, A. (n.d.). *Environmental Disaster Management in the Great Lakes: To What Extent are Governments in the Region Prepared?*

Samu, R., & Akıntuğ, B. (2020). Pre-disaster planning and preparedness: Drought and flood forecasting and analysis in Zimbabwe. *Water SA*, *46*(3), 448–457. https://doi.org/10.17159/wsa/2020.v46.i3.8655

Sandifer, P. A., Knapp, L. C., Collier, T. K., Jones, A. L., Juster, R. P., Kelble, C. R., Kwok, R. K., Miglarese, J. V., Palinkas, L. A., Porter, D. E., Scott, G. I., Smith, L. M., Sullivan, W. C., & Sutton-Grier, A. E. (2017). A conceptual model to assess stress-associated health effects of multiple ecosystem services degraded by disaster events in the Gulf of Mexico and elsewhere. *GeoHealth*, *1*(1), 17–36. https://doi.org/10.1002/2016GH000038

Sankaranarayanan, S., Prabhakar, M., Satish, S., Jain, P., Ramprasad, A., & Krishnan, A. (2020). Flood prediction based on weather parameters using deep learning. *Journal of Water and Climate Change*, *11*(4), 1766–1783. https://doi.org/10.2166/wcc.2019.321

Santosa, B. H. (2023). Exploring household flood resilience index using composite indicator method. *IOP Conference Series: Earth and Environmental Science*, *1201*(1). https://doi.org/10.1088/1755-1315/1201/1/012060

Sathya, K., Rahardjo, A. P., & Jayadi, R. (2021). Flash Flood Disaster Reconstruction for Estimating the Available Warning Time, the Case in Sempor River on 21stof February 2020, Mt. Merapi Slope, Yogyakarta Special Region. *IOP Conference Series: Earth and Environmental Science*, *930*(1). https://doi.org/10.1088/1755-1315/930/1/012080

Sattar, A., Goswami, A., Kulkarni, A. V., & Emmer, A. (2020). Lake evolution, hydrodynamic outburst flood modeling and sensitivity analysis in the central himalaya: A case study. *Water (Switzerland)*, *12*(1). https://doi.org/10.3390/w12010237

Schardong, A., Simonovic, S. P., & Tong, H. (2019). Use of quantitative resilience in managing urban infrastructure response to natural hazards. *International Journal of Safety and Security Engineering*, *9*(1), 13–25. https://doi.org/10.2495/SAFE-V9-N1-13-25

Schober, P., & Schwarte, L. A. (2018). Correlation coefficients: Appropriate use and interpretation. *Anesthesia and Analgesia*, *126*(5), 1763–1768. https://doi.org/10.1213/ANE.0000000000002864

Senthilkumar, P., & Arthur, M. P. (2023). A review of intelligent models for mapping city development and urban flooding. In *Land Degradation and Development* (Vol. 34, Issue 13, pp. 3793–3809). John Wiley and Sons Ltd. https://doi.org/10.1002/ldr.4742

Setiawan, O., & Nandini, R. (2022). Integration of LULC change/prediction and hydrological modeler for assessment of the effect of LULC Change on peak discharge in Sari Watershed, Sumbawa Island, Indonesia. *IOP Conference Series: Earth and Environmental Science*, *1109*(1). https://doi.org/10.1088/1755-1315/1109/1/012070

Sh Abed, B., Hussain, H. H., Abdul-Razzaq, K. A., & Al-Hilla, S. (2020). Finite Element Modeling of Saint-Venant Equations for Shatt-Al Hilla. In *Journal of Techniques* (Vol. 2, Issue 1). http://journal.mtu.edu.iq

Silva, H. A., & Moura, A. S. (2020). Teaching Introductory Statistical Classes in Medical Schools Using RStudio and R Statistical Language: Evaluating Technology Acceptance and Change in Attitude Toward Statistics. *Journal of Statistics Education*, *28*(2), 212–219. https://doi.org/10.1080/10691898.2020.1773354

Singh, A., Dawson, D., Trigg, M., & Wright, N. (2021). A review of modelling methodologies for flood source area (FSA) identification. In *Natural Hazards* (Vol. 107, Issue 2, pp. 1047–1068). Springer Science and Business Media B.V. https://doi.org/10.1007/s11069-021-04672-2

Sofia, G., Roder, G., Dalla Fontana, G., & Tarolli, P. (2017). Flood dynamics in urbanised landscapes: 100 years of climate and humans' interaction. *Scientific Reports*, *7*. https://doi.org/10.1038/srep40527

Soliman, M., Morsy, M. M., & Radwan, H. G. (2022a). Assessment of Implementing Land Use/Land Cover LULC 2020-ESRI Global Maps in 2D Flood Modeling Application. *Water (Switzerland)*, *14*(23). https://doi.org/10.3390/w14233963

Soliman, M., Morsy, M. M., & Radwan, H. G. (2022b). Assessment of Implementing Land Use/Land Cover LULC 2020-ESRI Global Maps in 2D Flood Modeling Application. *Water (Switzerland)*, *14*(23). https://doi.org/10.3390/w14233963

Šoltész, A., Zelenáková, M., Cubanová, L., Šugareková, M., & Abd-Elhamid, H. (2021). Environmental impact assessment and hydraulic modelling of different flood protection measures. *Water (Switzerland)*, *13*(6). https://doi.org/10.3390/w13060786

South African Weather Service. (2023). *Annual State of the Climate of South Africa 2022*.

Stephens, S. A., Paulik, R., Reeve, G., Wadhwa, S., Popovich, B., Shand, T., & Haughey, R. (2021). Future changes in built environment risk to coastal flooding, permanent inundation and coastal erosion hazards. *Journal of Marine Science and Engineering*, *9*(9). https://doi.org/10.3390/jmse9091011

Stoleriu, C. C., Urzica, A., & Mihu-Pintilie, A. (2020). Improving flood risk map accuracy using high-density LiDAR data and the HEC-RAS river analysis system: A case study from north-eastern Romania. *Journal of Flood Risk Management*, *13*(S1). https://doi.org/10.1111/jfr3.12572

Sudalaimuthu, K., Jesudhas, C. J., Ramachandran, U. R., Somanathan, A. K., Ganapathy, S., & Jeyakumar, R. B. (2022). Development of digital elevation model for assessment of flood vulnerable areas using Cartosat-1 and GIS at Thamirabarani river, Tamilnadu, India. *Environmental Quality Management*, *32*(1), 75–85. https://doi.org/10.1002/tqem.21842

Supriatna, Mukhtar, M. K., Wardani, K. K., Hashilah, F., & Manessa, M. D. M. (2022). CA-Markov Chain Model-based Predictions of Land Cover: A Case Study of Banjarmasin City. *Indonesian Journal of Geography*, *54*(3), 365–372. https://doi.org/10.22146/IJG.71721

Swain, K. C., Singha, C., & Nayak, L. (2020). Flood susceptibility mapping through the GIS-AHP technique using the cloud. *ISPRS International Journal of Geo-Information*, *9*(12). https://doi.org/10.3390/ijgi9120720

Tamiru, H., & Dinka, M. O. (2021). Artificial Intelligence in Geospatial Analysis for Flood Vulnerability Assessment: A Case of Dire Dawa Watershed, A wash Basin, Ethiopia. *Scientific World Journal*, *2021*. https://doi.org/10.1155/2021/6128609

Tariq, M. A. U. R., Farooq, R., & van de Giesen, N. (2020). A critical review of flood risk management and the selection of suitable measures. In *Applied Sciences (Switzerland)* (Vol. 10, Issue 23, pp. 1–18). MDPI AG. https://doi.org/10.3390/app10238752

Theron, E., Bills, C. B., Calvello Hynes, E. J., Stassen, W., & Rublee, C. (2022). Climate change and emergency care in Africa: A scoping review. In *African Journal of Emergency Medicine* (Vol. 12, Issue 2, pp. 121–128). African Federation for Emergency Medicine. https://doi.org/10.1016/j.afjem.2022.02.003

Thieken, A. H., Bessel, T., Kienzler, S., Kreibich, H., Müller, M., Pisi, S., & Schröter, K. (2016). The flood of June 2013 in Germany: How much do we know about its impacts? *Natural Hazards and Earth System Sciences*, *16*(6), 1519–1540. https://doi.org/10.5194/nhess-16-1519-2016

Thomas Steven Savage, J., Pianosi, F., Bates, P., Freer, J., & Wagener, T. (2016). Quantifying the importance of spatial resolution and other factors through

global sensitivity analysis of a flood inundation model. *Water Resources Research*, *52*(11), 9146–9163. https://doi.org/10.1002/2015WR018198

Tom, R. O., George, K. O., Joanes, A. O., & Haron, A. (2022). Review of flood modelling and models in developing cities and informal settlements: A case of Nairobi city. In *Journal of Hydrology: Regional Studies* (Vol. 43). Elsevier B.V. https://doi.org/10.1016/j.ejrh.2022.101188

Toonen, W. H. (2019). *Analysis of Main Periods of Catastrophic Floods in the Yesil River Basin*.

Tuozzolo, S., Langhorst, T., de Moraes Frasson, R. P., Pavelsky, T., Durand, M., & Schobelock, J. J. (2019). The impact of reach averaging Manning's equation for an in-situ dataset of water surface elevation, width, and slope. *Journal of Hydrology*, *578*, 123866. https://doi.org/10.1016/J.JHYDROL.2019.06.038

U-Din, S., Nazir, M. S., & Sarfraz, M. (2022). The climate change and stock market: catastrophes of the Canadian weather. *Environmental Science and Pollution Research*, *29*(29), 44806–44818. https://doi.org/10.1007/s11356-022-19059-4

Unduche, F., Tolossa, H., Senbeta, D., & Zhu, E. (2018). Evaluation of four hydrological models for operational flood forecasting in a Canadian Prairie watershed. *Hydrological Sciences Journal*, *63*(8), 1133–1149. https://doi.org/10.1080/02626667.2018.1474219

Van Khanh Triet, N., Viet Dung, N., Fujii, H., Kummu, M., Merz, B., & Apel, H. (2017). Has dyke development in the Vietnamese Mekong Delta shifted flood hazard downstream? *Hydrology and Earth System Sciences*, *21*(8), 3991–4010. https://doi.org/10.5194/hess-21-3991-2017

Vousdoukas, M. I., Voukouvalas, E., Mentaschi, L., Dottori, F., Giardino, A., Bouziotas, D., Bianchi, A., Salamon, P., & Feyen, L. (2016). Developments in large-scale coastal flood hazard mapping. *Natural Hazards and Earth System Sciences*, *16*(8), 1841–1853. https://doi.org/10.5194/nhess-16-1841-2016

Wang, H., Yun, R., Zhang, J., & Zhao, R. (2022). Sensitivity analysis of the flash flood hazard by coupling variable fuzzy method and mutual entropy. *Journal of Flood Risk Management*, *15*(2). https://doi.org/10.1111/jfr3.12792

Wang, W., Yang, S., Gao, J., Hu, F., Zhao, W., & Stanley, H. E. (2020). An Integrated Approach for Assessing the Impact of Large-Scale Future Floods on a Highway Transport System. *Risk Analysis*, *40*(9), 1780–1794. https://doi.org/10.1111/risa.13507

Wang, Y., Hong, H., Chen, W., Li, S., Pamučar, D., Gigović, L., Drobnjak, S., Bui, D. T., & Duan, H. (2019). A hybrid GIS multi-criteria decision-making

method for flood susceptibility mapping at Shangyou, China. *Remote Sensing*, *11*(1). https://doi.org/10.3390/rs11010062

Wu, Y., Peng, F., Peng, Y., Kong, X., Liang, H., & Li, Q. (2019). Dynamic 3D simulation of flood risk based on the integration of spatio-temporal GIS and hydrodynamic models. *ISPRS International Journal of Geo-Information*, *8*(11). https://doi.org/10.3390/ijgi8110520

Yamamoto, T., Kazama, S., Touge, Y., Yanagihara, H., Tada, T., Yamashita, T., & Takizawa, H. (2021). Evaluation of flood damage reduction throughout Japan from adaptation measures taken under a range of emissions mitigation scenarios. *Climatic Change*, *165*(3–4). https://doi.org/10.1007/s10584-021-03081-5

Yang, Q., Zhang, S., Dai, Q., & Yao, R. (2020a). Assessment of community vulnerability to different types of urban floods: A case for Lishui City, China. *Sustainability (Switzerland)*, *12*(19). https://doi.org/10.3390/SU12197865

Yang, Q., Zhang, S., Dai, Q., & Yao, R. (2020b). Improved framework for assessing vulnerability to different types of urban floods. *Sustainability (Switzerland)*, *12*(18). https://doi.org/10.3390/su12187668

Yang, T. H., & Liu, W. C. (2020). A general overview of the risk-reduction strategies for floods and droughts. *Sustainability (Switzerland)*, *12*(7). https://doi.org/10.3390/su12072687

Yang, X., Chen, H., Wang, Y., & Xu, C. Y. (2016). Evaluation of the effect of land use/cover change on flood characteristics using an integrated approach coupling land and flood analysis. *Hydrology Research*, *47*(6), 1161–1171. https://doi.org/10.2166/nh.2016.108

Yariyan, P., Avand, M., Abbaspour, R. A., Torabi Haghighi, A., Costache, R., Ghorbanzadeh, O., Janizadeh, S., & Blaschke, T. (2020). Flood susceptibility mapping using an improved analytic network process with statistical models. *Geomatics, Natural Hazards and Risk*, *11*(1), 2282–2314. https://doi.org/10.1080/19475705.2020.1836036

Yigitcanlar, T., Regona, M., Kankanamge, N., Mehmood, R., D'costa, J., Lindsay, S., Nelson, S., & Brhane, A. (2022). Detecting Natural Hazard-Related Disaster Impacts with Social Media Analytics: The Case of Australian States and Territories. *Sustainability (Switzerland)*, *14*(2). https://doi.org/10.3390/su14020810

Yu, Q., Wang, Y., & Li, N. (2022). Extreme Flood Disasters: Comprehensive Impact and Assessment. *Water (Switzerland)*, *14*(8). https://doi.org/10.3390/w14081211

Zhang, B., Wang, S., & Wang, Y. (2021). Probabilistic Projections of Multidimensional Flood Risks at a Convection-Permitting Scale. *Water Resources Research*, *57*(1). https://doi.org/10.1029/2020WR028582

Zhang, D., Shi, X., Xu, H., Jing, Q., Pan, X., Liu, T., Wang, H., & Hou, H. (2020). A GIS-based spatial multi-index model for flood risk assessment in the Yangtze River Basin, China. *Environmental Impact Assessment Review*, *83*. https://doi.org/10.1016/j.eiar.2020.106397

Zhang, J., Min, Y., Feng, B., & Duan, W. (2021). Research and application of key technologies for dynamic control of reservoir water level in flood season. *Water (Switzerland)*, *13*(24). https://doi.org/10.3390/w13243576

Zhang, W., Zhang, X., Liu, Y., Tang, W., Xu, J., & Fu, Z. (2020). Assessment of flood inundation by coupled 1d/2d hydrodynamic modeling: A case study in mountainous watersheds along the coast of southeast China. *Water (Switzerland)*, *12*(3), 1–14. https://doi.org/10.3390/w12030822

Zhu, X., Nie, S., Wang, C., Xi, X., Li, D., Li, G., Wang, P., Cao, D., & Yang, X. (2020). Estimating terrain slope from ICESat-2 data in forest environments. *Remote Sensing*, *12*(20), 1–19. https://doi.org/10.3390/rs12203300

Zischg, A. P. (2022). Confronting complexity. In *Journal of Flood Risk Management* (Vol. 15, Issue 4). John Wiley and Sons Inc. https://doi.org/10.1111/jfr3.12865